University of Alberta

Characterization of the anti-apoptotic properties of flavivirus capsid proteins

by

Matthew Daniel Urbanowski

A thesis submitted to the Faculty of Graduate Studies and Research in partial fulfillment of the requirements for the degree of

Doctor of Philosophy

Cell Biology

Spring 2014
Edmonton, Alberta

Abstract

The introduction of WNV into North America in 1999 was followed by rapid spread throughout the continent. Today, WNV is an endemic pathogen in the west, with thousands of cases of severe infection reported annually. In addition to traditional vaccine research, there is an urgent need to understand the contributions of individual virus components to the infection process. This includes the capsid protein, which has until recent times has been thought only to be a structural protein. As the sole component of the nucleocapsid, the capsid protein serves the essential function of both providing structure to the virion and protecting the viral genome. However, recent research would suggest that in addition to these functions, capsid can serve to modulate the host cell environment to create a more permissive environment for viral replication and spread.

Viruses such as WNV that exhibit slower replication kinetics must employ strategies to avoid host responses which attempt to prevent viral replication. One such critical strategy is the prevention of cell death. A growing number of reports in the literature have described mechanisms whereby viral proteins can blunt the apoptotic response to permit efficient virus replication. This can be mediated through enhanced activity of the ubiquitous and highly regulated PI3K/Akt pathway. Indeed, WNV appears to utilize this pathway to prolong cell survival during infection.

In my thesis, I describe the anti-apoptotic properties of WNV and other flavivirus capsids, and demonstrate their ability to suppress apoptosis triggered by ligation of Fas. In concordance with this, I show that those capsids which block apoptosis triggered by anti-Fas enhance phosphorylation of Akt. The inhibition of this kinase through the use of the inhibitor LY294002 prevents WNV capsid mediated suppression of apoptosis triggered by Fas ligation.

In support of this first study, I also demonstrate that capsid proteins are able to promote cellular proliferation, even in the absence of growth factors. Curiously, this phenomenon includes those capsid proteins which do not protect against anti-Fas. The characterization of these properties of flavivirus capsid proteins provides greater insight into the biology of the viruses they are derived from.

Acknowledgements

First, I must sincerely thank my mentor Dr. Tom C. Hobman for his hard work and perserverence in assisting me on my journey to becoming a scientist. Scientific research is a challenging and demanding endeavour which requires not only dedication, but rigourous training. I am incredibly fortunate to have had his expert guidance during my graduate studies. It has certainly prepared me very well for the road ahead.

I would also like to thank the numerous friends and lab mates that I have had the pleasure of working with over the years, whose acquaintance has enriched my life. Thank you for your friendship, collaboration, and for sharing in this journey. You know who you are, and you have my most heartfelt thanks.

Finally, I must express my gratitude to my wife and and best friend Camille Hamula. Throughout the years she has been my dearest companion, and my greatest supporter. Her love, kindness and understanding allowed me to keep going, even when I was uncertain. Words truly cannot express how greatful I am to her for everything she has done to enrich my life.

List Of Tables

List of Figures

List of Abbreviations and Nomenclature

µ	micro
^{o}C	degrees Celcius
AcGFP	*Aquorea corelescens* Green Fluorescent Protein
BBB	Blood Brain Barrier
cDNA	complementary Deoxyribonucleic Acid
CNS	Central Nervous System
cryo-EM	cryo-Electron Microscopy
DAPI	4',6-diamidino-2-phenylindole
DENV	Dengue Virus
DMEM	Dulbecco's Modified Eagle Medium
DMSO	Dimethyl Sulfoxide
DNA	Deoxyribonucleic Acid
dNTPs	deoxynucleotide Triphosphates
EBOV	Ebola Virus
EDTA	ethylenediaminetetraacetic acid
ER	Endoplasmic Reticulum
FBS	Fetal Bovine Serum
g	g force
GST	Glutathione S-Transferase
HCV	Hepatitis C Virus
HEPES	4-(2-hydroxyethyl)-1-piperazineethanesulfonic acid
JEV	Japanese Enchephalitis Virus
kDa	kiloDalton
LD	Lipid Droplet
m	milli
M	Moles per Litre
mRNA	messenger Ribonucleic Acid
MVEV	Murray Valley Encephalitis Virus
PBS	Phosphate Buffered Saline
PBS-T	Phosphate Buffered Saline Tween
PCD	Programmed Cell Death
PCR	Polymerase Chain Reaction
pH	power of Hydrogen
PVDF	Polyvinylidene Fluoride
RdRP	RNA-dependent RNA Polymerase
RNA	Ribonucleic Acid
RNAi	RNA interference

SDS-PAGE	Sodium Dodecyl Sulfate Polyacrylamide Gel Electrophoresis
SLEV	St. Louis Encephalitis Virus
ssRNA	singel stranded RNA
TagRFP	Tag-Red Fluorescent Protein
TEMED	Tetramethylethylenediamine
TNFR	TNF Receptor
TNFα	Tumor Necrosis Factor alpha
TRAIL	TNF Related Apoptosis Inducing Ligand
U	Enzyme unit
UAR	Upstream AUG Region
UTR	Untranslated Region
V	Volts
v/v	volume per volume
VSV	Vesicular Stomatitis Virus
w/v	weight per volume
WNV	West Nile Virus
YFV	Yellow Fever Virus

Chapter 1

Introduction

1.1 West Nile Virus

1.1.1 Overview

The outbreak of West Nile Virus (WNV) in New York during the summer of 1999 heralded the arrival of an arbovirus previously unknown in North America. Although there were relatively few cases in this initial outbreak, WNV has since spread throughout North America. In 2012, there were 5674 reported cases in the United States and 450 in Canada. Alarmingly, half of reported North American cases result in the development of neuroinvasive infection. This neuroinvasive disease is characterized by the development of meningoencephalitis, paresthesia, neuropathy and death in 10-12% of affected individuals (Centers for Disease Control, 2012). Those who recover from neuroinvasive WNV infection can experience severe long term pain and impairment of motor function. Patients who develop long term *sequellae* have reduced quality of life, increased healthcare costs, and often reduced employability (Berg et al., 2010; Carson et al., 2006; Nolan et al., 2012).

Since the 1999 New York outbreak, significant resources have been applied in an attempt to define and understand the mechanisms by which WNV causes disease in humans. In addition to programs which seek to limit the numbers of mosquito vectors, surveillance initiatives have sought to track the emergence and spread of new strains (Anez et al., 2013; Chung et al., 2013; Ergunay et al., 2013; Friesen and Johnson, 2013; Kilpatrick and Pape, 2013; Lampman et al., 2013). Perhaps most importantly, research into the molecular mechanisms by which

WNV replicates, spreads, and initiates pathogenesis in a human host has revealed many aspects of WNV biology. The development of animal models has aided greatly in understanding the mechanism of WNV pathogenesis, while molecular tools have provided insight into the specific mechanisms by which disease occurs (Machain-Williams et al., 2013; Szretter et al., 2012; Wicker et al., 2006).

The consequences of virus infection can be thought of as the result of both the simple and complex interactions of viral macromolecules with the host. Therefore, to develop a comprehensive understanding of how WNV causes disease in humans, studying the contribution of individual viral proteins to the final disease outcome is essential. Examining the interactions between virus proteins and RNA with host factors allows for more rational design of anti-viral drugs and vaccines. Particularly, it has become clear in recent years that that the so-called structural proteins of WNV play important non-structural roles during infection (Bhuvanakantham et al., 2009; Bhuvanakantham and Ng, 2013; Urbanowski and Hobman, 2013; Hunt et al., 2007).

1.1.2 West Nile Virus: Molecular Characteristics and Life Cycle

1.1.2.1 West Nile Virus phylogenetic organization

West Nile Virus belongs to the family of viruses known as the *Flaviviridae*. With rare exception, all of the viruses in this family are spread by arthropod vectors, and are medically relevant (reviewed in (Mackenzie et al., 2004)). Within

this family are four genera: *Flavivirus*, *Hepacivirus*, *Pegivirus* and *Pestivirus*. By far the largest of these is the genus *Flavivirus*, which currently contains 67 members including WNV. The classification of WNV includes many strains which have been characterized during outbreaks and regular surveillance. The phylogeny of WNV is broadly divided between two line ages (Mackenzie and Williams, 2009 and Figure 1.1). Additional lineages have been proposed, but the majority of strains isolated are still classified into either 1 or 2. Lineage 1 viruses are primarily associated with human outbreaks, and increased severity of disease compared to lineage 2. Lineage 1 strains have a broad geographic distribution, and this group includes the strain which was first introduced into New York in 1999. The origins of this strain are believed to be in Israel, where a highly similar virus was isolated and characterized one year previously (Lanciotti et al., 1999). This event led to the eventual spread of WNV throughout North America, and the emergence of several highly related WNV strains.

The group of lineage 2 viruses, which includes the first strain isolated from the West Nile region of Uganda in 1937, is generally associated with less pathogenic infections in humans. These strains are more commonly seen in zoonoses of a wide variety of animals, including horses in Sub-Saharan Africa and Europe. Since their discovery, both lineages of WNV have spread geographically due to increased international travel as well as animal habitat and climate changes (Mackenzie and Williams, 2009).

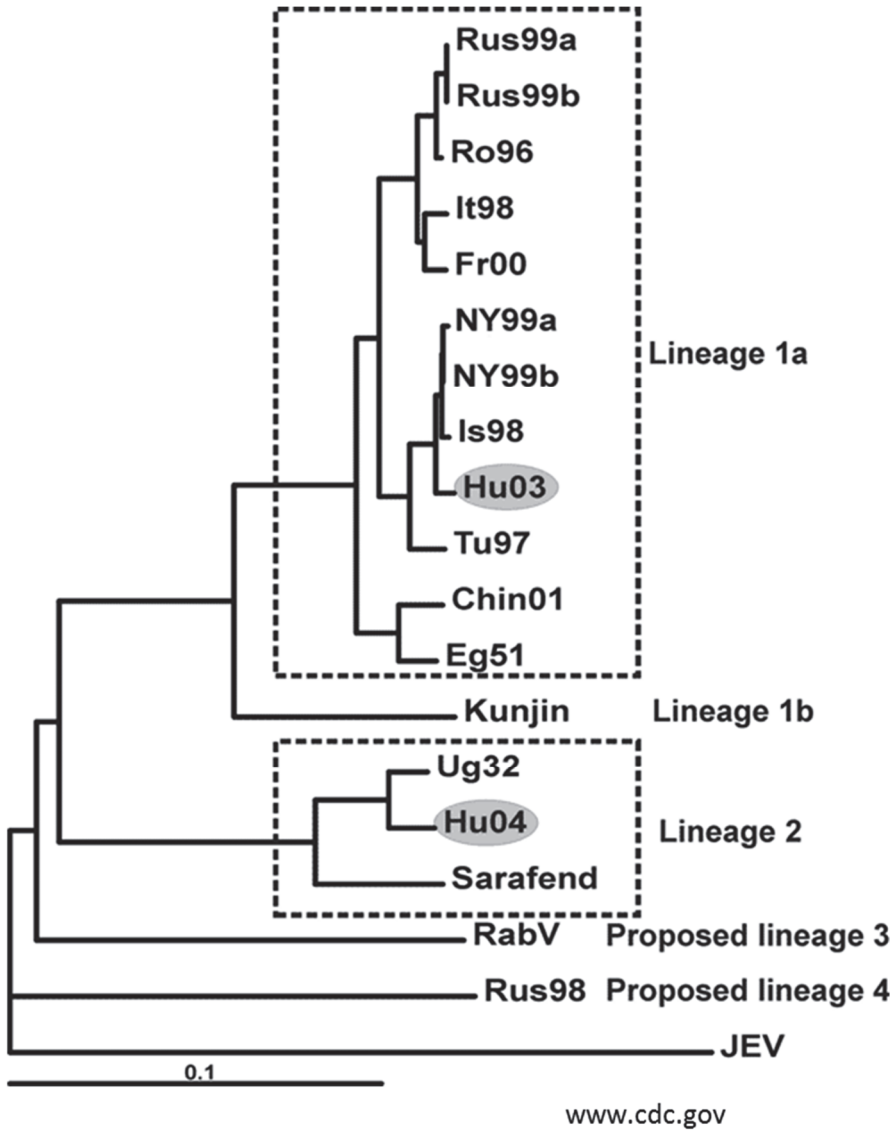

Figure 1.1. **Phylogenetics of West nile virus strains**. Dashed lines surround the two major lineages of WNV, Lineage 1a and Lineage 2. The most recent additions to these lineages (Hu03 and Hu04) are denoted with a grey oval. Two additional lineages have been proposed, currently with only one member each. For reference, the JEV lineage is shown.

1.1.2.2 Virion structure

Mature WNV particles are approximately 60-80 nm in diameter and have a relatively smooth surface (Figure 1.2). This is chiefly due to the lack of glycoprotein spikes, which are found on the surface of many other enveloped RNA viruses (e.g. togaviruses, retroviruses and rhabdoviruses) (Checkley et al., 2011; Plemper, 2011). The host-derived lipid bilayer of the mature virion contains multiple embedded "rafts" of the viral E protein, which are arranged in 3 parallel sets of dimers (Figure 2). Each monomer contains a single fusion peptide that is capped during virion assembly by the prM protein (Lorenz et al., 2002). Also an envelope protein, prM is arranged in trimers allowing the "pr" peptide to make contact with the fusion peptide of E. The removal of the pre-peptide "pr" by a cellular furin-like protease exposes the fusion peptide of E, and allows for structural rearrangements that give rise to the mature virion. Although both E and M are transmembrane proteins, mutational analyses and cryo-EM studies suggest that their transmembrane domains do not interact with each other (Zhang et al., 2003). Additionally, the transmembrane domains of E and M do not penetrate past the lipid bilayer to make contact with the nucleocapsid.

Contained within the host-derived envelope is a single copy of the virus genome, surrounded by multiple copies of the capsid protein arranged into a nucleocapsid shell. Curiously, the nucleocapsid lacks any discernable icosahedral symmetry. There is no distinct protein density detectable

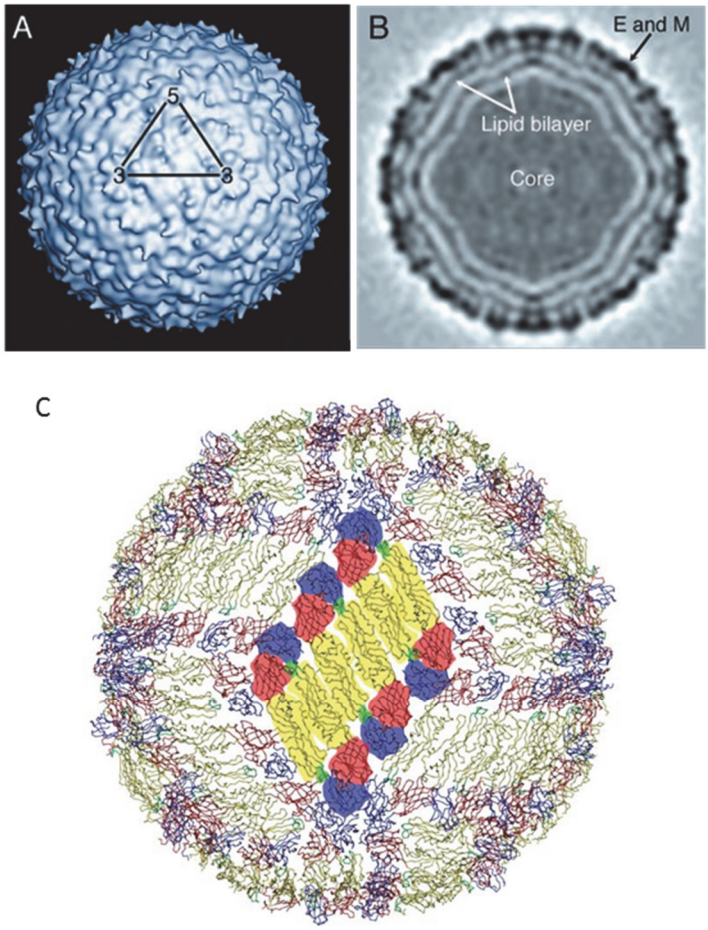

Figure 1.2. **Structure and organization of the flavivirus virion.** A surface shaded model derived from the 17Å cryo-EM structure, with both the 5 and 3 –fold axes of symmetry shown (A). The image in (B) depicts a cryo-EM cross section of the WNV virion, with various densities visible. The locations of the nucleocapsid core, lipid bilayer, and E and M proteins is indicated. In (C), a representation of the WNV virion structure highlighting the arrangement of E protein anti-parallel dimers in groups of 3 on the surface of the virion (red and blue-tipped structures) (Adapted from Kuhn *et al*, 2002).

surrounding the virus genome (Zhang et al., 2007). This strongly suggests that there is no ordered nucleocapsid structure present in WNV particles.

1.1.2.3 West Nile Virus genome structure and organization

The single-stranded RNA genome of WNV is approximately 11 000 bases and encodes a single open reading frame that is flanked by 5' and 3' untranslated regions (UTR) (Figure 1.3). *Cis*-acting elements within the coding sequence and UTRs are known to play important roles in the virus life cycle. Complementary sequences in both the 5' and 3' UTR, which are collectively referred to as the cyclization sequence 5'-3' UAR, were discovered via folding prediction algorithms (Trent et al., 1987; Khromykh et al., 2001; Thurner et al., 2004). Mutational analyses revealed that this sequence pair is essential for replication of WNV (Alvarez et al., 2008; Zhang et al., 2008). In addition, a 5' sequence element that includes part of the capsid-coding region, was found to have a complementary sequence in the 3' UTR (Trent et al., 1987). Studies using infectious clones and replicons showed that interaction between these two sequences is critical for replication of RNA, but not for translation of input RNA (Khromykh et al., 2001); (Lo et al., 2003). These studies were the first to show that genome cyclization through the interaction of 5' and 3' *cis*-acting elements is required for RNA replication.

In addition to RNA sequences that are necessary for replication, the WNV genome possesses a 5' cap. This cap structure is generated by the viral

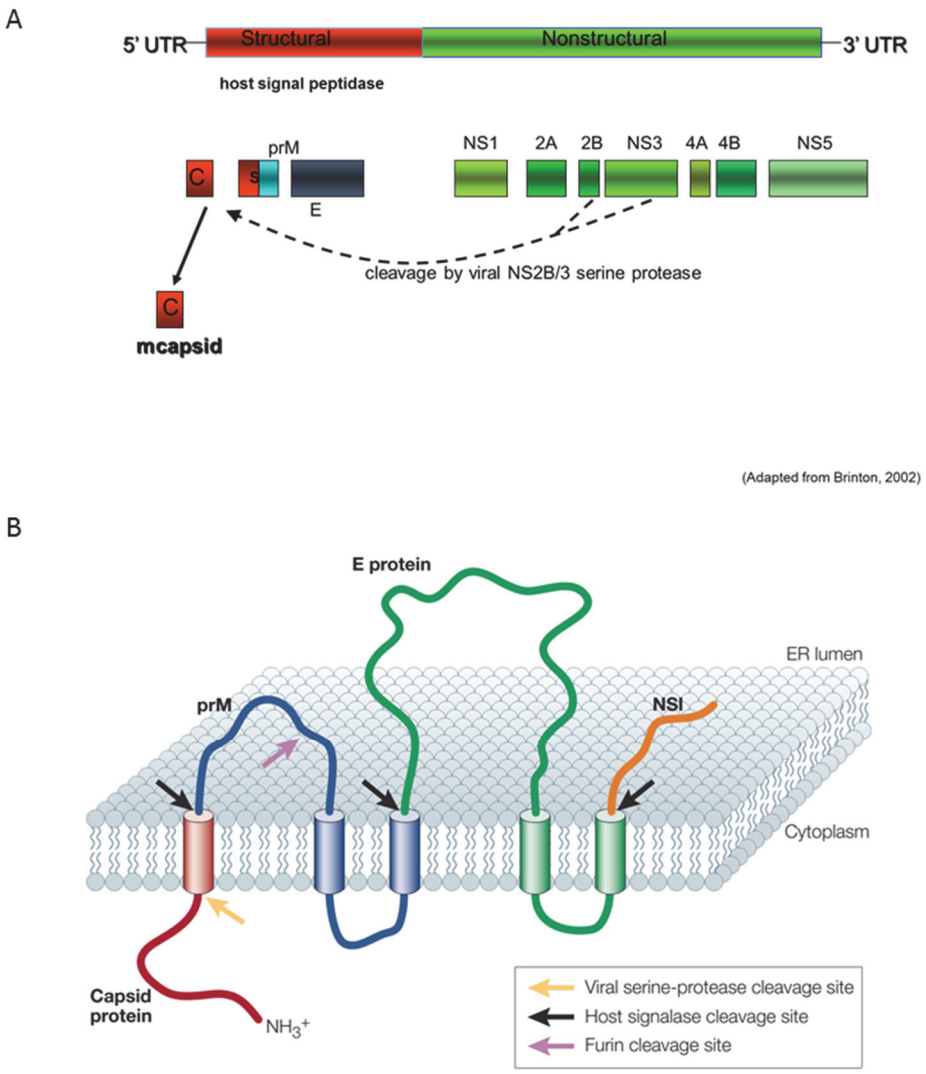

Figure 1.3. Structure and organization of the West Nile genome and polyprotein. The WNV genome is approximately 11kb and is currently thought to encode 3 structural and 7 non-structural proteins. The names and relative positions of the various final protein products is indicated in (A). Topology of the structural region of the WNV polyprotein, with protease cleavage sites indicated. Of note is the fact that capsid is the only protein which is not at least partially exposed to the lumen of the ER during proteolytic processing Adapted from Brinton, 2002 (A), and Mukhopadhyay S *et al*., 2005 (B).

methyltransferase activity of the NS5 protein, which also contains the RNA-dependent RNA polymerase. Methylation occurs at two distinct sites: the N-7 position of the terminal guanosine, and the 2'-O position of the penultimate 5' nucleotide (Dong et al., 2008). Although lack of methylation at the N-7 position does not affect translation of the viral genome, it is required for infection. In contrast, 2'-O methylation is not required for productive infection but does play a critical role in evasion of the innate immune response in mammalian cells (Zhou et al., 2007). Viruses that lack 2'-O methyltransferase activity are greatly attenuated *in vivo*, exhibiting almost no lethality in the mouse model of WNV infection (Daffis et al., 2010).

1.1.2.4 Viral protein synthesis, processing and topology

Following uncoating of the virion after entry, the viral genome is exposed to the host translation machinery in the cytoplasm. Due to the fact that the WNV genome is of positive (+) sense, an RNA-dependent RNA polymerase (RdRp) is not required to first synthesize a copy of the genome before viral protein can be produced. Cap-dependent translation leads to the production of a single polyprotein, which is co-translationally inserted into the membranes of the ER. This polyprotein is immediately processed by viral and cellular proteases to produce 3 structural (capsid, prM and E) and 7 non-structural (NS1, NS2A, NS2B, NS3, NS4A, NS4B, NS5) proteins (Figure 1.3). All cleavages which occur on the

cytoplasmic side of the endoplasmic reticulum (ER) are carried out by the viral protease (NS2B/3), while those in the ER lumen are performed by the host protease, signal peptidase (Reviewed in (Lindenbach and Rice, 2003)). With the exception of capsid, all WNV proteins are at least partially exposed to the ER lumen during their proteolytic processing and maturation (Figure 1.3). Multiple WNV proteins are subject to N-linked glycosylation, including E, prM, and NS1. Of these, glycosylation of the E and prM proteins has been most extensively studied. This post-translational modification is important for viral pathogenesis. Specifically, N-linked glycosylation of the E protein affects virus assembly and infectivity in cell culture models as well as neuroinvasion in a mouse model of infection (Hanna et al., 2005; Beasley et al., 2005). The glycosylation of prM has also been demonstrated to affect release of infectious particles in cell culture models of infection.

1.1.2.5 The West Nile Virus life cycle

WNV is maintained in an enzootic cycle in nature. In North America the virus is thought to cycle between over 40 species of mosquitos and 70 species of birds (Enserink, 2002). In birds, infection with the less pathogenic lineage 2 strains can lead to viremia for up to 100 days. However, infection by lineage 1 strains leads to significantly higher mortality among avians. In fact, the presence of many dead birds in populated areas can herald the arrival of WNV before a human outbreak.

Following the bite of an infected mosquito, WNV is thought to infect and replicate in keratinocytes, subcutaneous dendritic cells, and Langerhans cells. Entry of the virus into cells depends upon binding to an as of yet poorly defined cellular receptor (Figure 1.4). Following interaction of the viral membrane proteins with this receptor, the virion is taken up by receptor-mediated endocytosis and transported to endosomes (reviewed in (Smit et al., 2011) and (Enserink, 2002). The low-pH environment of endosomes leads not only to structural changes in the nucleocapsid, but also the envelope proteins, resulting in fusion of the virion envelope with the endosomal membrane (Gollins and Porterfield, 1986). The capsid is subsequently shed from the viral genome in a process known as uncoating. When the genome is exposed to the cytoplasm, it acts as an mRNA for translation of the viral polyprotein.

Processing of the viral polyprotein on the membranes of the ER (Section 1.1.2.4 and reviewed in (Suthar et al., 2013) gives rise to the 10 viral proteins necessary for the formation of replication complexes and assembly of new virions. The ER surface also serves is the site where viral RNA is copied to create a negative-sense genomic RNA ((-)ssRNA), which is used as a template for production of (+)ssRNA genomes by NS5, the viral RdRp. Nascent genomes are encapsidated by the capsid protein on the membranes of the ER in a poorly understood assembly process. Following encapsidation, the virion acquires a host-derived envelope by budding into the lumen of the ER. This envelope contains multiple copies of both the E and prM proteins, embedded into the

membrane. While transiting the secretory pathway, the virion is considered "immature" because the E protein exists in a fusion incompetent configuration in which its fusion peptide is blocked by the pre-peptide of M (Section 1.1.2.2). Most likely this feature evolved to prevent spurious fusion of virus particles with cellular endomembranes. Prior to secretion of virions from infected cells, a maturation event occurs in which the pre-peptide of M is cleaved, exposing the fusion peptide of the E protein. This cleavage is carried out by the cellular protease, furin, located in the Golgi apparatus (Stadler et al., 1997). The infectious mature virion is then released from the host cell via exocytosis. It is important to note that although this maturation cleavage event is an obligate part of the WNV life cycle, it is not highly efficient. Many virus particles are produced which contain immature prM, and at least one study has demonstrated that these particles are infectious (Mukherjee et al., 2011).

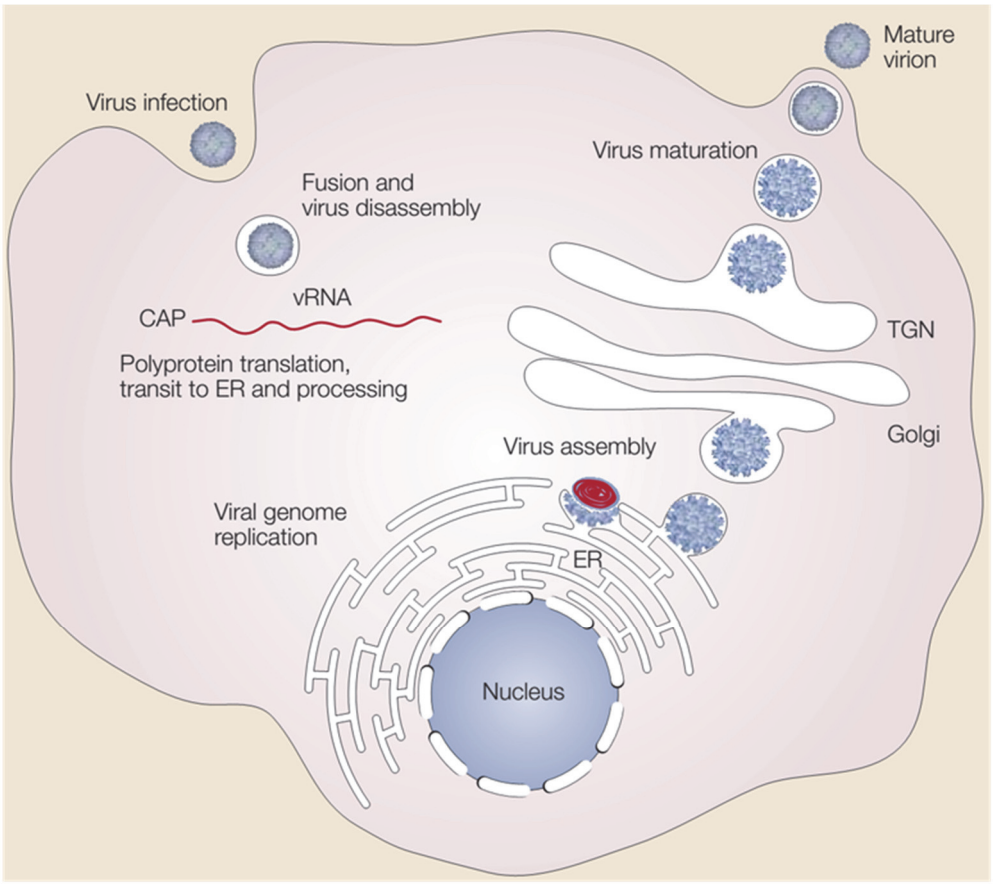

Figure 1.4. **The West Nile virus life cycle.** Incoming WNV virions bind to an as of yet poorly defined receptor and are then internalized via endocytosis. Following acidification, the viral envelope fuses with the endosomal membrane and the nucleocapsid is released into the cytoplasm where it disassembles. Subsequently, the viral RNA is able to act directly as a message to direct the synthesis of the WNV polyprotein. This leads to the production of the 3 structural and 7 non-structural proteins. The viral RNA can then be copied to (-) sense RNA so that additional copies of the (+) sense ssRNA can be produced. This occurs in association with membranes, and requires the viral RdRp (NS5), as well as other non-structural proteins. Viral nucleocapsids are then assembled on the membranes of the rough ER and then bud into the ER. The immature virions transit the secretory pathway, and undergo a maturation cleavage event at the TGN, which creates mature, infectious particles. The virions are then released from the cell via exocytosis. Adapted from Mukhopadhyay S *et al*., 2005.

1.1.3 The capsid protein: biochemistry and structure

1.1.3.1 Biochemistry: Proteolytic cleavage

The mature WNV capsid protein is 105 amino acid residues long and is produced from the polyprotein at the ER by cleavage of its C-terminus from the signal peptide of prM (Figure 1.3). The viral protease cleavage occurs C-terminal to a cluster of positively charged amino acids, directly before a small residue such as glycine or serine. This initial event is necessary for the subsequent cleavage of the prM signal peptide from prM by the host signal peptidase. The research group of Mario Lobigs conducted experiments with a C-prM precursor from Murray Valley Encephalitis Virus (MVEV). Transfected cells expressing the fusion protein could not process the signal peptide of prM. However, when microsomes prepared from these cells were treated with trypsin, the capsid protein was released, and the prM signal peptide was cleaved (Stocks and Lobigs, 1995). Additionally, Amberg and Rice examined the role of coordinated processing of C-prM in Yellow Fever virus (YFV). By employing several mutants in which residues near or at the cleavage site were converted to alanines, they also demonstrated a strict requirement for coordinated processing in the production of infectious virus (Amberg and Rice, 1999). These data strongly support a coordinated cleavage model in which the viral NS2B/3 protease must act before the host signal peptidase. Indeed, mutant MVEV strains in which the cleavages occur

independently of each other, replicate to much lower titres and have morphological defects in the nucleocapsid structure (Lobigs et al., 2010).

1.1.3.2 Capsid structure

The X-ray crystal structure of the WNV (subtype Kunjin) capsid protein was determined though crystallization in 2004 (Dokland et al., 2004). This study showed that the capsid protein is composed of four α-helical regions (α1-α4) separated by short loops, and is thought to exist as a dimer *in vivo* (Figure 5). Helices α2 and α4 in one monomer are anti-parallel to the α2 and α4 helices in the other monomer of a dimer. The surface of the capsid protein is positively charged, owing to a relatively high number of arginine and lysine residues. Most of this surface is made up of helices α1 and α4. A conserved hydrophobic region spans helices α2 and α3, and it is likely that this region is exposed on the surface of the nucleocapsid. Mutational analysis of the hydrophobic regions of helices α1 and α2 showed that infectious virus could be recovered when second-site mutations were introduced in α4. However, α3 helix mutants could not be rescued by compensating mutations in another helix (Kofler et al., 2002; Kofler et al., 2003). This suggests that dimerization is likely maintained by the α4 helix, and that the residues in the hydrophobic regions of capsid are not explicitly required for assembly of infectious virus.

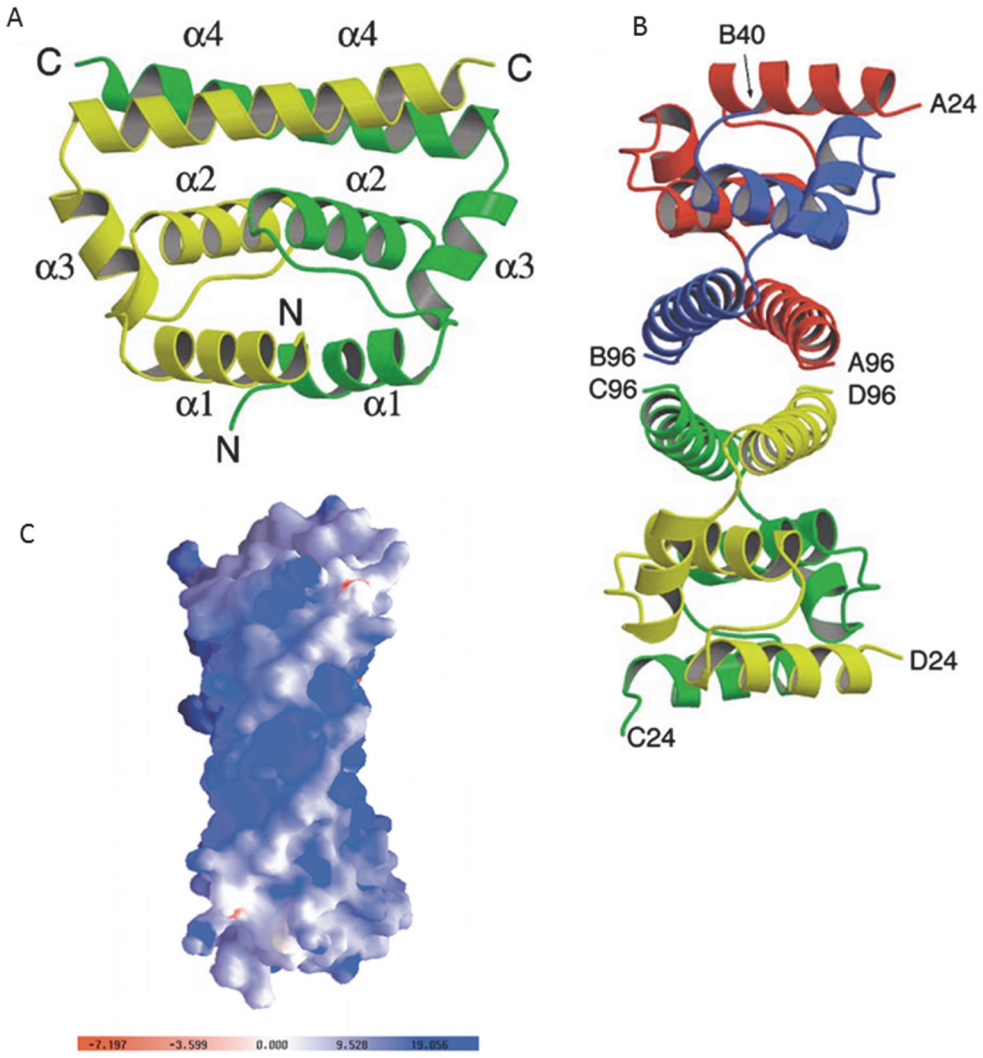

Figure 1.5. **Crystal structure of West Nile virus capsid protein.** (A) The structure of a dimer is shown, with one monomer marked as green, while the other is marked as yellow. Both the N- and C-termini are indicated, and the locations of helices α1 - α4 are also shown. In (B) the structure of a WNV tetramer, which serves as a building block for the long ribbons seen in the crystal structure itself. The view seen is down the "tunnel" created by the two dimers. In (C), an electrostatic surface potential model demonstrates the high level of positive charge present on the surface of the WNV capsid tetramer. A red color indicates a more negative charge, while blur indicates a more positive charge. Areas which are white are neutral. The view of the tetramer is the same as in (B). Adapted from Dokland *et al., 2004.*

1.1.4 Flavivirus capsid proteins and their non-structural roles

1.1.4.1 The case for non-structural roles

Virus capsid proteins, including those of flaviviruses have classically been studied in terms of their roles in nucleocapsid assembly. However, over the last 10 years or more, it has become clear that RNA virus capsid proteins have important non-structural functions (reviewed in (Urbanowski et al., 2008). As an integral and abundant part of the virion, capsid proteins are exposed to the host cell *milieu* very early during infection. Moreover, these proteins are produced in vast excess for what is required for virus assembly. As such, there are large pools of capsid available for other functions. The subcellular localization of flavivirus capsids in infected cells is also of note. Although virions are assembled on the membranes of the ER, a large pool of capsid localizes to the nuclei of host cells (Hunt et al., 2007). Given that this pool of capsid cannot directly participate in virion assembly, it seems likely that this capsid cohort interacts with host factors in the nucleus, possibly to manipulate the host cell environment in favor of virus replication.

1.1.4.2 Proteolytic processing

A growing number of publications have reported the interaction of flavivirus capsids with host cell factors, many of which affect cellular pathways relevant to viral infection. For example, Japanese enchephalitis virus (JEV) capsid

protein is a substrate of the cysteine protease cathepsin L and cleavage between residues 18 and 19 of capsid generates a truncated protein that is important for JEV pathogenesis. A mutant JEV encoding a capsid lacking this cleavage site, exhibits reduced neuroinvasion and less lethality in mice. Curiously, this mutant JEV replicates normally in Vero, PK15, and C6/36 cells but poorly in neuronal (N18) and macrophage (RAW 264.7) cells (Mori et al., 2007).

1.1.4.3 Interaction with nuclear proteins

The localization of flavivirus capsids to the nucleus, and specifically the nucleolus is a pan flavivirus phenomenon. As previously discussed, this pool of capsid is in a prime position to interact with cellular factors to influence the host environment. Indeed, recent evidence suggests that flaviviruses can manipulate the nucleolar proteome to favor replication. One such example of this is the interaction of the nucleolar protein B23 with JEV capsid protein. The nucleolar localization of JEV capsid creates a prime opportunity for it to interact with B23 in the nucleolus. Expression of JEV capsid causes translocation of nucleolar B23 into the cytoplasm of infected cells. However, when a mutant virus encoding a capsid protein that cannot bind to B23 was employed, B23 did not translocate to the cytoplasm. In addition, expression of a dominant negative form of B23 that did not bind to capsid decreased viral replication (Tsuda et al., 2006).

WNV capsid has also been reported to interact with the nuclear protein, I_2^{PP2A}, an inhibitor of protein phosphatase 2A (PP2A). GST pulldown and co-

immunoprecipitation assays were used to determine that this interaction is mediated by the C-terminal half of capsid and the N-terminal half of I_2^{PP2A} (Hunt et al., 2007). This interaction appears to have functional consequences for the host cell as expression of WNV capsid was shown to significantly decrease AP-1 transcription activity, a process that is regulated by PP2A. Indeed this phosphatase complex is a key regulator of many cellular processes, including anti-viral signaling, programmed cell death and the cell cycle. By affecting this key regulator, WNV capsid may repress the expression of anti-viral genes or inhibit one or more phosphorylation dependent reactions of the innate immune response (Hunt et al., 2007)

Further support for the importance of the nuclear pool of flavivirus capsid proteins comes from studies on the interaction of WNV capsid with the nucleolar helicase DDX56. Originally found to interact with capsid in a multi-tissue yeast two-hybrid assay, it was confirmed to bind WNV capsid in a co-immunoprecipitation assay as well. Co-localization studies indicate that capsid and DDX56 overlap extensively in the nucleolus of cells expressing WNV capsid alone. Interestingly, WNV infection leads to the dislocation and degradation of DDX56 in the cytoplasm. This is inhibited by the proteasomal inhibitor MG132, but not by leptomycin B. This suggests that although the activity of the proteasome is required, active nuclear transport via Crm1 is not. The most critical observation is that RNAi mediated depletion of DDX56 leads to a 100x drop in WNV titres (Xu et al., 2011). This is not due to a decrease in viral protein

production, but rather a defect in the assembly of infectious virions; specifically, less viral RNA is packaged into virions in cells that are depleted of DDX56. Furthermore, the helicase activity of DDX56 is necessary for the role that it plays in production of infectious virions. Infection of cells overexpressing a helicase-dead mutant DDX56 recapitulates the results of the RNAi studies, leading to a significant drop in infectious titres (Xu and Hobman, 2012). These studies suggest that although DDX56 is translocated to the cytoplasm and degraded, its presence is required during the WNV life cycle for packaging of viral RNA.

1.1.4.4 Interaction with cellular lipids and membranes

Flavivirus capsids also influence cellular lipid and membrane dynamics to create a permissive environment for the production of infectious virus. To date, most studies have focused on how DENV and Hepatitis C virus (HCV) capsids affect these critical cellular processes. The interaction of DENV capsid with lipid droplets (LD) is reportedly important for virus assembly. Imaging studies by Samsa *et al.* determined that during DENV infection, the number of LDs in infected cells was significantly increased and that capsid protein extensively colocalizes with LDs. Two hydrophobic residues (L50 and L54) in helix α2 are required for the interaction of DENV capsid with LDs. Mutation of these residues results not only a loss of association with LD, but reduced RNA replication as well as virus titres (Samsa et al., 2009). ER-derived LDs may act as a "sink" to concentrate capsid on platforms rich in viral RNA, thereby enhancing encapsidation. In support of this

hypothesis, treatment of DENV-infected cells with the fatty acid synthase inhibitor, C75, reduced the number of LDs and had a significant effect on virus replication (Koyama et al., 2008; Namatame et al., 2004; Yamazaki et al., 2009). Specifically, addition of C75 to cells infected with DENV decreased viral titers by as much 1000x, depending on the concentration used. This result underscored the importance of the interaction between capsid and LDs, and has created new avenues for further study. However, inihibition of replication due to effects of C75 on other cellular processes cannot be ruled out.

Subsequent to this discovery, nuclear magnetic resonance and atomic force microscopy based studies expanded our understanding of the ways in which DENV capsid interacts with LDs during its life cycle. A 2012 study reported that in addition to the α2 helix, the disordered N-terminus of the DENV capsid protein interacts with LDs. Specifically, a peptide composed of amino acid residues 14-23 of DENV capsid was shown to bind strongly to LDs. Additionally, this peptide inhibited binding of full-length DENV capsid to LDs in a competitive manner. It is of note that the LD-binding regions of DENV capsid are located on one side of its structure, suggesting that capsid contains an LD interaction surface. This phenomenon is not limited to DENV, as the residues involved in LD interaction are conserved among flaviviruses, including WNV (Martins et al., 2012). Among the genus *Flavivirus*, DENV and HCV are the only viruses whose capsid associates with LDs, however, it is possible that the central hydrophobic patches and the disordered N-termini of other flavivirus capsids play function similarly. Indeed,

the core protein of HCV has been reported to interact with lipid droplets (Barba et al., 1997). Although a detailed discussion of the experimental evidence is not warranted here, this interaction is important for virus replication and pathogenesis.

Alterations in metabolic pathways that affect LDs have been linked to different pathologies and as such, have been the subject of intense study of late, and their relationship to flavivirus infections is no exception. Viruses require that a number of cellular resources be made available during the replication cycle in order to promote optimal replication and infectious particle production. One critical aspect of this process is the re-arrangement and re-purposing of cellular membranes for envelopment of encapsidated genomes. Here, flavivirus capsid proteins appear to manipulate these critical events through LDs. Future *in vivo* studies can determine the usefulness of LDs as a therapeutic target, as well as identify new lipid and membrane targets in the host cell.

1.2 Programmed cell death – Apoptosis

1.2.1 Overview

The ability of cells to commit suicide evolved early in the history of eukaryotic life. In fact, this phenomenon seems to predate the evolution of metazoan life. This assertion supported by the discovery of apoptosis in yeast (reviewed in (Carmona-Gutierrez et al., 2010)). Being able to clear damaged or

infected cells is critical to the survival of an organism. The inability to carry out Programmed Cell Death (PCD) in the appropriate circumstances underlies the etiology of several diseases such as cancer. As a regular and essential process, the orderly and stepwise destruction of cells occurs in normal development and following insult and/or injury. Naturally, this includes infections with pathogens, such as viruses.

1.2.2 The apoptotic cascade

1.2.2.1 The extrinsic initiation pathway

Programmed cell death or PCD has been classified into three major types thus far (for an overview, see (Fuchs and Steller, 2011). Type I PCD, also known as apoptotic cell death, is activated via two distinct classes of initiator pathways (Figure 6 and reviewed in (Spencer and Sorger, 2011)). Type II PCD or autophagic cell death is characterized by the consumption of cellular organelles by large vacuoles. Type III PCD is the most recently described form, and occurs in a caspase-independent manner. This mode of programmed cell death is still poorly understood. The extrinsic pathway is triggered through activation of extracellular death receptors of the Tumor Necrosis Factor Receptor (TNFR) superfamily, which bind specific ligands. This family of receptors includes TNFR, Fas and TRAIL. Upon activation of these receptors, initiator caspases such as caspase-8 and caspase-10 are recruited to the intracellular portion of the death receptor, where they

become activated. This occurs through the formation of protein complexes containing the inactive “pro” form of the initiator caspase. Critical to the formation of such complexes are the Fas-Associated Death Domain (FADD) and TNF Receptor-Associated Death Domain (TRADD) proteins. These proteins act as adaptors that bridge death receptors and caspases. Complex formation involves homotypic interactions between the Death Domains (DD) in these adaptors and those present in caspases. The complex of receptor, adaptor and caspase is typically referred to as the Death-Induced Signaling Complex (DISC). It is important to note that several other proteins may be recruited to DISC, including those that perform regulatory roles.

Following formation of DISC, the initiator caspase undergoes autocatalytic cleavage to produce the activated, shorter form of the caspase. This then leads to cleavage and activation of effector caspases such as caspase 3, whose protease activity directly acts on cellular substrates that are critical for the integrity of the cells. Breakdown of these structural components leads to the hallmarks of apoptotic cell death including nuclear DNA fragmentation, destruction of cytoskeletal networks, blebbing and packing of cellular contents into small membrane bound vesicles known as apoptotic bodies.

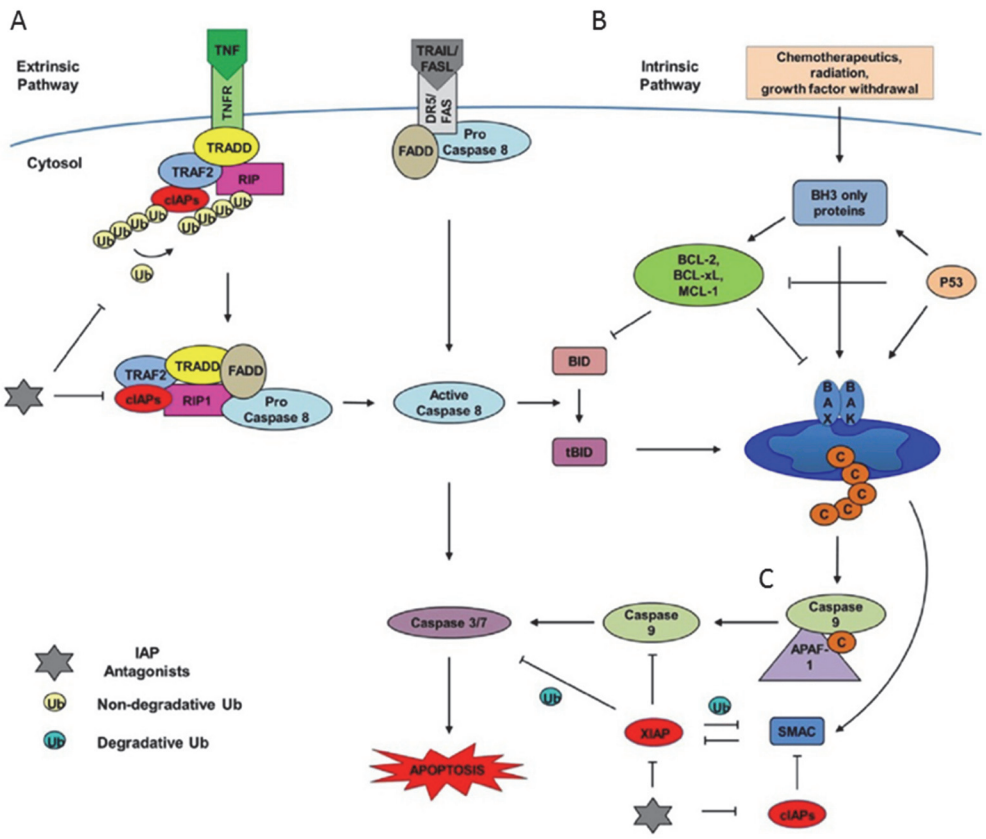

Figure 1.6. **Major components of the extrinsic and intrinsic apoptosis pathways.** The important events in both the extrinsic (A) and intrinsic (B) initiation pathways are indicated. (A) Upon binding of an appropriate ligand, adapter proteins such as TRADD and FADD are recruited to the intracellular domains of death receptor proteins. These adapters then facilitate the binding of accessory proteins such as TRAF2, cIAPS, or RIPK1, but most notably caspase-8. This caspase is then autocatalytically activated via cleavage, and can then activate executioner caspases 3 and 7, which go on to directly cleave cellular substrates. Additionally, caspase-8 can produce t-BID via direct cleavage of BID, which transits to mitochondria to effect cytochrome c release. (B) Intrinsic activation occurs following a cellular stress such as radiation or prolonged growth factor withdrawal. Through a variety of sensors such as pro-apoptotic BH3 only proteins and p53, Bax and Bak become activated, and via pore formation stimulate the release of cytochrome c from the mitochondria. This subsequently leads to the formation of the apoptosome (C), activation of caspases-3 and -7, and apoptosis. Note that various pro-survival inhibitor proteins can act at many steps of the process to block activation. Adapted from Apoptosis Xu *et al.,* 2013

1.2.2.2 Death receptor-mediated apoptosis: Fas and TNFR

As described above, extrinsic apoptosis can be triggered through the activation of death receptors at the cell surface. These receptors bind death ligands, which can be soluble, or membrane-bound. The ligation of these receptors sets in motion the recruitment of caspase-8 (and accessory factors) to the intracellular domains of the death receptors. This leads to the formation of DISC and initiation of the apoptotic cascade (section 1.2.1.1).

The Fas receptor or CD95 consists of an intracellular domain, a transmembrane domain, and an extracellular domain (Lavrik and Krammer, 2012). It belongs to the TNFR superfamily, a class of trimeric extracellular receptors (reviewed in (Cabal-Hierro and Lazo, 2012). Upon activation of CD95, the Fas receptors oligomerize. This receptor complex is then internalized via endocytosis, allowing the subsequent interaction of FADD with the DD of Fas. DISC is then formed, leading to cleavage and activation of caspase-8.

The Fas receptor binds a trimeric ligand, known as FasL (CD95L). This ligand is expressed on the cell surface and may act in an autocrine or paracrine fashion. For example, the interaction of Fas/FasL has important roles in the homeostasis of an organism. The activation of cytotoxic T-lymphocytes stimulates the expression of CD95, the effects of which T-cells show resistance to early during activation. However, the longer these cells are activated, the more sensitive they become to apoptosis induced by autocrine Fas activation (Aguirre et al., 2013; Brenner et al., 2008; Zhang et al., 2004). This mechanism is necessary for

preventing an unbridled cytotoxic T-cell response from damaging the host during responses to foreign antigens. Moreover, the cytotoxic T-cell response against some target cells is mediated by paracrine Fas/FasL ligation. Finally, a collection of 3131 tumor samples examined by the Broad Institute showed significant levels of CD95 deletions (Beroukhim et al., 2010). This study and others suggest that Fas is a tumor suppressor which is critical to the elimination of cancerous cells in humans.

Other TNFR family members play key roles in cellular homeostasis too. Similar to Fas, the TNF receptor is expressed on the surface of many different cell types. Several isoforms of TNFR are known, but *TNFR1α* and *TNFR1b* are the most extensively studied (reviewed in (Cabal-Hierro and Lazo, 2012)). TNFα differs from FasL in that in addition to being produced as a plasma membrane anchored form, it also exists as a soluble cytokine, which is produced by cleavage of a hydrophobic region that acts as a membrane tether. It is important to note that both the membrane bound form (TNF) and the soluble form (sTNF) are biologically active trimers. However, their exact functions *in vivo* remain controversial (Waters et al., 2013).

TNFα has several important roles, including the regulation of immune effector cells and the induction of inflammatory responses. Typically produced by monocytes, this cytokine is capable of inducing pyrexis, as well as inhibiting viral replication and tumorigenesis. Of critical importance is the fact that TNFα can induce apoptosis in many cell types. It is not surprising that disruptions in the

normal production of and response to TNFα are linked to the etiology of many diseases (Bluml et al., 2012; Cantarini et al., 2012; Methner and Zipp, 2013; Speeckaert et al., 2012).

The induction of apoptosis via TNFα occurs in a manner which is very similar to that induced by FasL. Upon ligand binding, receptor oligomerization leads to endocytosis of the receptor complex. Following internalization, the DD of the TNFR binds to the DD of TRADD, an adaptor that functions similarly to FADD. TRADD can also interact with other TNFR family members including Fas. The activation of caspase-8 occurs following the formation of DISC, and the apoptotic cascade is activated.

1.2.2.3 The intrinsic initiation pathway

Apoptosis can be triggered intracellularly through what is known as the intrinsic pathway. The chief players in this mechanism are mitochondria, the key energy producers of the cell (reviewed in (Galluzzi et al., 2012; Galluzzi et al., 2012). The triggers for this apoptotic mechanism are numerous, and include DNA damage, oxidative damage, and ER stress. Infection with pathogens can also trigger apoptosis intrinsically, through the aforementioned stresses, or via recognition of foreign molecular patterns such as dsRNA by Toll-like receptor 3 (TLR3) (Daffis et al., 2008; Kong et al., 2008; Vercammen et al., 2008; Wang et al., 2004). These stimuli lead to the activation of Bax, which is mediated by BH3 only Bcl-2 family members such as BIM, or PUMA. In addition to these BH3 only

sensors, the transcription factor p53 can directly activate Bax and/or Bak. Moreover, p53 can transactivate Bax transcription in response to cellular stresses such as DNA damage. Bax activation manifests as oligomerization at the mitochondria, leading to the release of apoptogenic proteins such as cytochrome *c*, and endonuclease G. Ultimately, this stimulates the formation of a multimeric complex composed of Apaf-1 and cytochrome *c*, which is known as the apoptosome (Figure 6 and (Fiandalo and Kyprianou, 2012)). It is at this point that the intrinsic and extrinsic pathways intersect, as the apoptosome activates caspase-3, which then goes on to cleave target structural components and other vital cellular substrates.

1.2.3 Regulation of apoptosis: The PI3k/PTEN/Akt/mTOR pathway

1.2.3.1 Controlling cell death

Given the significant consequences of activating a cell death pathway, it is imperative that regulatory mechanisms exist to prevent an inappropriate response. An overly sensitive apoptotic response may mean that healthy cells are killed too frequently, while cells that are refractory to apoptosis may allow a pathological condition to develop unchecked. Thus, both survival and apoptotic signaling pathways must exist, and the fate of the cell is ultimately determined by the balance of pro-death and survival signaling.

1.2.3.2 PI3K and PTEN

Signaling through the PI3K/PTEN/Akt/mTOR pathway is a key anti-apoptotic mechanism. This group of enzymes regulates multiple cellular processes including of mRNA translation, metabolism, cell cycle progression and cell survival (reviewed in (Markman et al., 2013; Slomovitz and Coleman, 2012; Song et al., 2012; Ciuffreda et al., 2010)). At the apex of this pathway is PI3K, a heterodimer consisting of an 85 kDa regulatory subunit and a 110 kDa catalytic subunit. This kinase complex is activated via recruitment to the intracellular domains of Receptor Tyrosine Kinases, which are activated by binding of a ligand, usually a growth factor (Figure 7). Specifically, the p85 subunit of PI3K binds the phosphorylated tyrosine residues on the receptor tyrosine kinase through a Src-homology 2 (SH2) domain (For an example of this, see (Kazlauskas and Cooper, 1990). The substrates of PI3K are membrane phospholipids such as phosphatidylinositol 4-phosphate and phosphatidylinositol 4,5-bisphosphate. The transfer of phosphate from ATP to the D-3 position of the phosphoinositide moiety catalyzed by PI3K forms the second messenger lipids phosphatidylinositol 3,4-bisphosphate and phosphatidylinositol 3,4,5-triphosphate. Formation of these phospholipids leads to recruitment of kinases to the plasma membrane and subsequent downstream signaling.

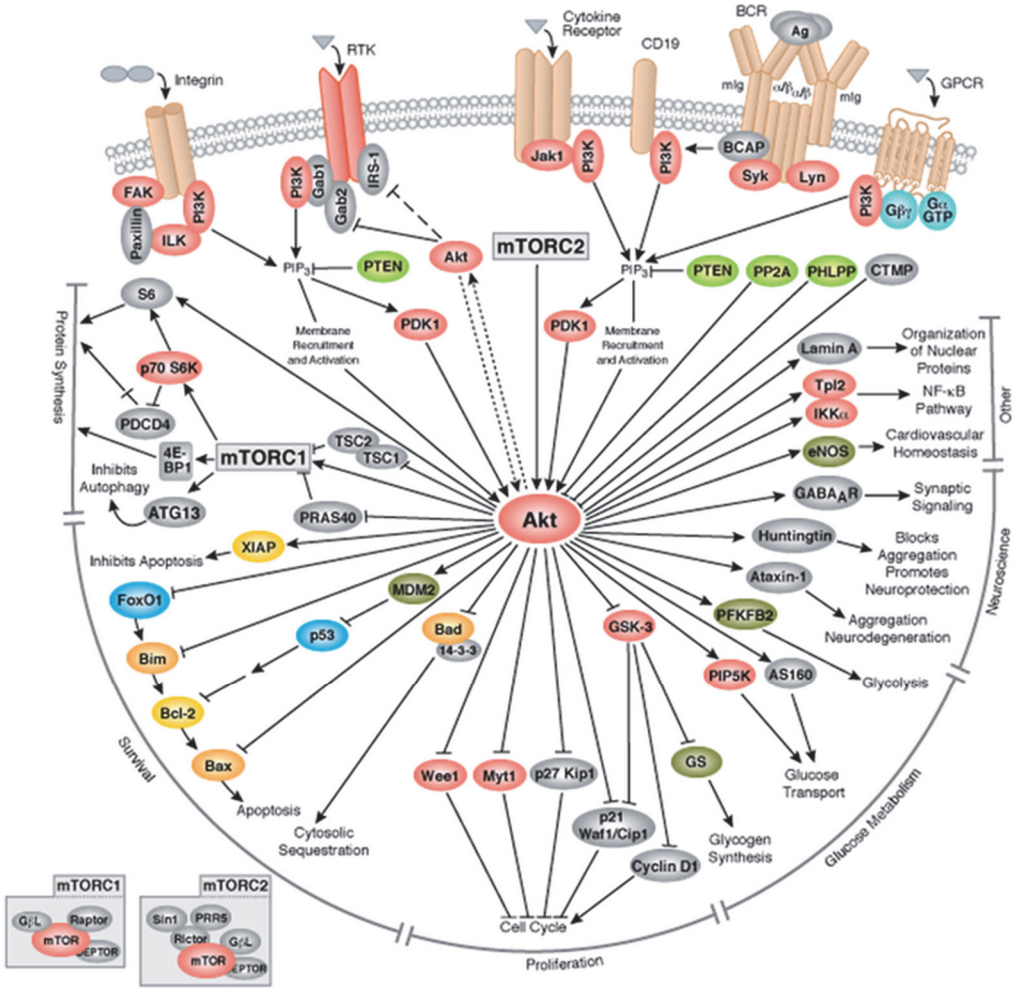

Figure 1.7. The PI3K/Akt signaling axis regulates a multitude of critical cellular processes. Diagram of the many known interactions between the kinase Akt/PKB and its substrates, showing both its centrality and importance as a regulatory factor. Substrates are arranged via known primary function and include protein synthesis, survival, proliferation, glucose metabolism, neurological and others which are not classified. Akt is stimulated via the actions of growth factor receptors, which upon ligand binding stimulate PI3K to phosphorylate PIP_3. This triggers the recruitment of Akt to the plasma membrane where it interacts with its activating kianses, PDK1 and PDK2 (mTORC2). Following sequential phosphorylation at Thr308 and Ser473 respectively, Akt is then free to move to the cytoplasm and/or nucleus to phosphorylate its substrates. Akt is subject to negative regulation by a variety of phosphatases, which serve to limit its growth and division enhancing properties. Adapted from www.cellsignal.com

Negative regulation of this process is made possible primarily through the actions of the phosphatase PTEN, which is a tumor suppressor (Song et al., 2012). As phosphoinositides such as phosphatidylinositol 3,4,5-triphosphate act to recruit kinases to the plasma membrane, dephosphorylation of these lipids reduces activation of downstream substrates. In addition, PTEN has multiple substrates including growth factor receptors, transcription factors and kinases. Although all of its substrates are not currently known, a consensus has emerged that the activity of PTEN is important for preventing aberrant survival signaling. In support of this, *PTEN* gene deletions are found in a vast majority of cancers (Slomovitz and Coleman, 2012; Song et al., 2012).

1.2.3.3 Akt: Activation

A key factor in survival signaling that PI3K recruits to the plasma membrane is the serine/threonine kinase Akt (Ahmed et al., 1993; Bellacosa et al., 1993). Following phosphorylation of the inositol lipids, Akt is recruited to the plasma membrane via its N-terminal pleckstrin homology domain. Akt is then activated via phosphorylation of two key residues: threonine 308 and serine 473. However, some evidence suggests that tyrosine phosphorylation of Akt is critical for activation, a concept which is supported by mutational studies of tyrosine residues in Akt (Chen et al., 2001). These phosphorylation events occur in a specific order, and T308 must be phosphorylated initially by Phosphoinositide-

Dependent Kinase 1 (PDK1) (Alessi et al., 1997; Alessi et al., 1998; Cohen et al., 1997; Dieterle et al., 2013; Meier and Hemmings, 1999). Full activity of Akt then depends on the transfer of phosphate to S473 by the mammalian Target of Rapamycin Complex 2 (Figure 1.7). This kinase complex is also a downstream target of Akt, which allows for mammalian Target of Rapamycin Complex 2 to play a role in regulating Akt activity. Following activation, Akt dissociates from the cell membrane and proceeds to phosphorylate both cytoplasmic and nuclear substrates.

1.2.3.4 Akt: downstream signaling events

Akt phosphorylates a large number of substrates that regulate a variety of cellular processes, including anti-apoptotic signaling (reviewed in (Carnero, 2010; Hers et al., 2011)). By phosphorylating pro-apoptotic BH3 Bcl-2 family members such as Bad and Bim, Akt blocks their pro-apoptotic function at mitochondria. Another substrate of Akt is Glycogen Synthase Kinase 3 Beta (GSK-3β), an enzyme whose activity can promote cell death. Akt can phosphorylate GSK-3β, and this inhibits its activity. This relieves repression of glycogen synthesis, and promotes cell survival (Doble and Woodgett, 2003; Woodgett, 2001). Akt also regulates pro-apoptotic genes through inactivating phosphorylation of pro-apoptotic transcription factors such as Foxo-3a, whose function is to induce expression of the pro-apoptotic genes including Fas/CD95L and Bim (Brunet et al., 1999).

Finally, Akt can act through other kinase complexes to enhance mRNA translation. The two major complexes regulated by Akt, mTORC1 and mTORC2 are thus named due to the presence of the serine/threonine kinase mammalian Target of Rapamycin (mTOR). This kinase modulates mRNA translation by phosphorylating components of the translation machinery such as $p70^{s6k}$ and eukaryotic Initiation Factor 4E Binding Protein 1 (eIF4EBP1). Phosphorylation of eIF4EBP1 releases eIF4E, which then binds the 5' UTRs of mRNAs. Together with other factors, the rate-limiting step of translation initiation is enhanced, leading to increased protein synthesis. Activation of $p70^{s6k}$ promotes phosphorylation of ribosomal protein S6, which also enhances translation (Gingras et al., 2001; Gingras et al., 2001; Malik et al., 2013; Raught and Gingras, 1999).

The PI3k/PTEN/Akt/mTOR signaling network is positioned to receive and integrate a vast number of inputs from extra and intracellular signals. This allows for important "decisions" regarding cell fate to be determined by the balance of pro-apoptotic and pro-survival signals. In support of this concept, mutations which allow PI3K signaling to proceed unchecked are strongly associated with oncogenesis, while those which ablate signaling are often lethal *in utero*.

1.3 Viral modulation of programmed cell death

1.3.1 Overview

Throughout the course of evolution eukaryotic cells have been constantly assailed by viral infections, a process which has had considerable influence on the evolution of cellular mechanisms. For example, sacrificial defense mechanisms have evolved whose function is to prevent the replication and spread of viruses within a multicellular organism. By killing virus-infected cells, the replication and spread of the virus is interrupted and the host has a greater chance of eliminating the pathogen. By balancing the threat of viral spread with the need to minimize damage to the host, infected organisms can more successfully defend against a foreign invader. This simple concept underlies the mechanism of several types of PCD, which can be triggered by viral infection. However, viruses have evolved mechanisms for evading or subverting these cellular processes to maximize fitness in a given context. This can entail both the promotion and inhibition of apoptosis. Distantly related viruses often employ similar strategies, a hallmark of convergent evolution. Here, I discuss the various strategies that DNA and RNA viruses employ to alter the course of an apoptotic response to gain advantage during infection.

1.3.2 Inhibition of apoptosis

1.3.2.1 Blockade and/or degradation of pro-apoptotic proteins: p53

A common strategy that viruses use to inhibit apoptotic programs is to block or degrade cellular proteins that promote PCD. One such example is the tumor suppressor p53. This transcription factor is a key regulator of cell cycle progression and cell fate decisions (Lee and Bernstein, 1993; Shaw et al., 1992; Yonish-Rouach et al., 1991). When activated, p53 translocates to the nucleus where it promotes transcription of pro-apoptotic genes such as *Bax* and *Bak* whose protein products act at the mitochondria (Matissek et al., 2013). Bax and/or Bak oligomerizes to form pores in the mitochondrial outer membrane. This leads to release of cytochrome c, formation of the apoptosome, and activation of executioner caspases. Death receptor signaling also impinges upon Bax and Bak but this requires cleavage of Bid to produce t-Bid, which then translocates to the mitochondria to promote the release of apoptogenic factors (Li et al., 1998; Wang et al., 1996). Alternatively, during intrinsic apoptosis, p53 can directly trigger conformational changes in Bax and Bak that leads to their oligomerization (Chipuk et al., 2004). The activity of p53 also controls expression of *Fas* and *TNFR*, allowing for direct regulation of death receptor levels (Lin et al., 2002). Given that p53 controls the expression and activation of so many potent pro-apoptotic genes, it is not surprising that many viruses have developed strategies to block its function.

Viral proteins can interfere with the function of p53 by redirecting the cellular protein degradation machinery to significantly reduce its levels. Human Papillomavirus E6 protein can form complexes with the cellular protein E6AP and

p53 to block its function (Beer-Romero et al., 1997; Talis et al., 1998) E6AP is an ubiquitin ligase that targets p53 to the proteasome for destruction (Huang et al., 1999; Thomas and Banks, 1998). Similarly, the adenovirus proteins E1B-55K and E4orf6, cooperate to recruit p53 to a multiprotein complex containing Cul5, Elongins B and C, and the RING-H2 finger protein Rbx1, an E3 ligase that promotes ubiquitination of p53 (Nayak et al., 2008; Pennella et al., 2010; Querido et al., 2001) These mechanisms prevent p53-mediated apoptosis, and together with other factors can lead to oncogenic transformation of persistently infected cells.

Finally, some viruses can block p53 function without promoting its degradation. The SV40 large-T antigen is a well characterized antagonist that sequesters p53 in inactive complexes, thus rendering it unable to transactivate transcription of pro-apoptotic genes (Carbone et al., 1997).

1.3.2.2 Viral mimicry of Bcl-2

Anti-apoptotic proteins of the Bcl-2 family are potent inhibitors of the apoptotic program. By way of example, overexpression of *Bcl-2*, *Bcl-XL* and *Bcl-w* can effectively block cell death triggered by a variety of stimuli (reviewed in (Youle and Strasser, 2008). Aberrant expression of these anti-apoptotic genes underlies the etiology of many cancers. For example, anti-apoptotic Bcl-2 family members are overexpressed in many types of malignant tumors (Oltersdorf et al., 2005). Given that these proteins are such potent antagonists of apoptosis, many viruses encode Bcl-2 family orthologues that are capable of blocking cell death.

The E1B-19K protein of adenovirus is one such example. Although this viral protein has only moderate sequence similarity to Bcl-2, it functions in a similar manner. Through direct binding, E1B-19K inhibits oligomerization of Bax and thereby blocks release of cytochrome *c* from the mitochondria. Infection of cells with E1B-19K deletion mutant viruses leads to enhanced apoptosis and greater cytopathic effects (Huang et al., 1997).

Herpesviruses also encode anti-apoptotic proteins that mimic the function of Bcl-2. In fact, all γ-herpesviruses whose genomes have been sequenced encode anti-apoptotic Bcl-2 orthologues. BHRF1 protein of Epstein Barr virus (EBV) is structurally similar to Bcl-2 family members, but lacks the ability to bind several pro-apoptotic proteins, such as Bax and PUMA (Henderson et al., 1993). However, it does interact with a limited pool of the BH3-only protein Bim to block apoptosis in primary cell lines (Desbien et al., 2009; Kvansakul et al., 2010). Another γ-herpesvirus, Kaposi's sarcoma-associated virus encodes a protein known as KSbcl-2, which blocks apoptosis as efficiently as Bcl-2 or Bcl-XL. However, KSbcl-2 does not dimerize with cellular Bcl-2 proteins. This interesting property allows it to escape the normal regulatory mechanisms imposed by interaction with Bax and Bak (Cheng et al., 1997).

Some RNA virus proteins seem to have Bcl-2-like functions. The capsid protein of Rubella virus (RV) inhibits the function of Bax (Ilkow et al., 2011). Although it doesn't prevent oligomerization of Bax, the pore-forming activity of this protein is blocked. By intercalating into Bax oligomers, RV capsid inhibits the

release of cytochrome *c* triggered by both staurosporine and anti-Fas. The RV capsid does not harbor any significant sequence similarity to Bcl-2 family proteins.

By encoding proteins which closely mimic the function of a family of highly anti-apoptotic proteins, viruses can escape destruction by both innate and adaptive immune mechanisms that trigger cell death. An unfortunate consequence of this is a greatly increased risk of tumorigenesis. Indeed, γ-herpesvirus Infections are associated with the formation of various tumors, a likely consequence of prolonged inhibition of cell death pathways (reviewed in (Speck and Virgin, 1999).

1.3.2.3 Viral activation of the PI3K/Akt signaling axis

In addition to directly blocking pro-apoptotic BH3 only proteins, viruses have evolved strategies to enhance activation of mitogenic and pro-survival signaling pathways. The PI3K/Akt signaling network is often targeted by viruses in order to promote cell survival and/or enhance cellular functions needed for viral replication.

Flaviviruses have recently come to light as important agonists of this signaling pathway (Das et al., 2010; Lee et al., 2005; Scherbik and Brinton, 2010; Yang et al., 2012). Activating phosphorylation of Akt on serine-473 increases sharply early after flavivirus infection. Typically, the increase in phospho-Akt levels can be detected within 30 minutes of infection, and can last up to 24 hours, an effect that varies with the particular flavivirus and with the cell line employed.

With respect to WNV, infection of MEF cells results in phosphorylation of Akt at serine-473 within 2 hours. Levels of phospho-Akt remain high for at least 24 hours, after which time they decline. Treatment of cells with the PI3-K inhibitor LY294002 blocked phosphorylation of Akt and earlier activation of caspase-3 was observed in infected cells. This was also accompanied by lower virus titres. The enhanced phosphorylation of Akt was shown to be dependent on calcium, as treatment with the calcium ionophore BAPTA-AM severely diminished Akt activation. In this context, Akt activation by WNV appears to prevent early cell death during infection, allowing time for RNA replication and virus particle formation. Similar results have been reported for DENV and JEV indicating that activation of Akt signaling is a common feature of flavivirus infection in mammalian cells at least.

Akt phosphorylation induced by flavivirus infection may do more than just promote survival. Similar to WNV, DENV and JEV, PI3K/Akt signaling is likely important during early phases of HCV infection. However, evidence suggests that pathway is important for development of a chronic infection. Interestingly, when antibodies against HCV receptors caludin-1 and CD81 were used to block HCV entry, Akt activation still occurred (Liu et al., 2012). This suggests that engagement of these receptors is responsible for the effects seen. Blockade of Akt activity through pre-treatment with the inhibitor Akt-V inhibited HCV replication, while treatment post-infection did not. These data suggest that HCV employs activation of Akt for multiple purposes, including virus entry and cell survival. The specific

spatial and temporal aspects of how PI3K/Akt activation acts at each stage of the viral life cycle is not yet clear.

1.3.3 Viral promotion of apoptosis

1.3.3.1 Early cell killing

Although many viruses employ strategies to reduce PCD, some have adapted to actually promote cell death as a means of maximizing fitness. In some cases, it may be more advantageous for a virus to escape the selective pressure of the immune system by rupturing cells early to promote release of infectious virus. Generally, these types of viruses tend to replicate faster than those that block cell death pathways.

1.3.3.2 Direct induction of apoptosis in infected cells: Bax and Bak

As viruses are obligate intracellular parasites, host cells have evolved mechanisms to detect the presence of specific intracellular molecular patterns. Various signaling pathways are activated in order to shut down viral replication or kill the host cell before the virus can escape and spread. A number of viruses have adapted to enhance the apoptotic cascade and thus maximize their replication and spread.

One such example is Sindbis Virus (SV), an alphavirus which has been studied with much interest as an oncolytic therapy due to its ability to kill infected

cells rapidly (Granot et al., 2011; Huang et al., 2012; Quetglas et al., 2010). Upon initiating an infection, SV triggers activation of Protein Kinase R (PKR) (Gorchakov et al., 2004). This kinase, which is activated when it binds dsRNA, phosphorylates multiple cellular substrates that inhibit translation and trigger cell death. The major target of PKR is eIF2a, a component of the cellular translation initiation machinery. When phosphorylated, eIF2a inhibits translation at the initiation step. This leads to accumulation of translational stress signals, and the eventual induction of apoptosis (Srivastava et al., 1998). In addition to translational stress, the action of BH3 only Bcl-2 family member Bad is required. Bad can act in a pro- or anti-apoptotic depending on its phosphorylation state, a process that is regulated by Jun Kinase (JNK). Non-phosphorylated Bad forms heterodimers with Bcl-2 and Bcl-xL and prevents them from blocking the pro-apoptotic activity of Bax and Bak, thus allowing apoptosis to proceed (Moriishi et al., 2002). Upon phosphorylation, Bad is sequestered by 14-3-3 proteins, and thus Bcl-2 and Bcl-xL are able to inhibit Bax and Bak. Another Bcl-2 family member known as Mcl-1 can also inhibit Bak activation. During infection with SV, translational arrest reduces the expression of Mcl-1. In combination with phosphorylation of Bad, apoptosis is triggered via Bak (Moriishi et al., 2002; Venticinque and Meruelo, 2010).

Another virus that triggers rapid apoptosis through Bak is the negative strand RNA virus, Vesicular Stomatitis Virus (VSV). Due in part to inhibition of host gene expression by VSV M protein, intrinsic apoptosis is triggered rapidly by VSV infection (Balachandran et al., 2000; Clinton et al., 1978; Koyama, 1995). VSV

infection also promotes degradation of Mcl-1, which together with Bcl-xL blocks the pro-apoptotic action of Bak. Indeed, Bak plays a significant role in VSV-induced apoptosis. Whereas RNAi-mediated suppression of *Bax* has little effect on VSV-induced apoptosis, loss of *Bak* expression greatly reduces activation of caspase-3 and subsequent apoptosis (Pearce and Lyles, 2009; Schache et al., 2009). Interestingly, death receptor-mediated apoptosis is suppressed during VSV infection. Understanding how viruses manipulate apoptotic signaling has implications for cancer therapy. Some VSV strains with mutations in the M gene do not block expression of pro-apoptotic genes (that are suppressed by wild type VSV). These VSV mutants cause even more rapid apoptosis via Fas-, PKR-, and Daxx-dependent pathways (Gaddy and Lyles, 2007). By controlling the progression of apoptosis, VSV is able to maximize the benefits of cell death and virus release.

1.3.3.3 Bystander apoptosis: induction of extrinsic pathways

While virus-infected cells can undergo apoptosis directly, in many cases, they can also induce the death of uninfected "bystander" cells. This has the effect of suppressing various aspects of the immune system, or breaking down barriers that normally prevent viruses from spreading between compartments.

Ebola virus (EBOV) infection triggers extensive death in many different cell types during human infection (Ray et al., 2004). In particular, lymphoctyes appear to be targets of bystander apoptosis during EBOV infection. Studies suggest that

both extrinsic and intrinsic pathways are triggered in lymphocytes during EBOV infection (Bradfute et al., 2010). Mice that are $FADD^{-/-}$ or Bcl-2 overexpressors demonstrate significantly reduced levels of lymphocyte apoptosis during EBOV infection. Although these mice demonstrate greatly reduced levels of lymphocyte apoptosis, they do not demonstrate enhanced levels of survival during EBOV infection (Bradfute et al., 2010). Currently, it is unclear whether this is due to particular differences between mouse and human physiology, or if the massive loss of lymphocytes due to bystander apoptosis is truly unimportant for disease outcome (Wolf et al., 2011). Further studies will determine in more detail how EBOV affects cell fate through both direct and indirect mechanisms.

Flavivirus infections have also been reported to induce death of uninfected cells, a phenomenon that may contribute to the progression of disease in human infections. In cases of severe WNV disease, death of neurons in the CNS is observed, together with meningoencephalitis and flaccid paralysis. The virus is thought to enter the CNS via breakdown of the blood-brain barrier (BBB), which normally excludes pathogens from transiting the circulation to the CNS (Bradbury, 2005; Diamond and Klein, 2004; Paterson, 2005; Solomon and Vaughn, 2002). Although death of infected neurons has been observed, studies have also demonstrated that infection of neurons is inefficient and many uninfected neurons die as well (Darman et al., 2004). In addition to triggering inflammation, studies on human clinical samples and with hamster models have demonstrated reduced levels of the primary excitatory amino acid transporter (EAAT) in spinal

grey matter. This neuronal and neuroglial receptor maintains levels of extracellular glutamate via reuptake. Suppression of EAAT leads to a reduction of uptake and higher levels of glutamate, which mediates excitotoxicity and neuronal apoptosis. Strikingly, regions of the CNS with reduced EAAT expression contained very few infected neurons. This may indicate that in severe cases of WNV disease, neuronal death in the CNS is mediated through bystander effects due to glutamate toxicity, as well as inflammation (Blakely et al., 2009). A more thorough understanding of these mechanisms and the means by which WNV infection causes CNS damage will lead to the development of better neuroprotective therapies.

Bystander cell death is a common phenomenon in many different types of viral infection and is commonly associated with pathological effects that viruses have in their host organisms. This can be mediated by a broad range of stimuli including cytokines, membrane bound ligands, and neurotransmitters.

1.4 Objectives

WNV has emerged as an important arboviral pathogen in North America. Globally, it has had significant impact on countries in which it has become endemic. At the outset of this study, multiple publications reported that WNV capsid protein is a pro-apoptotic protein. However, given that capsid is the first protein made in WNV infected cells, it is difficult to understand how this is beneficial for a relatively slowly replicating virus. Moreover, many studies indicate

that WNV causes little cytopathic effect in most cells types. In contrast, recent evidence suggests that WNV and other flaviviruses actually activate survival signaling early in infection. The objective of my thesis research was to characterize the effects that WNV and other flavivirus capsids have on cell survival. I hypothesize that WNV capsid is actually an anti-apoptotic protein, capable of delaying the onset of apoptotic cell death during WNV infection. The results described in chapter 3 provide evidence that WNV capsid protein is not a pro-apoptotic protein, but rather, its expression significantly reduces the amount of apoptotic cell death during anti-Fas challenge. This effect is dependent on PI3K, and is the first report to demonstrate the anti-apoptotic properties of WNV capsid. These results led me to hypothesize that other flavivirus capsids possess such protective effects as well. In chapter 4, I describe the ability of other flavivirus capsids to inhibit the activation of caspases during anti-Fas challenge. I also examine the response of capsid expressing cells to another apoptotic agonist, TNFα. Depending upon the virus capsid and apoptotic agonist, a range of protective effects were observed.

Chapter 2

Materials and Methods

2.1 Materials

2.1.1 Reagents

Reagents listed below were used according to manufacturer's instructions, unless specifically stated.

Table 2.1 Commercially prepared reagents

Reagent	***Source***
40% acrylamide	Bio-Rad
Agar	Sigma-Aldrich
Agarose, Ultrapure	Invitrogen
Alamar Blue (resazurin salt)	Sigma-Aldrich
Ammonium persulfate	Invitrogen
Ampicillin	Sigma-Aldrich
Bacto-tryptone	Becton, Dickinson & Company
Bacto-yeast extract	Becton Dickinson & Company
Bovine serum albumin (BSA)	Sigma-Aldrich
Bromophenol Blue	Sigma-Aldrich
Chloroform	Sigma-Aldrich
Complete^{TM} EDTA-free protease inhibitor	Roche
Diatomaceous earth	Sigma-Aldrich
Dimethyl sulfoxide (DMSO)	Sigma-Aldrich
Disodium hydrogen orthophosphate	Thermo Fisher-Scientific
Dithiothreitol (DTT)	Sigma-Aldrich
Dulbecco's modified Eagle's medium (DMEM)	Invitrogen
Ethidium bromide solution	Sigma-Aldrich
Ethanol	Commercial Alcohols

Table 2.1 (Continued)

Reagent	***Source***
Ethylenediaminetetraacetic acid (EDTA)	EMD Chemicals
Fetal Bovine Serum	Invitrogen
Glycine	Calbiochem
4-(2-hydroxymethyl)-1-piperazineethanesulphonic acid (HEPES)	Thermo Fisher Scientific
Hydrochloric acid	Thermo Fisher Scientific
Kanamycin	Sigma-Aldrich
Lipofectamine 2000	Invitrogen
Magnesium chloride hexahydrate	EMD chemicals
Methanol	Thermo Fisher Scientific
2-Mercaptoethanol	Thermo Fisher Scientific
N,N,N',N'-tetramethylenediamine (TEMED)	Sigma-Aldrich
Nonidet P-40 (NP-40)	Sigma-Aldrich
OptiMEM	Invitrogen
Paraformaldehyde	Thermo Fisher Scientific
Pencillin-streptomycin solution (100x)	Invitrogen
Phenol, buffer-saturated	Sigma-Aldrich
Phenol:Chloroform:Isoamyl Alcohol	Sigma-Aldrich
Polybrene	Sigma-Aldrich
Potassium Acetate	Anachemia
Potassium chloride	Becton, Dickinson & Company
Potassium hydroxide	Becton, Dickinson & Company
Prolong Gold with DAPI	Invitrogen
2-propanol	Thermo Fisher Scientific
Skim Milk Powder	Carnation

Table 2.1 (Continued)

Reagent	***Source***
Sodium chloride	Thermo Fisher Scientific
Sodium dodecyl sulfate (SDS)	Bio-Rad
Sodium hydroxide	Acros Organics
TransIT-LT1	Mirus Bio
Tris base	EMD Chemicals
Triton X-100	EMD Chemicals
0.25% Trypsin-EDTA	Invitrogen
Tween-20	Thermo Fisher Scientific
Ultrapure distilled water	Invitrogen

Table 2.2 Molecular size standards

Standard	***Source***
GeneRuler 1 kb DNA Ladder Plus (SM1333)	Fermentas
PageRuler Pre-stained Protein Ladder	Fermentas

Table 2.3 DNA/RNA modifying enzymes, buffers

Enzyme	***Source***
Antarctic Phosphatase	New England Biolabs
Benzonase	Novagen
DNase I, amplification grade	Invitrogen
Restriction endonucleases	Invitrogen
RNase A	New England Biolabs
RNase H	New England Biolabs
T4 DNA ligase	Invitrogen

Table 2.4 Detection systems

System	*Source*
FluorChem FC	Alpha Innotec Corp.
FluorChem Q	Cell BioSciences
Hamamatsu EMCCD Camera (C9100-13)	
ImageJ analysis software	National Institutes of Health
Immobilon-FL PVDF membrane	Millipore
IX-81 motorised microscope base	Olympus
Moxi-Z Cell Counter	Orflo
MX3005P	Stratagene
Odyssey Infrared Imaging System	LiCor
Volocity acquisition and analysis software	Perkin-Elmer
Yokagawa CSU X1 spinning disk confocal scan-head	Yokagawa
Supersignal WestPico chemiluminescent substrate	Thermo Scientific
Ultraviolet transilluminator	Thermo Fisher Scientific

Table 2.5 Multi-component systems

System	*Source*
Expand High Fidelity PCR System	Roche
PerfeCTa SYBR Green SuperMix, UNG, Low Rox	Quanta Biosciences
QIAEX II gel extraction kit	Invitrogen
QIAGEN plasmid maxi kit	QIAGEN
QIAprep spin miniprep kit	QIAGEN
QIAquick PCR purification kit	QIAGEN
Total RNA Isolation Mini kit	Agilent

2.1.2 Commonly used buffers

The buffers listed in the following table were used in various parts of this work. Their composition is detailed below.

Table 2.6 Buffers and solutions

Name	***Composition***
5x protein sample buffer	62.5 mM Tris-Hcl (pH 6.8), 50% (v/v) glycerol, 2% (w/v) SDS, 0.01% (w/v) bromophenol blue, 5% (v/v) 2-Mercaptoethanol
6x DNA gel loading buffer	40% (w/v) sucrose, 0.25% (w/v) bromophenol blue, 0.25% (w/v) xylene cyanol FF
Alkaline lysis buffer	200 mM NaOH, 1% (w/v) SDS
Bacteria resuspension buffer	50 mM tris-HCl (pH 8.0), 10 mM EDTA, 100 µg/mL RNase A
Dialysis Buffer	10mM Hepes pH 7.9, 0.1mM EDTA, 0.1mM DTT, 0.1M potassium acetate, 10% glycerol
Diatomaceous earth	100 mg/mL diatomaceous earth, 6 M guanidine-HCl, 20 mM EDTA, 50 mM Tris-HCl (pH 8.0)
Diatomaceous earth wash buffer	50% (v/v) isopropanol, 200 mM NaCl, 5 mM EDTA, 20 mM Tris-HCl (pH 7.5)
IPP Buffer	10mM Hepes pH 8, 100mM NaCl, 0.1% Triton, 10% glycerol
LB growth media	1% (w/v) Bacto-tryptone, 0.5% (w/v) Bacto-yeast extract, 0.5% (w/v) NaCl, 0.1% (v/v) 1M NaOH
Neutralization buffer	3.0 M Potassium acetate (pH 5.5)
Phosphate-buffered saline (PBS)	137 mM NaCl, 2.7 mM KCl, 8mM Na2HPO4 (pH 7.4)
PBS-T	137 mM NaCl, 2.7 mM KCl, 8mM Na2HPO4 (pH 7.4), 0.05% Tween-20

Table 2.6 (Continued)

Name	***Composition***
Rinsing buffer	50mM ammonium bicarbonate, 125mM NaCl (pH 8)
SDS-PAGE running buffer (Tris-Glycine)	192 mM glycine, 0.1% (w/v) SDS, 25 mM Tris base (pH 8.3)
SDS-PAGE running buffer (Tris-HEPES)	100 mM HEPES, 0.1% (w/v) SDS, 100 mM Tris bas (pH 8.0)
TAE	40 mM Tris-Acetate, 1mM EDTA (pH 8.0)
TpA	10mM Hepes pH 7.9, 1.5mM $MgCl_2$, 10mM KCl
TpB	50mM Hepes pH 7.9, 1.5mM MgCl2, 0.5mM DTT, 1.26M Potassium Acetate, make to 25ml with H2O and add 75mL glycerol
Tris-buffered saline (TBS)	137 mM NaCl, 2.7 mM KCl, 24 mM Tris-HCl (pH 7.4)
TBS-T	137 mM NaCl, 2.7 mM KCl, 24 mM Tris-HCl (pH 7.4)
Western blot transfer buffer	200 mM glycine, 25mM Tris base (pH 8.3), 20% (v/v) methanol, 0.1% (w/v) SDS

2.1.3 Oligonucleotides

Table 2.7 Oligonucleotides

Name	***Restriction Sites***	***Sequence***	***Usage (Section)***
AcGFP-Fwd	NheI	5’-GATCGCTAGCATGGTGAGCAAGGGCGCCGA	2.2.2.3
AcGFP-Rev	SacII	5’-GTACCCGCGGTCACGTACAGCTCATCCA	2.2.2.3

Table 2.7 (Continued)

Name	***Restriction Sites***	***Sequence***	***Usage (Section)***
DENV-Cap-myc-Fwd	SpeI	5’-TAGCACTAGTGCCACCATGGAACAAAAACTCATCTCAGAAGAGGATCTGAATGACCAACGGAAAAAGGC	2.2.2.6
DENV-Cap-Rev	XhoI	5’-GTACCTCGAGTTATCTGCGTCTCCTATTCAAGA	2.2.2.6
JEV-Cap-myc-Fwd	BamHI	5’-TGACGGATCCGCCACCATGGAACAAAAACTCATCTCAGAAGAGGATCTGATGACTAAAAAACCAGGAGGGC	2.2.2.6
JEV-Cap-Rev	XhoI	5’-GTACCTCGAGTTATCTTTTGTTTTGCTTTCTGCC	2.2.2.6
MCS (+)	SpeI, BamHI, MluI, SalI, ClaI and XhoI	5’-GTACACTAGTACTGGATCCACTACGCGTATAGTCGACAAGATCGATATACTCGAGCATG	2.2.2.2
MCS (-)	SpeI, BamHI, MluI, SalI, ClaI and XhoI	5’-CATGCTCGAGTATATCGATCTTGTCGACTATACGCGTAGTGGATCCAGTACTAGTGTAC	2.2.2.2

Table 2.7 (Continued)

Name	***Restriction Sites***	***Sequence***	***Usage (Section)***
MVEV-Cap-myc-Fwd	BamHI	5’-TAGCGGATCCGCCACCATGGAACAAAAACTCATCTCAGAAGAGGTCTGATGTCTAAAAAACCAGGAGGAC	2.2.2.6
MVEV-Cap-Rev	XhoI	5’-GTACCTCGAGTTATCTTTTCTTTTGTTTTTTGCC	2.2.2.6
SLEV-Cap-myc-Fwd	SpeI	5’-TAGCACTAGTGCCACCATGGAACAAAAACTCATCTCAGAAGAGGATCTGTCTAAAAAACCAGGAAAACC	2.2.2.6
SLEV-Cap-Rev	XhoI	5’-GTACCTCGAGTTATCCTTCTTGCTTGGCCGCCGGT	2.2.2.6
WNV-Cap-Fwd1	SpeI	5’-GTACACTAGTGCCACCATGTCTAAGAAACCAGGAGG	2.2.2.4
WNV-Cap-Fwd2	EcoRI	5’-GATCGAATTCGCCACCATGTCTAAGAAACCAGGAGG	2.2.2.1
WNV-Cap-myc-Fwd	SpeI	5’-TAGCACTAGTGCCACCATGGAACAAAAACTCATCTCAGAAGAGGATCTGTCTAAGAAACCAGGAGGGCC	2.2.2.6

WNV-Cap-Rev1	XhoI	5’-GATCCTCGAGTTATCTTTTCTTTTGTTTTGAGC	2.2.2.4, 2.2.2.6
WNV-Cap-Rev2	BamHI	5’-GTACGGATCCTTATGCTCCTACGCTGGCGATCAGGCC	2.2.2.1
YFV-Cap-myc-Fwd	SpeI	5’-TAGCACTAGTGCCACCATGGAACAAAAACTCATCTCAGAAGAGGATCTGTCTGGTCGTAAAGCTCAGGG	2.2.2.6
YFV-Cap-Rev	XhoI	5’-GTACCTCGAGTTATTAACGGCGTTTCCTTGAGG	2.2.2.6

2.1.4 Plasmid Vectors

Table 2.8 Plasmid vectors

Plasmid	***Source***
pCMV-VSV.G	Charles Rice (Rockefeller University)
pCMVNY99	Vladimir Yamshchikov (Southern Research Institute)
pGag-Pol	Charles Rice (Rockefeller University)

Table 2.8 (Continued)

Plasmid	***Source***
pIDT-SMART	IDT
pIRES2-AcGFP1	Clontech
pIRES2-AcGFP1-WNV Capsid	Constructed in this study
pTRIP.CMV.iresRFP-DEST	Charles Rice (Rockefeller University)
pTRIP-MCS-RFP	Constructed in this study
pTRIP-MCS-AcGFP	Constructed in this study
pTRIP-MCS-AcGFP-myc-WNV-Capsid	Constructed in this study
pTRIP-MCS-AcGFP-myc-WNV-Capsid-NT	Constructed in this study
pTRIP-MCS-AcGFP-myc-WNV-Capsid-CT	Constructed in this study
pTRIP-MCS-AcGFP-myc-WNV-Capsid-PxxP	Constructed in this study
pTRIP-MCS-AcGFP-myc-WNV-Capsid-KA	Constructed in this study
pTRIP-MCS-AcGFP-myc-WNV-Capsid-NLS	Constructed in this study
pTRIP-MCS-AcGFP-myc-MVEV Capsid	Constructed in this study
pTRIP-MCS-AcGFP-myc-SLEV Capsid	Constructed in this study
pTRIP-MCS-AcGFP-myc-JEV Capsid	Constructed in this study
pTRIP-MCS-AcGFP-myc-DENV Capsid	Constructed in this study
pTRIP-MCS-AcGFP-myc-YFV Capsid	Constructed in this study
pTRIP-MCS-AcGFP-WNV Capsid	Constructed in this study

2.1.5 Antibodies

Table 2.9 Primary Antibodies

Antibody	***Dilution***	***Application****	***Source***
Guinea Pig anti-WNV Capsid	1:2000	WB	T. Hobman, University of Alberta
Mouse anti-Actin (ab3280)	1:3000	WB	Abcam
Mouse anti-CD95 – Activating (05-201)	1:1000	WB	Millipore
Mouse anti-myc (4A6)	1:2000	WB	Millipore
Mouse anti-myc (9E10)	1:1000	IIF	T. Hobman, University of Alberta
Mouse anti-Striatin-3B (MAB2291)	1:500	IIF	Abnova
Rabbit anti-Akt (4685)	1:1000	WB	Cell Signaling
Rabbit anti-caspase-3 (Asp175) (9664)	1:200, 1:1000	FC, WB	Cell Signaling
Rabbit anti-caspase-8 (Asp391) (9496)	1:100, 1:1000	FC, WB	Cell Signaling
Rabbit anti-GAPDH (ab9485)	1:3000	WB	Abcam
Rabbit anti-GFP	1:25000	WB	L.G. Bertihaume, University of Alberta
Rabbit anti-Phospho-Akt (Ser473) (4058)	1:1000	WB	Cell SIgnaling
Rabbit anti-WNV Capsid	1:1000	WB	T. Hobman, University of Alberta

*- IB: immunoblot; IIF: indirect immunofluorescence; IP: immunoprecipitation

Table 2.10 Secondary antibodies

Antibody::Conjugate	***Dilution***	***Application****	***Source (product ID)***
Donkey anti-mouse::Alexa488	1:1000	IIF	Invitrogen (A21202)
Donkey anti-mouse::Alexa680	1:10 000	WB	Invitrogen (A10038)
Donkey anti-rabbit::Alexa488	1:1000	IIF	Invitrogen (A21206)
Donkey anti-rabbit::Alexa647	1:1000	IIF	Invitrogen (A31573)
Goat anti-mouse::Alexa647	1:1000	IIF	Invitrogen (A21236)
Goat anti-mouse::Alexa750	1:10 000	WB	Invitrogen (A21037)
Goat anti-mouse::HRP	1:5000	WB	Jackson ImmunoResearch Laboratories
Goat anti-rabbit::HRP	1:5000	WB	Jackson ImmunoResearch Laboratories
Goat anti-rabbit::Alexa594	1:1000	IIF	Invitrogen (A11037)
Goat anti-rabbit::Alexa750	1:10 000	WB	Inivitrogen (A21039)

*- IB: immunoblot; IIF: indirect immunofluorescence; IP: immunoprecipitation

2.1.6 Cell lines

Table 2.11 Mammalian cell culture lines

Cell line	***Source***
A549	ATCC
1HAEO	David Marchant, University of Alberta
HEK293T	ATCC
HEL/18	E. Gönczöl, Wistar Institute

2.2 Methods

2.2.1 Molecular Biology

2.2.1.1 Purification of plasmid DNA from Eschericia coli

The small scale preparation of plasmid DNA was carried out using the Qiagen Qiaprep spin mini prep kit (Table 2.5). All procedures were performed according to the manufacturer's instructions. Preparation procedures were performed on overnight 3-5 mL LB cultures of DH5α *E. coli,* transformed with plasmid DNA.

For large scale preparation of DNA, overnight cultures were processed either with the Qiagen Plasmid Maxi Kit (Table 2.5) or through a classical alkaline lysis procedure, followed by PEG precipitation. Plasmid harboring bacteria were grown overnight in a volume of 100mL LB and were pelleted via centrifugation at 5 000 x g for 10 minutes. Bacterial pellets were then resuspended in Qiagen buffer P1 (Table 2.5), and 20mg of lysozyme is added to the suspension. After 20 minutes of incubation on ice, 12mL of Qiagen buffer P2 (Table 2.5) is added and the mixture is carefully inverted to ensure adequate mixing and lysis. The lysate is then mixed with 10mL of buffer P3 (Table 2.5) and incubated on ice for 20 minutes. After centrifuging the lysate at 20 000 x g for 15 minutes, the supernatant is recovered and incubated for 30 minutes at 37 ^{o}C after addition of 100 µg of RNAse A. To isolate nucleic acids the cleared lysate is extracted twice with an equal volume of phenol : chloroform : isoamyl alcohol, followed by one

extraction with chloroform : isoamyl alcohol. To precipitate plasmid DNA, one volume of 2-propanol is added to the extract, followd by incubation at room temperature for 5 minutes. Following centrifugation at 20 000 x g for 15 minutes, the resulting pellet is dried and resuspended in 1.6 mL of 10 mM Tris-Hcl. To further remove impurities, the plasmid DNA is precipitated by the addition of 0.4 mL of 4 M NaCl and 2.0 mL of 13% PEG-8000 solution. The mixture is then incubated for 60 minutes on ice, and centrifuged at 20 000 x g for 15 minutes. After one wash with 70% ethanol and centrifugation as in the previous step, the pellet is dried and resuspended in 300 µL of 10 mM Tris-HCl.

2.2.1.2 Polymerase chain reaction

Target amplicons were produced using the Expand High Fidelity PCR System (Table 2.5). A typical reaction contained 10ng of plasmid DNA, 200 µM of each of the four dNTPs, and 300 nM of each primer. Expand High Fidelity enzyme mix was added at 2.6 U/reaction. All reactions were performed on a TC-312 thermocycler (Techne).

2.2.1.2 Restriction endonuclease digestion

Endonuclease digestion was normally carried out in a volume of 20 – 30 µL containing 1 – 5 µg of plasmid DNA and 5 – 10 U of restriction enzyme with the prescribed buffer (Table 2.3).

2.2.1.3 Desphosphorylation of linearized vectors

In order to reduce occurrences of plasmid vector self-ligation following restriction digest, vector DNA was treated with Antarctic Phosphatase according to manufacturer's recommendations (Table 2.3).

2.2.1.4 Agarose gel electrophoresis

To cast agarose gels for electrophoresis, ultrapure agarose (0.5% - 1.0% (w/v)) (Table 2.6) was dissolved in TAE via heating. Immediately before pouring, Ethidium Bromide was added to a final concentration of 0.5 µg/mL. The gel was then placed in an electrophoresis tank and sufficient TAE was added to submerge the gel. DNA samples were then mixed with 6x loading buffer (Table 2.6) and applied to the gel. Gels were typically run at 75 – 100 V until sufficient resolution was achieved. Bands of DNA were visualized using a UV transilluminator (Table 2.4) or a FluoroChem FC imaging system (Table 2.4).

2.2.1.5 Purification of DNA fragments

To purify PCR products following completion of PCR or restriction digest, a QIAquick PCR purification kit was used to remove proteins and salts, and short (<100 nt) cleavage products (Table 2.5). For purification of DNA fragments that could not be processed using the aforementioned kit, agarose gel electrophoresis was performed. This was followed by excision of the desired

bands with a razor blade and extraction from the gel via the Qiaex II gel extraction kit (Table 2.5).

2.2.1.6 Annealing of synthesized oligonucleotides

Oligonucleotides MCS(+) and MCS(-) (Table 2.7) which were suspended in 10 mM Tris-HCl at a concentration of 100 µM were mixed in equimolar amounts and heated to 95 °C for 3 minutes. After heating, the mixture was placed in a room temperature tube rack and allowed to anneal for ~30 minutes. Following this, the annealed oligonucleotide mixture was placed on ice before being subjected to restriction digest.

2.2.1.6 Ligation of DNA fragments

Restriction digested DNA fragments were ligated into plasmid vectors using a molar ratio of 6:1. A mass of 25 – 50 ng of vector DNA was typically use in ligation reactions which were carried out in a 20 µL volume. After addition of 2 – 5 U of T4 DNA ligase, reactions were mixed and incubated for at least 30 minutes at either room temperature (cohesive end ligations) or 16 ^{o}C (for blunt end ligations).

2.2.1.7 Transformation of Escherichia coli

Chemically competent subcloning efficiency DH5α (Invitrogen) and HB101 cells (Promega) were used during the course of these studies. For all

transformations, cells were transformed and subsequently cultured according to the manufacturer's instructions.

2.2.2 Construction of recombinant plasmids

A list of all oligonucleotide primers used in the construction of plasmids for these studies is available in Table 2.7. The sources of all plasmids used in these studies is listed in Table 2.8. All plasmids which were constructed during the course of this work were subjected to DNA sequencing to verify that the insert(s) did not contain mutations. This analysis was performed at The Applied Genomics Centre (TAGC, Department of Medical Genetics, University of Alberta).

2.2.2.1 pIRES2-AcGFP1-WNV Capsid

The plasmid pCMVNY99 was used as a template in a PCR containing the primers WNV-Cap-Fwd2 and WNV-Cap-Rev2. The resulting product of 477 bp was purified and subsequently digested with *EcoRI* and *BamHI*. The digested fragment was then ligated into pIRES2-AcGFP1 which had been digested with the same enzymes and purified.

2.2.2.2 pTRIP-MCS-RFP

The plasmid pTRIP.CMV.iresRFP-DEST was digested with *XhoI* and *SpeI*. Two complementary oligonucleotides (MCS (+) and MCS (-)) which were

annealed prior to digestion with *SpeI* and *XhoI* were then ligated into pTRIP.CMV.iresRFP-DEST to create pTRIP-MCS-RFP.

2.2.2.3 pTRIP-MCS-AcGFP

The plasmid pIRES2-AcGFP1 was used as a template in a PCR reaction containing primers AcGFP-FWD and AcGFP-Rev. The resulting reaction product of 740 bp was digested with *NheI* and *SacII.* The digested fragment was subsequently ligated in to pTRIP-MCS-RFP which was also digested with *NheI* and *SacII*.

2.2.2.4 pTRIP-MCS-AcGFP-WNV Capsid

The plasmid pCMVNY99 was used as a template in a PCR containing the primers WNV-Cap-Fwd1 and WNV-Cap-Rev1. The resulting product of 477 bp was purified and subsequently digested with *SpeI* and *XhoI*. The digested fragment was then ligated into pTRIP-MCS-AcGFP1 which had been digested with the same enzymes and purified.

2.2.2.5 pTRIP-MCS-AcGFP—myc-WNV Capsid –NT,CT,PxxP,KRA,NLS

DNA sequences encoding and N-terminal portion (NT) of WNV capsid (aa 1-57), the C-terminal portion (CT) (aa 48-105), WNV capsid with prolines 5 and 8 mutated to alanines (PxxP), WNV capsid with amino acids 85 and 86 (KK) and 103-105 (KKR) mutated to alanines (KRA), and WNV capsid with aa 85-105

deleted (NLS) were synthesized by IDT. All synthesized fragments were designed to contain *SpeI* and *XhoI* sites. The sequences were received in a shuttle vector (pIDT-SMART) provided by IDT. Following digestion with *SpeI* and *XhoI,* the fragments were purified and ligated into pTRIP-MCS-AcGFP which had also been digested and purified.

2.2.2.6 pTRIP-MCS-AcGFP-myc-MVEV, SLEV, WNV, JEV, DENV and YFV capsid

Full length cDNAs encoding the capsid proteins from MVEV (377 bp), SLEV (368 bp), WNV (507 bp), JEV (377 bp), DENV (359 bp) and YFV (365 bp) including an N-terminal c-myc epitope were synthesized by IDT. All constructs were designed to include *SpeI* and *XhoI* sites. After restriction digestion of the shuttle vectors containing the cDNAs, the purified fragments were ligated into pTRIP-MCS-AcGFP digested with *SpeI* and *XhoI*.

2.2.3 Culture and transfection of mammalian cell lines

2.2.3.1 Cell line maintenance

A549, HEK293T, and HEL/18 cells were cultured in DMEM containing 10% FBS, 20 mM HEPES (pH7.4). 1HAE0 cells were cultured in MEM containing 10% FBS. All cultures were incubated at 37°C in a humidified atmosphere with 5% CO_2.

2.2.3.2 Transient transfection of cell lines

A549 cells were transiently transfected with plasmid DNA using Lipofectamine 2000. Cells were seeded in 6-well dishes at a density of 2 x 10^5 cells/well 24 hours prior to transfection. Cells were then transfected with 1 μg of plasmid DNA and 1 μL of Lipofectamine 2000 in a total volume of 1mL of OptiMEM per well. Cells were incubated with the DNA-Lipofectamine 2000 complexes for 6 hours, at which time the medium was aspirated and replaced with fresh DMEM + 10% FBS. The dishes were returned to a humidified incubator at 37^{o}C with 5% CO_2 atmosphere for 24 or 48 hours before harvesting. Transfection of HEK293T cells was carried out using plasmid DNA and TransIT-LT1 transfection reagent. Twenty four hours prior to transfection, 2.5 x 10^6 cells were seeded into each 100 mm dish. For both co-immunoprecipitation experiments and production of lentivirus particles, 13 μg of plasmid DNA was mixed with 48 μL of TransIT-LT1 in a total volume of ~850 μL. Complexes were then added to cells in 7 mL of DMEM + 3% FBS and placed in the incubator for 6 hours. The medium was then aspirated and replaced with 10 mL of DMEM + 10% FBS in the case of co-immunoprecipitation experiments, or 10 mL of DMEM + 3% FBS in the case of lentivirus pseudovirion production.

2.2.4 Production and use of lentiviral particles

2.2.4.3 Production of lentivirus particles

To produce lentivirus pseudovirions for transduction of mammalian cell lines, HEK293T cells were transfected as described above and incubated for 48 hours before cell culture supernatants were harvested and replaced with 10 mL of fresh DMEM + 10% FBS. Harvested supernatants were placed on ice in the dark overnight. Twenty four hours after the first harvest, cell culture supernatants are again collected and combined with those from the previous harvest. Lentivirus containing medium is then centrifuged at 1000 xg for 10 minutes at 4^{o}C to pellet cellular debris. After addition of polybrene to a final concentration of 5 μg/mL, lentiviral preparations are aliquoted and stored at -80^{o}C until needed.

2.2.4.4 Transduction of mammalian cell lines

For transduction cell lines such as A549, HEL18 and 1HAEo, the procedure was performed in 6 or 12 well plates. For A549 cells, 1.0 x 10^5 cells were seeded into each well of a 6-well plate, or 5 x 10^4 cells in each well of a 12-well plate 24 hours prior to transduction. For HEL/18 cells, 2 x 10^5 cells were seeded into each well of a 6-well plate 48 hours prior to transduction. For 1HAE0 cells, 1.5 x 10^5 cells were seeded into wells of a 6-well plate. To transduce the cells medium was removed and replaced with DMEM + 3% FBS containing 5 μg/mL polybrene.

Lentiviral suspension was added at a multiplicity of transduction (MOT) of 10 and plates were then placed in a swinging bucket rotor and centrifuged at 1,200 xg for 60 minutes in a 37^{o}C centrifuge. Following centrifugation, the lentivirus containing medium was removed and replace with fresh complete medium.

2.2.4.5 Determination of lentiviral yield

In order to determine the number of transducing units per mL (TU/mL) in lentiviral preps, A549 cells were plated at a density of 2 x 10^5 cells/well 24 hours before transduction. Medium was then changed to DMEM + 3% FBS with 5 µg/mL polybrene. In most cases, 100 µL, 50 µL and 10 µL of each suspension to be titred were added to the cells and transduction was carried out as described. To prepare cells for analysis, medium was removed and cells were washed with PBS. After trypsinization and resuspension, cells were centrifuged at 500 xg for 5 minutes, washed once in PBS + 5% FBS and then resuspended in 400 µL of PBS + 5% FBS. Analysis was performed either on a BD FACSCanto II or BD Fortessa flow cytometer. Samples which demonstrated positivity for AcGFP in 15% or less of cells were used to determine the number of transducing units/mL as each positive event is due to a single transducing particle.

2.2.5 Microscopy

2.2.5.1 Indirect Immunofluorescence

A549 cells were cultured on glass coverslips 24 hours prior to transduction with lentiviruses expressing myc-tagged capsids. After 48 hours of incubation, cells were washed twice with PBS after aspiration of medium. The cells were then fixed with 2% PFA in PBS with incubation at 4^{o}C for 30 minutes. Following 3 washes with PBS, the cells are then permeabilized with 0.2% (v/v) Triton X-100 in PBS for 12 minutes. After 3 washes with PBS, non-specific binding sites are blocked by incubation in 1% BSA (w/v) in PBS for 1 hour at room temperature. Coverslips are then incubated with mouse anti-myc (9E10) antibody in 1% BSA in PBS for 1 hour in a humidified chamber at room temperature or overnight at 4°C. Following three washes with 1% BSA (w/v) in PBS, cells are incubated with secondary antibody in the same buffer for 30 minutes. Three washes in PBS-T are followed with 1 wash in PBS, after which the coverslips were mounted on glass slides in Prolong Gold with DAPI. Digital images were acquired with an Olympus IX-81 microscope (Table 2.4).

2.2.4.3 Image Manipulation

Images acquired with the confocal microscope were exported as multi-channel 16-bit/pixel TIFF files from Volocity acquisition and analysis software (Table 2.4). Files were then imported into ImageJ analysis software and either

single z-slices or projections of the entire stack of images were separated based on acquisition channel. Merged images were also created for the comparison purposes. All adjustments made to the images were linear in nature.

2.2.5 Protein gel electrophoresis and immunodetection

2.2.5.1 Sodium dodecyl sulfate polyacrylamide gel electrophoresis (SDS-PAGE)

Proteins in samples were electrophoretically separated using either Tris-glycine or Tris-HEPES chemistries. Regardless of buffer system used, a 5% stacking gel was paired with a 10, 12 or 15% resolving gel. Stacking gels were prepared by addition of pre-prepared acrylamide/bis-acrylamide to a final concentration of 5% to a solution containing 125 mM Tris-HCl (pH 6.8) (for Tris-glycine gels) or 375 mM Tris-HCl (pH 7.0) (for Tris-HEPES gels). In both cases, 0.1% ammonium persulfate and 0.1% TEMED were added before casting. Resolving gels were prepared at a final concentration of 10, 12 or 15% acrylamide/bis-acrylamide in a solution consisting of either 375 mM Tris-Hcl (pH 8.8) (Tris-glycine gels) or 375 mM Tris-HCl (pH 7.0) (Tris-HEPES gels). Before casting, APS and TEMEMD were added to a final concentration of 0.1%. Prior to electrophoresis, protein samples were mixed with 5x protein sample buffer (Table 2.6) and heated to 95°C for 3 minutes. Electrophoresis was performed using the Bio-Rad mini-protean III system and Tris-glycine or Tris-HEPES running

buffer (Table 2.6) at 100-200 V. Following completion of the run, gels were prepared for Immunoblot as described in section 2.2.5.2.

2.2.5.2 Immunoblot analysis

After SDS-PAGE was complete, proteins were transferred from gels to 0.45 µM polyvinylidene fluoride (PVDF) membranes. To activate PVDF for protein binding, membranes were soaked in methanol for 1 minute and then equilibrated in western blot transfer buffer (Table 2.6) for 10-15 minutes. Tris-HEPES gels were soaked in transfer buffer for at least 5 minutes with agitation before transfer set up. The Mini Trans-blot electrophoresis transfer cell (Bio-Rad) was used for immunoblot procedures. Transfer was performed at 100 V constant current for 90 minutes. The transfer apparatus was cooled through the use of an ice-pack. After the transfer had completed, the membranes were dried and reactivated through soaking in methanol. Following several washes, membranes were blocked for one hour in PBS-T or TBS-T (table 2.6) containing either 5% (w/v) skim milk powder or 5% (w/v) bovine serum albumin, respectively. All incubations of membranes are carried out with agitation from a lab rocker. For all immunoblots except those for phospho-Akt the LiCor Odyssey system was used. PBS-T was used in washes and the preparation of antibody suspensions. For phospho-Akt blots, horseradish peroxidase conjugated secondary antibodies were used, TBS-T was employed throughout. The PVDF membranes were incubated in primary antibodies diluted as described in Table

2.9 in either PBS-T containing 5% (w/v) skim milk powder for either 1 hour at room temperature, or overnight at 4°C. When anti-phospho epitope antibodies were employed, primary antibody dilutions were performed in TBS-T + 5% (w/v) bovine serum albumin, and incubated with membranes overnight. Following incubations, membranes were washed 2 times in either PBS-T or TBS-T for total time of 10 minutes. Secondary antibody incubations were performed in either PBS-T with 5% (w/v) skim milk powder for fluorescently tagged antibodies, or TBS-T + 5% (w/v) bovine serum albumin for horseradish peroxidase conjugated secondary antibodies. Dilutions were performed as described in Table 2.10. Finally, membranes were washed in either PBS-T or TBS-T three 3 times for a total of 45 minutes before detection as described in section 2.2.5.3 or 2.2.5.4.

2.2.5.3 Detection of horseradish peroxidase conjugated secondary antibodies

Membranes were incubated in Supersignal West Pico chemiluminescent substrate (Table 2.4) for 2 minutes, at which point they were either exposed to film (Table 2.4) or imaged using the FluorChem Q photographic detection system (Table 2.4).

2.2.5.4 Detection of fluorophore conjugated secondary antibodies

Membranes were rinsed twice in PBS and placed on the scanner bed of the Odyssey infrared imaging system (Table 2.4). The membranes were scanned at 84 µM resolution on a quality setting of "high".

2.2.6 Cell viability determination

2.2.6.1 Cell counting

A549 cells which were seeded in 12-well plates were transduced at an MOT of 10 with lentiviruses expressing MVEV, SLEV, WNV, JEV, DENV and YFV capsids, as well as an AcGFP only control. Cells were then incubated for 24 hours in complete medium. Cells were trypsinized, resuspended, and counted using the Orflo Moxi-Z cell counter to count only those objects which conform to a curve-fitting algorithm which measures cellular diameter. Duplicate samples were then shifted into serum-free DMEM and allowed to incubate for a further 48 hours. Counts were then repeated to determine the number for cells after 48 hours of serum starvation. Results are expressed as the fold change of each capsid expressing sample in reference to the AcGFP control after 48 hours of serum-free medium treatment.

2.2.6.2 Alamar blue assay for cell viability

To assess oxidative respiration and thus viability in cells expressing flavivirus capsids, 3000 A549 cells were seeded into 96-well plates and transduced at an MOT of 10 with lentiviruses expressing MVEV, SLEV, WNV, JEV, DENV and YFV capsids, as well as an AcGFP only control. Cells were allowed to incubate for 48 hours in complete medium before addition of 400mM Alamar blue stock

solution to a final concentration of 10% v/v. Cells were then incubated for 4 hours in a cell culture incubator before being read on a Perkin Elmer EnVision fluorescent plate reader. Excitiation at 530 nm is followed by collection of emission between 570 nm and 600 nm. Results are expressed as Relative Fluorescence Units (RFU).

2.2.7 RNA Techniques

2.2.7.1 Cellular RNA isolation

Total RNA, not including small RNAs such as microRNAs were isolated from A549 cells using the Agilent Total RNA Isolation Mini Kit. All procedures were carried out according to the manufacturer's recommendations. Briefly, 2 x 10^5 cells were seeded into each well of a 6-well plate. After 24 hours of incubation, an entire 6-well plate was transduced with the indicated lentivirus and all wells were harvested from each plate following 48 hours of incubation. Cellular RNA was eluted in 30 µL of ddH_2O and yield was determined via spectrophotometric measurement.

2.2.7.2 RNA quality control for microarray hybridization

The total RNA samples prepared in section 2.2.7.1 were sent to the Alberta Transplant Applied Genomics Center (ATAGC, University of Alberta) for analysis with an Agilent BioAnalyzer 2100. In order to be acceptable for use in microarray hybridization, samples had to have a determined RNA Intergrity

Number of ≥8.0. This value is determined by the BioAnalyzer software automatically.

2.2.7.3 Microarray analysis of gene expression

Samples were submitted to the ATAGC (University of Alberta) and 300 ng of total RNA was labeled according to ATAGC protocol. Labeled RNA was then hybridized by an ATAGC technician to PrimeView Human Gene Expression microarrays, according to the manufacturer's recommendations.

Chapter 3

The West Nile Virus Capsid Protein Inhibits Fas-mediated Apoptosis

A version of this chapter has been published as
"Urbanowski M.D., Hobman T.C. (2013). The West Nile virus capsid protein blocks apoptosis through a phosphatidylinositol 3-kinase-dependent mechanism. J. Virol. *87(2)*:872-81."

3.1 Rationale

The capsid protein of West Nile Virus (WNV) has in the past been described only in terms of its critical structural functions, which serve to encapsidate the viral genome and facilitate infectious particle release. However, mounting evidence indicates that WNV capsid has important non-structural functions which alter the host environment to be more permissible for viral replication and spread. Studies from the Hobman lab and others have demonstrated that WNV capsid interacts with a number of cellular proteins to carry out important non-structural functions.

Previously published studies have suggested that the capsid protein of WNV is a pro-apoptotic protein which activates effector caspases and leads to cell death (Yang et al., 2008). However, this claim is not well supported as the form of capsid employed in these studies is not produced during viral infection (Amberg and Rice, 1999; Stocks and Lobigs, 1995). Additionally, the relatively slow replication kinetics of WNV are seemingly at odds with the concept of early activation of cell death pathways by a viral protein. Viruses with more rapid replication kinetics such as Vesicular Stomatitis Virus (VSV) and Sindbis Virus cause significant cell death in cultured cells within 24 hours (Koyama, 1995; Moriishi et al., 2002; Pearce and Lyles, 2009). Under the same conditions, WNV requires 48 to 72 hours to achieve a similar amount of cell death (Parquet et al., 2001). Given these facts and the evidence in published literature, I hypothesized that WNV capsid did not promote apoptosis, but blocked or slowed its progression. The

potential pro-survival properties of WNV capsid would allow WNV to delay the onset of cellular responses which have evolved to restrict and contain viral replication.

If WNV capsid is indeed an anti-apoptotic protein, then cells expressing WNV capsid should be resistant to one or more pro-apoptotic stimuli. In turn, this would result in reduced activation of apical and effector caspases and enhanced cell survival during apoptotic challenge. As a corollary, I hypothesized that WNV capsid would enhance activation of a pro-survival pathway to mediate the observed effects.

3.2 Results

3.2.1 A single isoform of WNV capsid is detectable in infected cells

As a first step we set out to confirm previously published reports which demonstrated that WNV capsid protein is produced as a single 105 aa species in infected cells. Although it has been reported that expression of WNV capsid induces apoptosis, it is important to point out that these studies employed a 123 amino acid residue form of capsid. Based on the spatial and temporal aspects of viral polyprotein processing in yellow fever and Murray Valley encephalitis virus-infected cells, we expected that the larger (123 amino acid residue) isoform of WNV capsid would be very transient or undetectable in infected cells. To test this directly, I expressed both the 105 amino acid and 123

amino acid isoforms form of WNV capsid in transfected cells and compared the electrophoretic mobilities of these proteins to the capsid protein in infected A549 and HEK293T cells (Figure 3.1). At all time points examined, the only species of capsid in the WNV infected cells that was detectable by immunoblotting, co-migrated with the 105 amino acid residue isoform. Based on these observations, I concluded that that the reported pro-apoptotic effects of the 123 amino acid isoform of WNV capsid are of questionable relevance to WNV biology and that further investigation of how the 105 amino acid isoform functions in cellular death signaling was warranted.

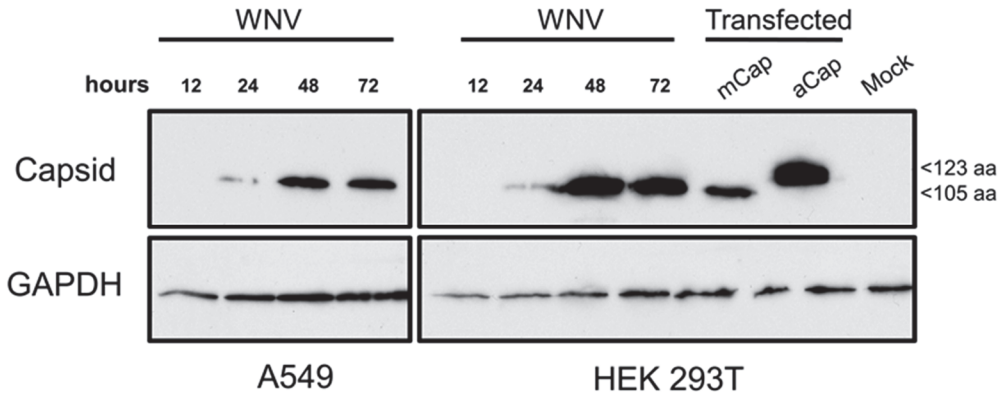

Figure 3.1. Only the 105 amino acid form of capsid protein is detected in WNV infected cells. A549 and HEK293T cells were infected with WNV at an MOI of 5 and at the indicated time points, cell lysates were prepared and analyzed by immunobloting with antibodies to capsid and GAPDH (loading control). As indicated, cells were transfected with plasmids pCMV5-mCap encoding the 105 amino acid form of capsid, or pCMV5-aCap, which encodes the 123 amino acid form of capsid.

3.2.2 Cells infected with WNV do not undergo caspase-dependent cell death until late in infection

Apoptosis in WNV infected cell lines has been previously reported, the kinetics of which depend on the cell line and MOI used. To determine the kinetics of apoptosis induction in WNV infected A549 cells, we performed a time course experiment where caspase activation was monitored at various times post-infection. Cells were infected with WNV and VSV at various MOIs. Infection of A549 cells with VSV is known to cause extensive cell death in less than 24 hours and therefore this virus served as a positive control for rapid induction of apoptosis. Mock and infected cells were harvested at 24, 48 and 72 hours post-infection, fixed, permeabilized and stained with an antibody that recognizes activated caspase-3 followed by an Alexa Fluor 647 labeled secondary antibody. Samples were then subjected to analyses by flow cytometry. Figure 3.2A shows that regardless of the MOI, WNV antigen was detectable at all time points with the exception of 24 hours when cells were infected with a an MOI of 0.1. For WNV samples, even though the majority of the cells were infected at 48 hours, the number of cells which were positive for active caspase-3 was below ~20%, even at an MOI of 3. This is in contrast to the data in Figure 3.2C which show that by 24 hours post-infection, ~30% of the VSV-infected cell population was positive for active caspase-3. None of these cells survived past the 48 hour time point and thus only one time point is shown. In contrast, less than 5% of WNV-infected cells were caspase-3 positive at 24 hours post-infection. Only after 72 hours did the level of

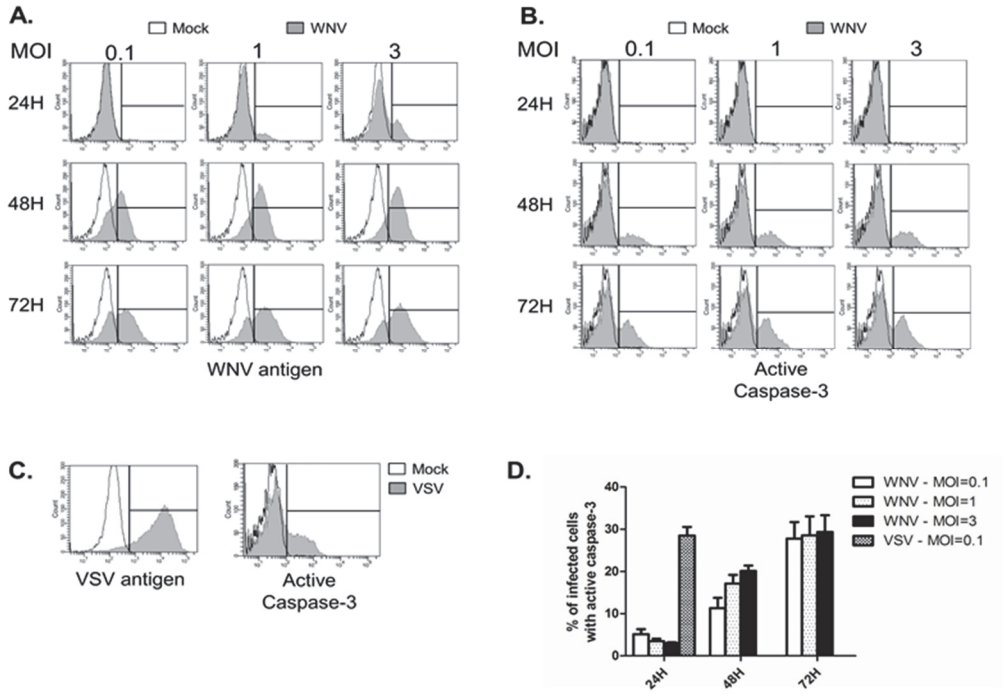

Figure 3.2 WNV does not cause significant activation of caspase-3 until late in infection. A549 cells were infected with WNV at an MOI of 0.1, 1 or 3, or VSV at an MOI of 0.1. At 24, 48, and 72 hours post-infection WNV infected cells were harvested. VSV infected cells were only harvested at 24 hours post infection because shortly after this time point, the majority of cells were dead. (A, B) Following fixation, WNV infected cells were incubated with mouse NS2B/3 (to detect virus antigen) and rabbit active-caspase-3 and then anti-mouse Alexa Fluor 488 and anti-rabbit Alexa Fluor 647. Samples were then subjected to flow cytometric analysis. Histogram overlays were constructed from representative experiments in which the fluorescent intensity distribution of mock-infected samples (unfilled histograms), is shown together with that of infected samples (grey histograms). An interval gate (vertical line) is indicated in each plot. Events to the right of the interval gate are considered positive for the given antigen. C. VSV infected cells were stained with a mouse monoclonal antibody (BW8G65) to VSV glycoprotein (virus antigen) or rabbit anti-active-caspase-3, and analyses were performed as in A and B. The results of three independent experiments are summarized in D. Standard error bars are shown.

apoptosis in WNV infected samples approach 30% (Figure 3.2D). These data suggest that although WNV infected A549 cells eventually undergo apoptosis, this does not occur until late in the infection cycle.

3.2.3 Expression of WNV capsid protects cells from Fas- but not staurosporine-dependent apoptosis, as determined by TMRM assay

Having established that induction of apoptosis is delayed in WNV infected A549 cells, I next determined whether expression of capsid, which is the first viral protein produced, affects the onset of apoptosis. I chose to assess whether capsid expression influenced cell death triggered by Fas (CD95) ligation. This pathway is well characterized and plays a physiologically relevant role in elimination of virus-infected cells. Twenty-four and 48 hours after transfection of A549 cells with pIRES2-AcGFP1 or pIRES2-AcGFP1-Capsid plasmids, cells were challenged with anti-Fas and cycloheximide for 6 hours. The membrane-permeable dye TMRM was used to detect the loss of mitochondrial membrane potential, which is indicative of commitment to apoptosis. After staining with TMRM, transfected cells were analyzed by flow cytometry. Gating on AcGFP expressing cells was used to differentiate transfected cells from non-transfected cells (Figure 3.3C). TMRM staining is brightest in cells that have intact mitochondrial membrane potential and the vertical line in the histogam represents the threshold between viable and apoptotic cells; apoptotic cells grouping to the left. The primary and summarized data in Figures 3.3A and 3.3D, show that at 24 and 48 hour time points, expression

of WNV capsid reduced the onset of Fas-induced apoptosis by 43% and 50% respectively compared to cells expressing AcGFP only. In these samples, treatment with anti-Fas antibody caused a negligible increase in apoptotic cells during the time course examined. These data suggest that capsid blocks execution of the Fas-dependent apoptotic program by delaying loss of mitochondrial membrane potential and the subsequent release of pro-apoptotic factors. Interestingly, WNV capsid failed to protect cells from mitochondrial membrane potential loss during treatment with staurosporine (2μM), a potent and pan-specific kinase inhibitor (Figure 3.3B). This suggests that the anti-apoptotic activity of WNV capsid is limited to pathways that rely upon the activity of specific kinases.

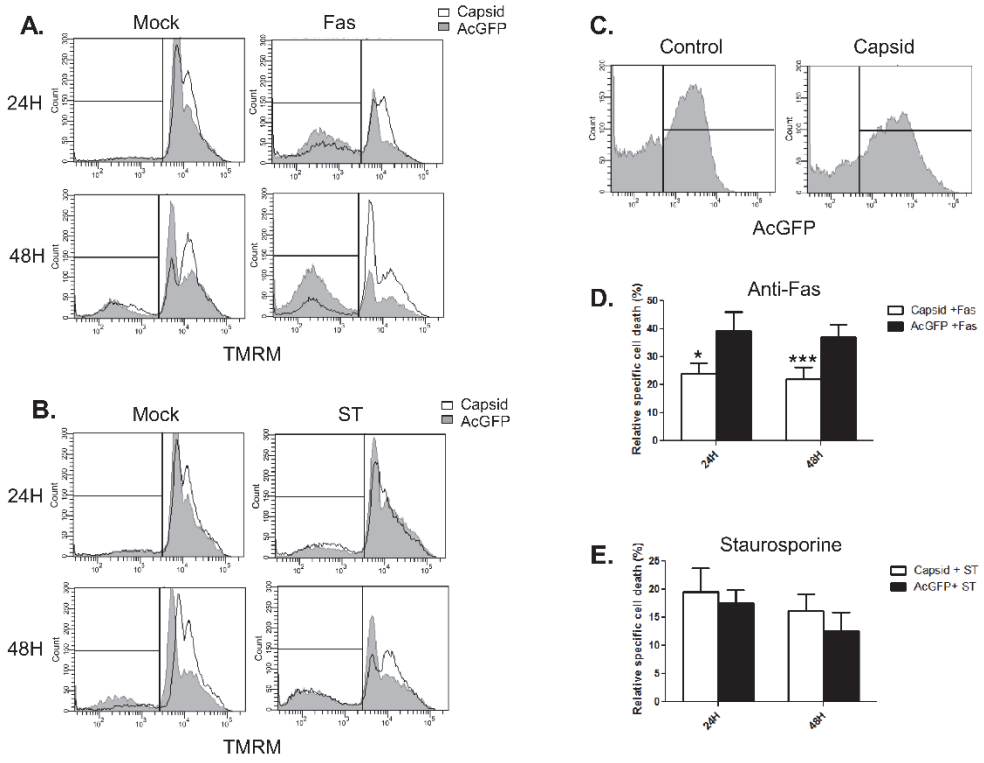

Figure 3.3 WNV capsid protects against anti-Fas challenge but not staurosporine treatment. A549 cells were transfected with plasmids encoding AcGFP alone (Control) or AcGFP and WNV capsid protein (Capsid). At 24 and 48 hours post transfection, cells were treated with DMSO, staurosproine (ST), mock treated, or treated with anti-fas and cycloheximide (Fas) for 6 hours. Cells were then incubated with the fluorescent mitochondrial dye TMRM and processed for live cell flow cytometry. Following FACS analyses, histogram overlays were constructed from a representative experiment in which capsid expressing cells (unfilled histograms) were compared to AcGFP only expressing cells (grey-filled histograms). Results from analyses are shown in A (anti-fas) and B (staurosporine). Individual events to the left of the interval gates in A and B were considered positive for cell death. Plots in C represent the distribution of AcGFP fluorescence in transfected cells. All points to the right of the vertical line were considered positive for AcGFP. The percentage of dead mock treated cells was subtracted from the percentage of dead cells in anti-Fas or staurosporine-treated samples. The resultant percentage was referred to as "relative specific cell death". Graphs in D and E show the average results from 3 experiments. Standard error bars are indicated. Note that only AcGFP positive events were analyzed for TMRM flurorescence. Statistical analyses (paired t-test) were performed and statistically significant differences are indicated (* = $p \leq 0.05$; *** = $p \leq 0.001$).

3.2.4 WNV capsid inhibits activation of caspase-3 and -8 during anti-Fas challenge

I then compared the relative activation of initiator (caspase-8) and executioner (caspase-3) caspases in control and WNV-capsid expressing cells that had been challenged with anti-Fas. For these experiments, I used recombinant lentiviruses to mediate capsid expression instead of plasmid-based transfection. Transduced A549 cells were fixed, stained sequentially with anti-active caspase-8 or -3 antibodies and then AlexaFluor 647 secondary antibody prior to flow cytometric analyses. Analyses revealed that expression of WNV capsid reduced activation of caspase-8 and caspase-3 in response to anti-Fas by 43% and 46%, respectively (Figure 3.4). These results are consistent with the data in Figure 3 showing that capsid protects cells against loss of mitochondrial membrane potential.

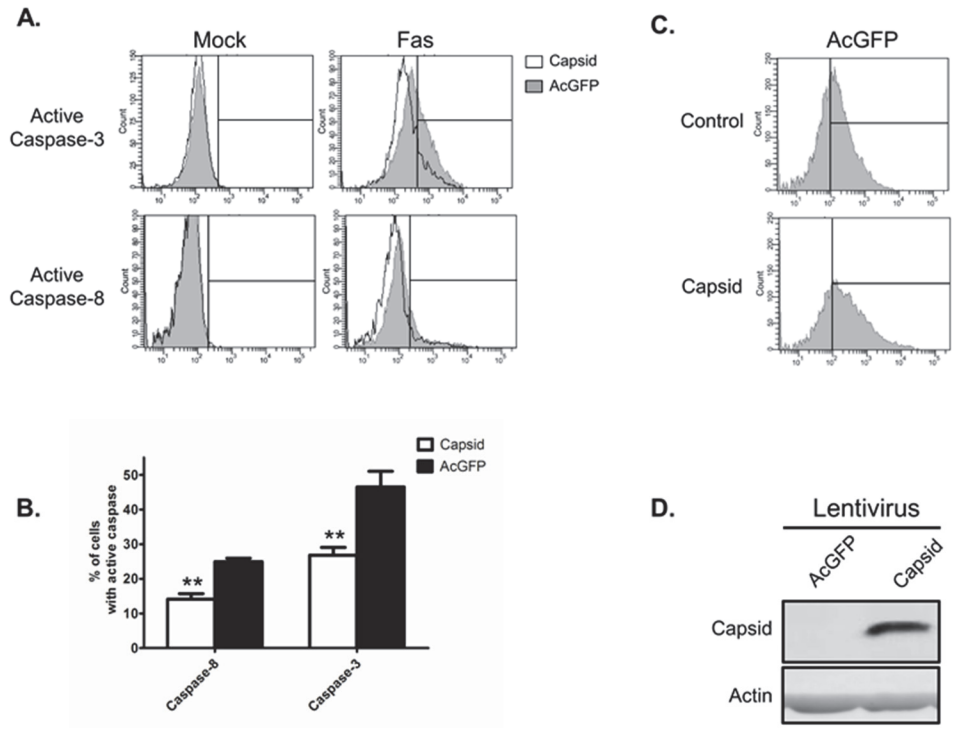

Figure 3.4 WNV capsid inhibits Fas-dependent activation of caspase-3 and -8. A549 cells were transduced with lentiviruses encoding AcGFP alone (AcGFP) or AcGFP and WNV capsid protein (Capsid) at a multiplicity of transduction of 3. Approximately 48 hours post transduction cells were treated with anti-fas (Fas) or mock treated (Mock). Samples were then processed for intracellular staining with antibodies to active caspase-3 or caspase-8, followed by staining with anti-rabbit Alexa Fluor 647 (A). Samples were then analyzed via FACS and histogram overlays were constructed from a representative experiment in which capsid expressing cells (unfilled histograms) were compared to AcGFP only expressing cells (grey-filled histograms). Individual events to the right of the interval gate in Figure 4A were considered positive for the given active caspase. Mock treated samples were used to establish a baseline for activated caspase staining. Note that only AcGFP positive cells were analyzed for the presence of active caspase. Results averaged from 3 independent experiments are shown in (B). Standard error bars are indicated. Histograms in C display levels of AcGFP expression and thus transduction in experimental samples. Events to the right of the interval gate are considered positive for AcGFP. Immunoblot data in panel D show that transduction of cells with lentiviruses encoding WNV capsid results in robust expression. Statistical analyses (paired t-test) were performed and statistically significant differences are indicated (** = $p \leq 0.01$).

3.2.5 WNV capsid inhibits Fas-mediated apoptosis in HEL/18 cells

Although I had already established that WNV capsid was able to inhibit the apoptotic program in A549 cells, I wished to assess the ability of WNV capsid to inhibit apoptosis in another cell line. Most continuous cell lines, including A549 are tumor derived. Given this, it was possible that the observed phenomenon was due to the abnormal functioning of one or more cellular processes. In order to ensure that the effects that I was observing were not cell line specific, I examined the activation of caspase-3 during anti-Fas challenge in HEL/18 primary human fibroblasts. In concordance with results obtained in A549 cells, WNV capsid expression reduced the number of cells that were positive for activated caspase-3 by 43% (Figure 3.5).

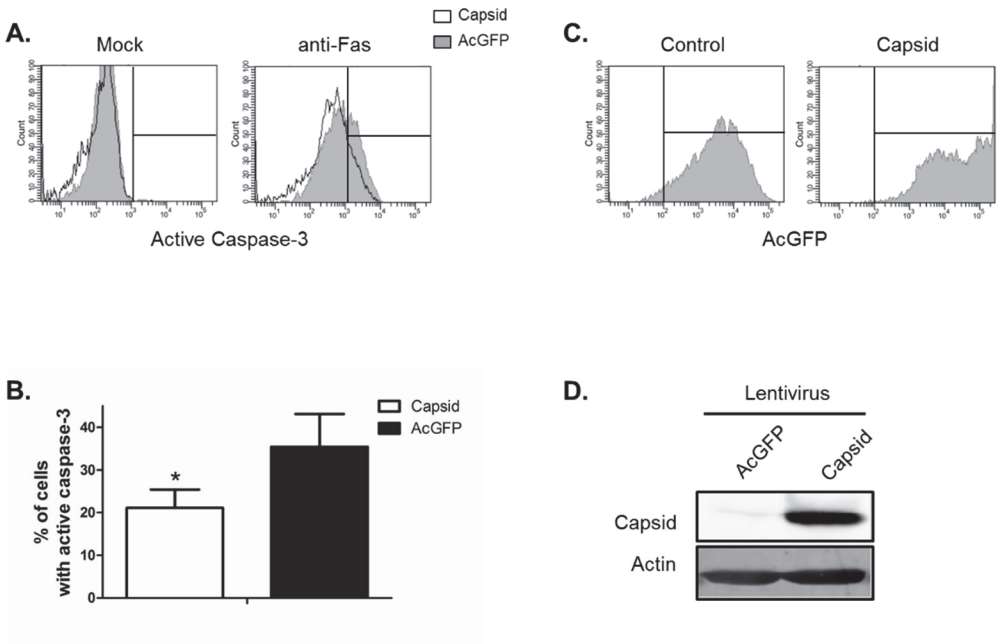

Figure 3.5 WNV capsid inhibits activation of caspase-3 in HEL/18 primary fibroblasts. HEL/18 cells were transduced with lentiviruses encoding AcGFP alone (AcGFP) or AcGFP and WNV capsid protein (Capsid) at a multiplicity of transduction of 3. At approximately forty-eight hours post-transduction, cells were treated with or without anti-Fas (Fas). Samples were then processed for intracellular staining with antibodies to active caspase-3, followed by staining with anti-rabbit Alexa Fluor 647. A. Samples were then analyzed via FACS and histogram overlays were constructed from a representative experiment in which capsid expressing cells (unfilled histograms) were compared to AcGFP only expressing cells (grey-filled histograms). B. Results averaged from 3 independent experiments are shown. Standard error bars are indicated. The asterisk indicates that the differences are statistically significant as determined by a paired t-test ($P \leq 0.05$). Histograms in C display levels of AcGFP expression and thus transduction in experimental samples. Immunoblot data in panel D show that transduction of cells with lentiviruses encoding WNV capsid results in robust expression. Statistical analyses (paired t-test) were performed and statistically significant differences are indicated (* = $p \leq 0.05$).

3.2.6 Expression of WNV Capsid increases Akt phosphorylation at Serine-473 and its protective effects are dependent on PI3K activity

Recent studies have revealed that anti-apoptotic/survival signaling is activated shortly after flavivirus infection. This signaling process involves the kinase Akt, which is activated by PI3K-dependent phosphorylation on serine 473. To determine if WNV capsid is involved in induction of survival signaling, I monitored the phosphorylation of Akt in capsid-expressing cells. Immunoblot analyses of these samples showed that WNV capsid increased phosphorylation of serine-473 by 2-fold (Figure 3.6A). Capsid-induced phosphorylation of Akt was abrogated in the presence of the PI3K inhibitor LY294002 (Figure 3.6B). We next asked whether PI3K activity is required for the protective effect of WNV capsid. Transduced A549 cells expressing AcGFP only or WNV capsid were challenged with anti-Fas and cycloheximide and/or LY294002. Immunoblot analyses confirmed that complete abrogation of Akt phosphorylation at serine-473 was achieved by treatment with LY294002 (Figure 3.7A). Data in Figure 3.7B show that in cells treated with LY294002, WNV capsid did not protect against anti-Fas (Figure 3.7C).

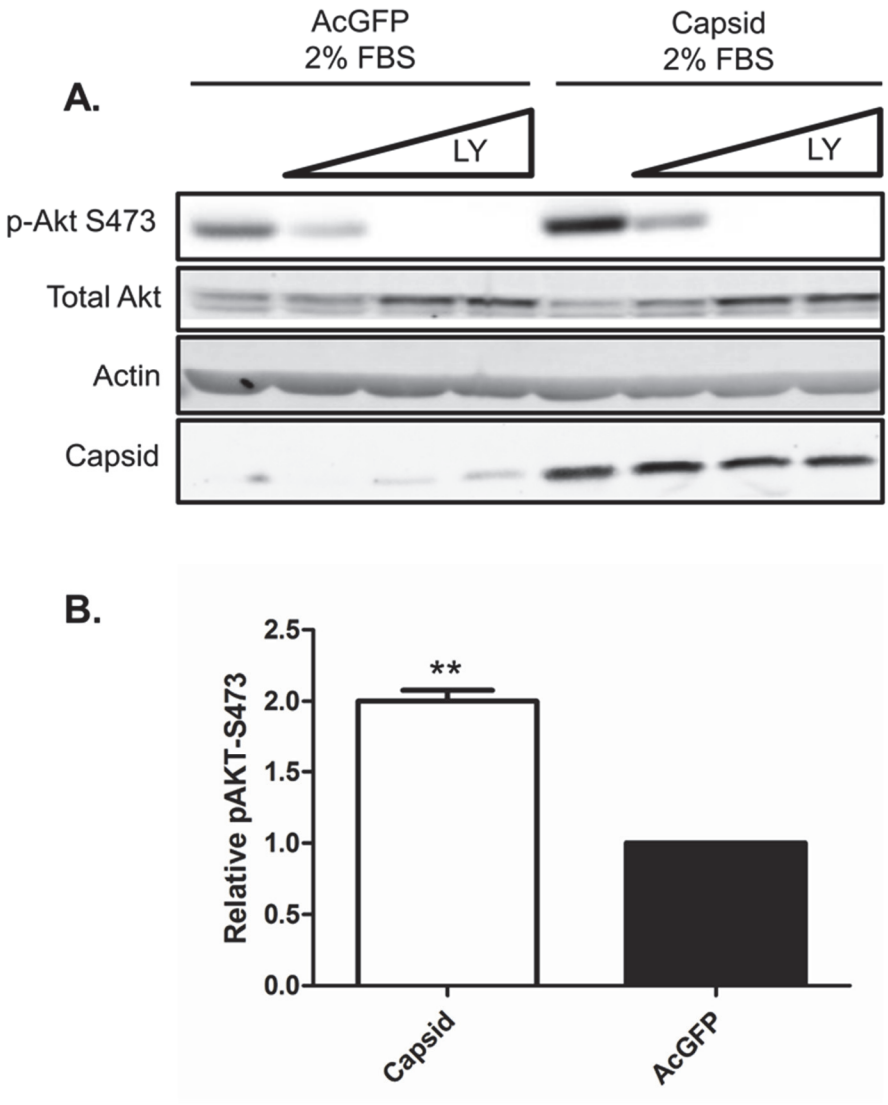

Figure 3.6 WNV capsid protein enhances phosphorylation of Akt at serine 473. A549 cells were transduced with lentiviruses expressing WNV capsid or AcGFP alone. After incubation in reduced serum conditions for 24 hours, cells were treated with increasing concentrations of LY294002 (6.25, 12.5, 25μM), or DMSO as a control. Cell lysates were collected and subjected to SDS-PAGE and immunoblotting for phospho-Akt-S473, WNV capsid and actin as a loading control in A. Levels of p-Akt were quantified relative to total Akt, and the results expressed as a fold-change with respect to the control. Three independent experiments are summarized in B. Statistical analyses (paired t-test) were performed and significant differences are indicated (** = $p \leq 0.01$). Standard error bar is shown.

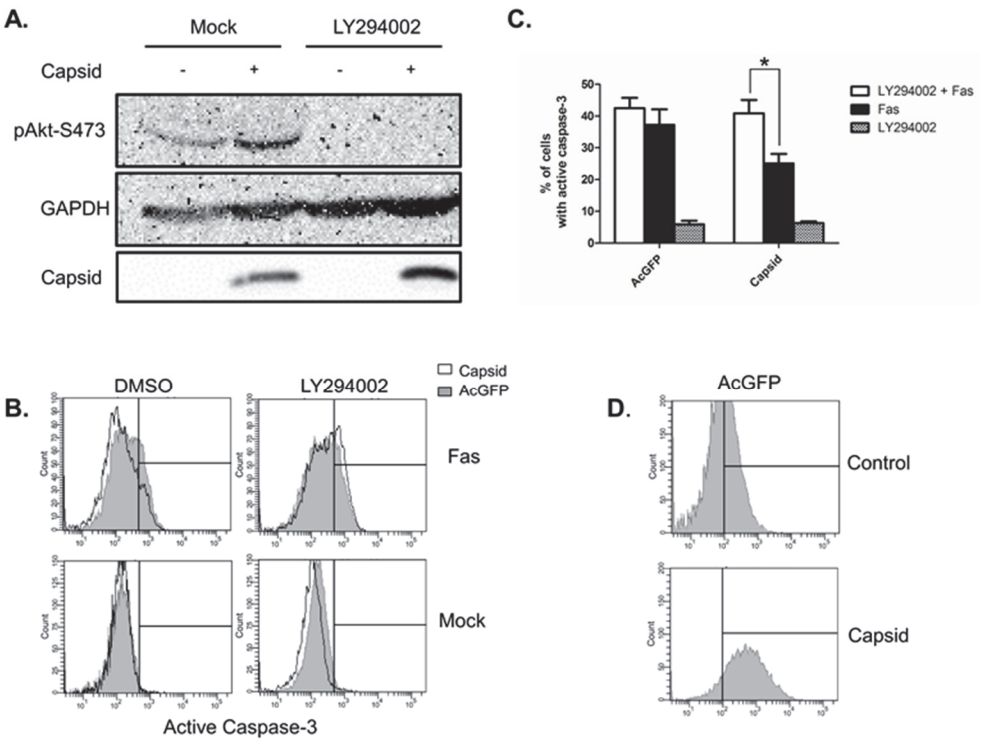

Figure 3.7 Inhibition of PI3 kinase abrogates protection by WNV capsid protein. A549 cells were transduced with lentiviruses encoding WNV capsid protein or AcGFP alone before challenge with anti-Fas with or without addition of LY294002. Resulting cell lysates were subjected to SDS-PAGE and immunoblotting with antibodies to phospho-Akt, WNV capsid and GAPDH (loading control) in A. Note that treatment with the PI3 kinase inhibitor (LY294002) reduces phospho-Akt regardless of whether capsid protein is expressed or not. Forty-eight hours post-transduction, cells expressing AcGFP or WNV capsid were treated with anti-Fas and LY294002 or DMSO. Samples were then processed for intracellular staining with antibodies to active caspase-3, followed by staining with anti-rabbit Alexa Fluor 647. Cells were then analyzed via FACS histogram overlays were constructed from a representative experiment in which capsid expressing cells (unfilled histograms) were compared to AcGFP only expressing cells (grey-filled histograms). Events to the right of the vertical line are considered positive in B. The results from 3 independent experiments were averaged and plotted in C. Standard error bars are indicated. Histograms in D display levels of AcGFP expression and thus transduction in experimental samples. Statistical analyses (paired t-test) were performed and statistically significant differences are indicated (* = $p \leq 0.05$).

3.3 Summary

In this section, WNV capsid was demonstrated to have a novel non-structural role which is to inhibit the progression of the apoptotic program in response to anti-fas challenge. The activation of the initiator caspase-8 and the executioner caspase-3 are reduced in anti-Fas challenged A549 cells expressing WNV capsid. Expectedly, the depolarization of mitochondrial membrane potential seen during the execution of apoptosis is significantly reduced by expression of WNV capsid. In addition to A549 cells, decreased activation of caspase-3 is observed in a primary cell line, HEL/18. Of note is the observation that WNV capsid does not offer any protection from challenge with the broad spectrum kinase inhibitor staurosporine. This is likely related to my data showing that the anti-apoptotic property of capsid is dependent on the activity of PI3-K. This kinase is known to be critical for the activation of many cell signaling networks. Most notably, PI3-K activity can activate many pro-survival mechanisms which allow cells to resist apoptotic agonists (Ji and Liu, 2008). In concordance with this, I have demonstrated that WNV capsid increases the phosphorylation of Akt/PKB, a kinase which is not only a substrate of PI3-K but a major player in the determination of cell fate. Through phosphorylation of downstream targets, Akt can promote cell survival by inactivating the pro-apoptotic functions of proteins such as Bax. Indeed, during these studies, published reports demonstrated that infection with WNV stimulates Akt phosphorylation early in infection. Inhibition of this effect via the PI3-K inhibitor LY294002 greatly enhances both the rapidity

of onset and magnitude of caspase-3 activation. It is tempting to speculate that the capsid protein is responsible for the enhancement of Akt phosphorylation observed during infection.

The exact events which lead to the enhanced phosphorylation of Akt, and subsequently enhanced cell survival are not yet clear. However, Akt activation has clearly been associated with phosphorylation of pro-apoptotic BH3-only proteins, blocking their function at mitochondria. At the same time, Akt mediated phosphorylation can enhance the activity and levels of anti-apoptotic proteins. Ongoing studies will determine the specific cellular factors required for WNV capsid to inhibit cell death. Clearly, a better understanding of how WNV manipulates cell fate decisions during infection will allow for more efficient and rational design of next generation anti-virals.

Chapter 4

Multiple flavivirus capsids inhibit apoptosis

4.1 Rationale

WNV belongs to a diverse genus of viruses that includes such members as JEV, DENV, MVEV, SLEV and YFV. All of these flaviviruses are medically relevant, and a vaccine is currently only available for YFV (Fernandez-Garcia et al., 2009; Sampath and Padmanabhan, 2009; Suthar et al., 2013). As a natural extension of my previous work, I wished to determine if other flavivirus capsids possessed anti-apoptotic properties. I hypothesized that flavivirus capsid proteins would protect cells from anti-Fas challenge. Given that the aforementioned flaviviruses share in common relatively slow replication kinetics and the ability to activate Akt during early infection, it is reasonable to assume that if other flavivirus capsid proteins demonstrate a protective effect it is likely dependent on PI3K (section 1.3.2.3 and Chapter 3). My previous studies examined the ability of WNV capsid to protect from both Fas- and staurosporine-mediated cell death. In the studies described in this chapter, I expanded the repertoire of apoptotic agonists to include TNFα, a ligand of TNFR.

If some flavivirus capsids protect against anti-Fas challenge but others do not, this information can provide direction in determining the mechanism of this phenomenon. Additionally, differential responses to different apoptotic stimuli will expand our understanding of the *in vivo* relevance of capsid mediated apoptosis blockade.

4.2 Results

4.2.1 Myc-tagged flavivirus capsids are expressed in A549 cells and localize to the nucleus.

Before proceeding to investigate the anti-apoptotic properties of the flavivirus capsid proteins, it was necessary to confirm the expression of each myc-tagged capsid construct, and compare their subcellular localizations using immunofluorescent imaging. As all of the flavivirus capsids under study are known to exhibit nuclear localization during infection, it was critical to determine that the presence of an N-terminal myc tag did not disrupt their subcellular localization (Bhuvanakantham et al., 2009; Isoyama et al., 2002; Mori et al., 2005; Sangiambut et al., 2008). Based on previous experience in our lab with Myc-tagged WNV capsids (Xu and Hobman, 2011), it was unlikely that this tag would affect the targeting of other flavivirus capsid proteins. Nevertheless, it was critical to rule out this possibility. A549 cells were transduced with lentivirus particles encoding Myc-tagged WNV, SLEV, MVEV, DENV, JEV and YFV capsid proteins and 48 hours later, were processed for indirect immunofluorescence imaging, or lysed for analysis by SDS-PAGE and immunoblotting. In Figure 4.1A, it can be seen that the myc-tagged capsid proteins are stably expressed and detectable with an anti-myc antibody. As a control for transduction efficiency, the marker protein AcGFP which is produced from the bicistronic pTRIP construct, was expressed a similar levels in all samples. As a loading control, anti-

GAPDH antibody was used (Figure 4.1A). After processing for indirect immunofluorescence, A549 cells expressing the indicated capsid constructs were examined for the presence of the myc-epitope. The nuclear dye DAPI was used as a counterstain. In all cases, flavivirus capsid proteins exhibited a predominantly reticular pattern surrounding the nucleus, and/or within nuclei in structures that were previously identified as nucleoli (Figure 4.1B and 4.1C). These observations are consistent with published literature documenting the subcellular localization of flavivirus capsid proteins (Hunt et al., 2007; Sangiambut et al., 2008).

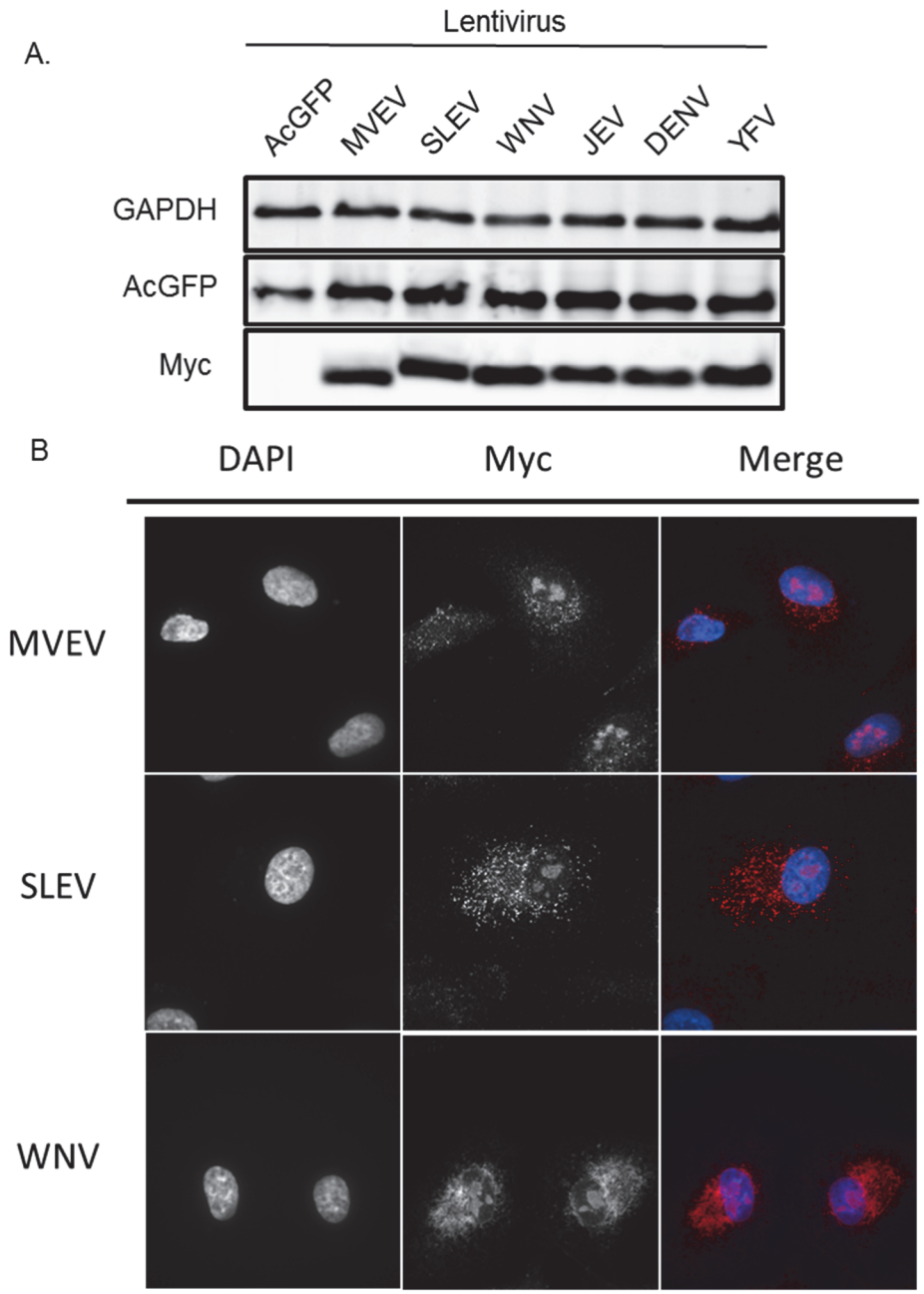

Figure 4.1. Expression and localization of Myc-tagged flavivirus capsid proteins. A549 cells were transduced with lentiviral particles expressing the indicated capsid proteins, and incubated for 48 hours before analyses by immunoblotting (A) or indirect immunofluorescence (B). In panel A, capsid were detected with anti-Myc, while AcGFP and GAPDH serve as transduction efficiency and loading controls respectively. In panel B, capsids were detected with anti-Myc and nuclei were stained with DAPI. A Z-stack composed of 0.25 µm slices was acquired for each channel, and an extended focus image was generated for each sample. Each channel was pseudo-colored prior to merging *(continued).*

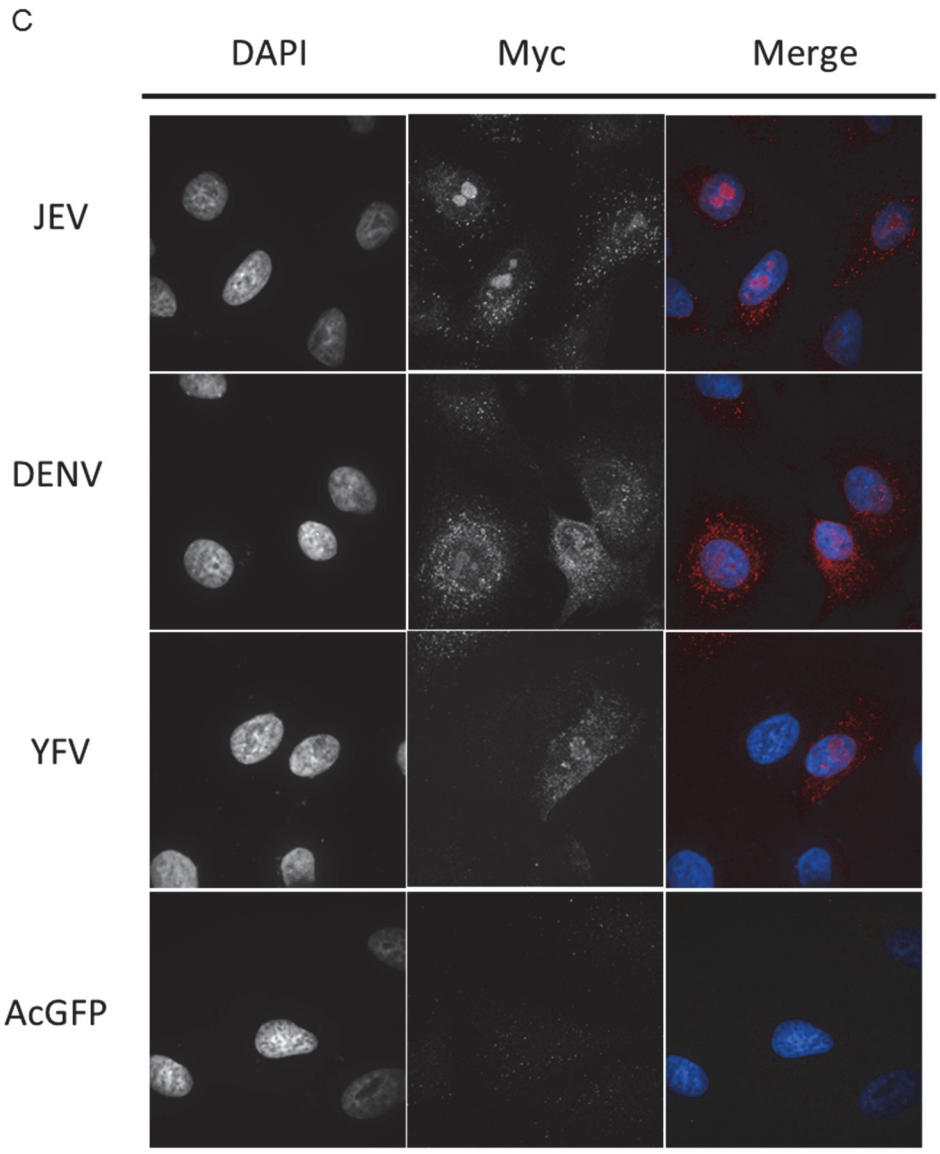

Figure 4.1 *(continued)*. Expression and localization of myc-tagged flavivirus capsid proteins.

4.2.2 Expression of flavivirus capsids does not affect expression of caspase-8 and -3.

Before beginning the examination of the effects of flavivirus capsid proteins on the progression of apoptosis, I determined if the expression of any of the myc-tagged flavivirus capsids effected the expression of caspase-8 and -3. For example, it is possible that reduced levels of activated caspase-8 and caspase-3 in capsid-expressing cells could in fact be due to diminished expression of the caspase zymogens.

Forty-eight hours post-transduction of A549 cells, lysates were prepared and levels of specific cellular proteins were examined via SDS-PAGE and immunoblot. Data in Figure 4.2 shows that relative to cells expressing AcGFP only, the levels of both pro-caspase-8 and -3 are not significantly affected by expression of flavivirus capsid proteins.

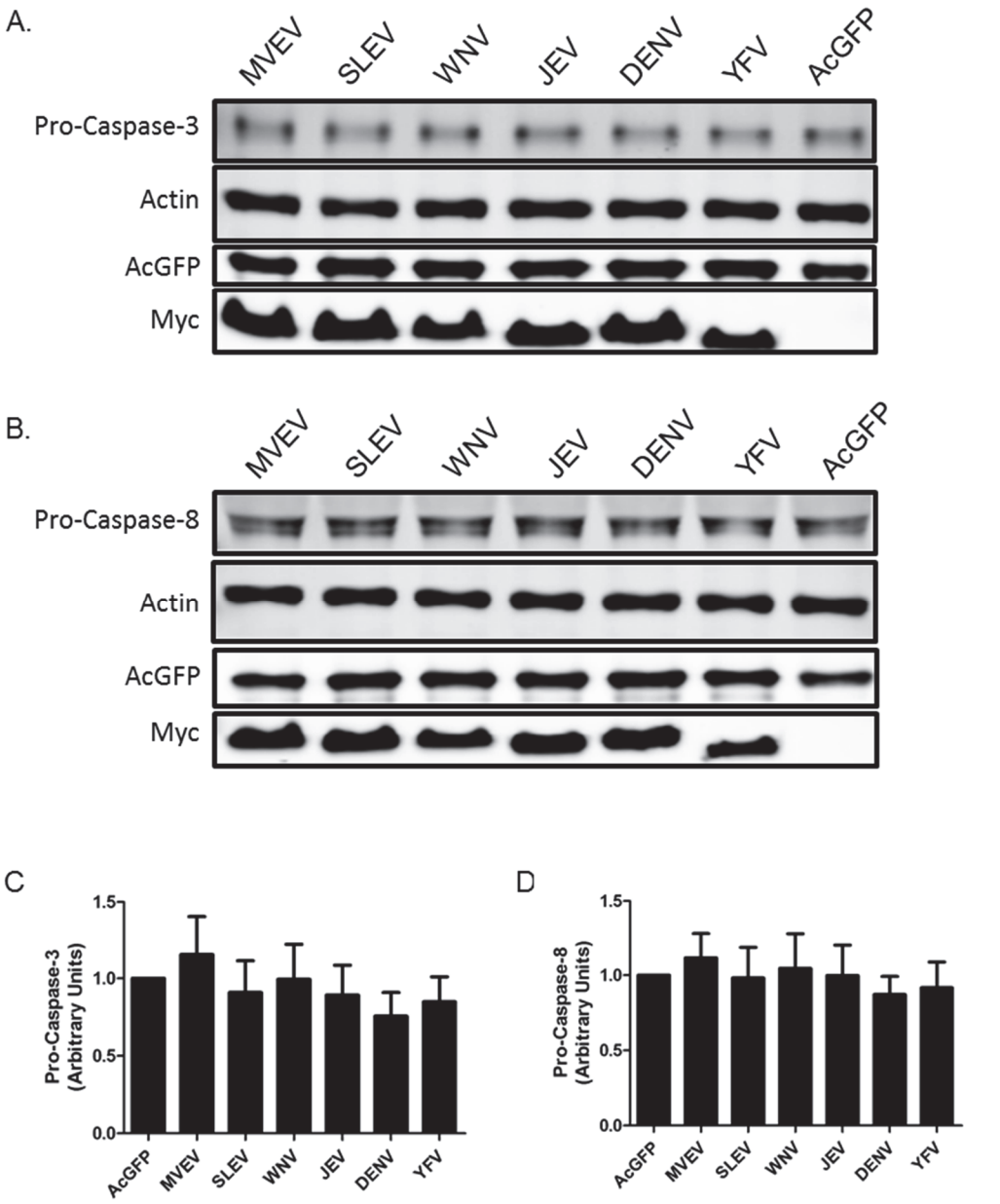

Figure 4.2. Flavivirus capsids do not affect expression of caspase 3 or 8. A549 cells were transduced with lentiviral particles encoding the indicated capsid proteins, and after 48 hours, cell lysates were subjected to immunoblot analyses. Immunoblotting for total caspase-3 (A) and total caspase-8 (B) was carried out in parallel with immunoblotting for AcGFP (as a transduction control), and Myc (to detect tagged capsid proteins). Anti-actin antibody was used as a loading control. In panels A and B, the intact pro form of the caspase is shown. Levels of pro-caspase-3 and -8 standardized to actin are shown in panels C and D. Graphs represent the results of three experiments. The levels of pro-caspase for each capsid expressing sample were standardized to those of AcGFP, giving a relative fold change value (Arbitrary Units). Standard error bars are shown.

4.2.3 Flavivirus capsids display a spectrum of protective effects against anti-Fas challenge

To directly compare the results of my previous studies on the anti-apoptotic properties of WNV capsid, I chose to examine the ability of various flavivirus capsids to protect against anti-Fas challenge. As described previously (Section 3.1), apoptotic status of cells was determined by monitoring the activation of caspase-8 and -3. Based on the studies with WNV capsid protein, I hypothesized that expression of other flavivirus capsids inhibit Fas-mediated apoptosis.

Following challenge with anti-Fas and cycloheximide, cells expressing myc-tagged MVEV, SLEV, WNV, JEV, DENV and YFV capsids or AcGFP only were fixed and stained with anti-caspase-8 and -3 antibodies. Only cells which were positive for AcGFP fluorescence were included in the flow cytometry analyses. Consistent with earlier results (Chapter 3), when challenged with anti-Fas, cells expressing WNV capsid exhibited a 35% reduction in caspase-3 activation compared to the AcGFP only (negative control). Two other capsids, those from SLEV and MVEV showed a statistically significant difference in caspase-3 activation of 25% and 24%, respectively (Figure 4.3). The activation of caspase-8 was reduced by 41% in WNV capsid expressing cells in comparison to the control. Only SLEV capsid expressing cells demonstrated a significant decrease in caspase-8 activation with a 28% reduction in positive cells. None of the other flavivirus capsid proteins affected activation of caspase-8 to a statistically significant degree (Figure 4.3).

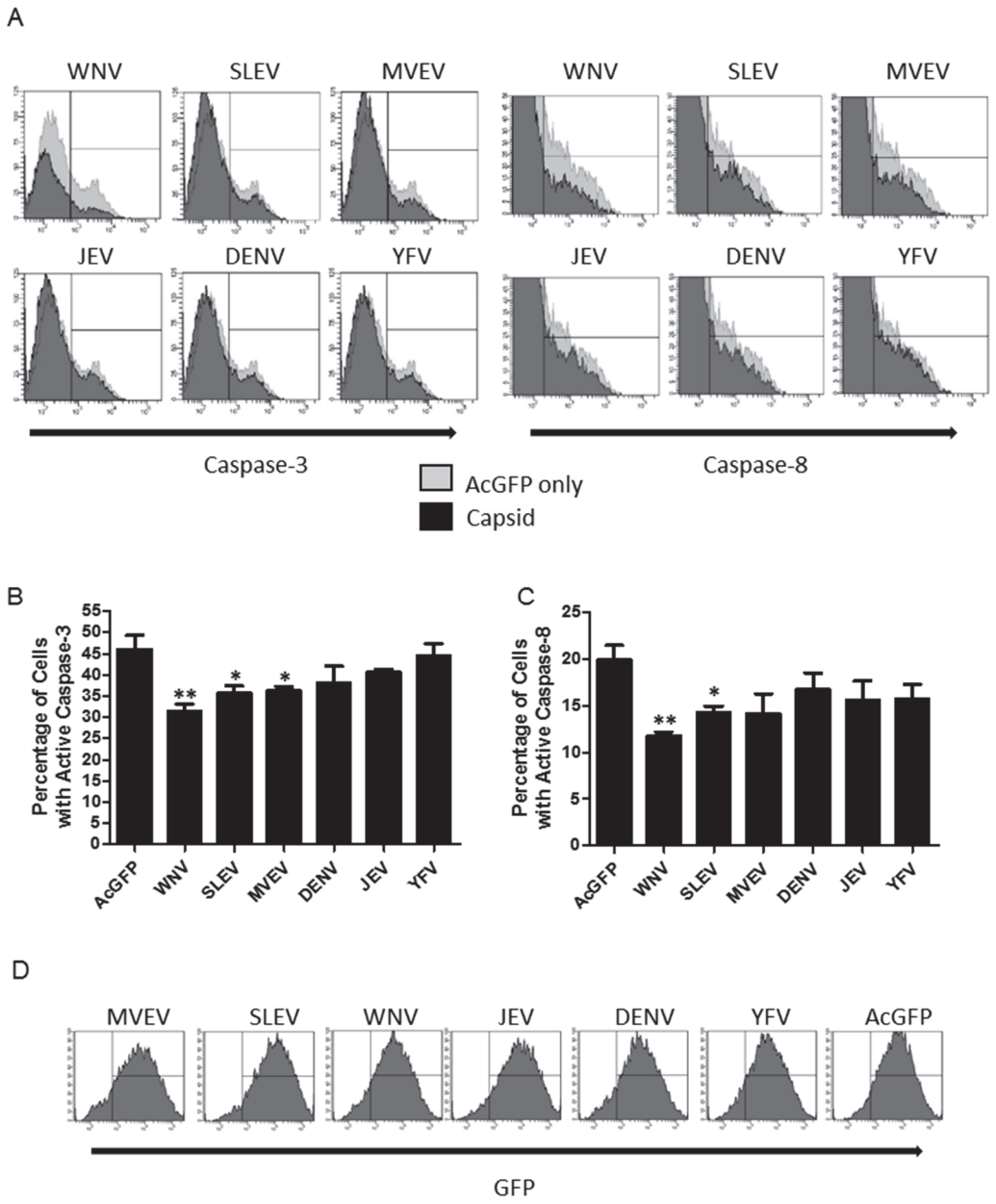

Figure 4.3. Multiple flavivirus capsids protect against anti-Fas challenge. Following transduction with lentiviruses encoding the indicated capsid proteins, cells were incubated for 48 hours before being challenged with anti-Fas for 8 hours. Following fixation and flow cytometric analysis, histogram plots were created (A) in which caspase-3 and -8 staining profiles for the indicated capsid proteins (dark histograms) are overlaid with those from the AcGFP only control (lighter gray historgrams). Events to the right of the vertical line are considered positive for the indicated active caspase. WNV capsid serves as a positive control for protection from apoptosis. The data from 3 experiments are summarized in B and C. Plots in D are histograms displaying the level of AcGFP fluorescence in each sample. Cells to the right of the vertical line are considered positive for AcGFP.

Results of statistical analyses (t-test) in B and C are indicated (*, $P \leq 0.05$) (**, $P \leq 0.01$).

The data in this section demonstrate that in addition to WNV capsid, SLEV and MVEV capsid protect from anti-Fas challenge to varying degrees. The protection afforded by these capsid proteins to anti-Fas challenge likely plays an important role during virus replication and spread in human hosts. Although the protection provided by MVEV against caspase-8 did not reach statistical significance, it is important to point out that the activity of the executioner caspase-3 is most important in carrying out the terminal steps in apoptosis (reviewed in (Salvesen, 2002)). That the activation of this caspase was significantly reduced in MVEV capsid expressing cells suggests that this capsid inhibits the execution of the apoptotic program.

4.2.4 Challenge of flavivirus capsid expressing cells with TNFα reveals differential responses to alternative death receptor ligands.

In addition to the Fas receptor, activation of other death receptors can initiate apoptosis via the extrinsic pathway (section 1.2.2.1). In order to examine if the effects observed with flavivirus capsids were specific to Fas activation, I challenged capsid expressing cells with TNFα and CHX in serum-free medium. As TNFα can exert both pro-survival and pro-apopotic effects depending on context, induction of a stress response such as that provided by CHX and serum-free conditions are necessary for effective induction of apoptosis. Interestingly, reduced activation of caspase-8 and -3 was not seen in flavivirus capsid-expressing cells (Figure 4.4). As a positive control to block apoptosis, cells were treated

with zVAD-fmk before TNFα challenge. In these samples, significant reductions in activation of both caspase-8 and -3 were observed. These data suggest that the protective effects of flavivirus capsids do not extend to all apoptotic agonists.

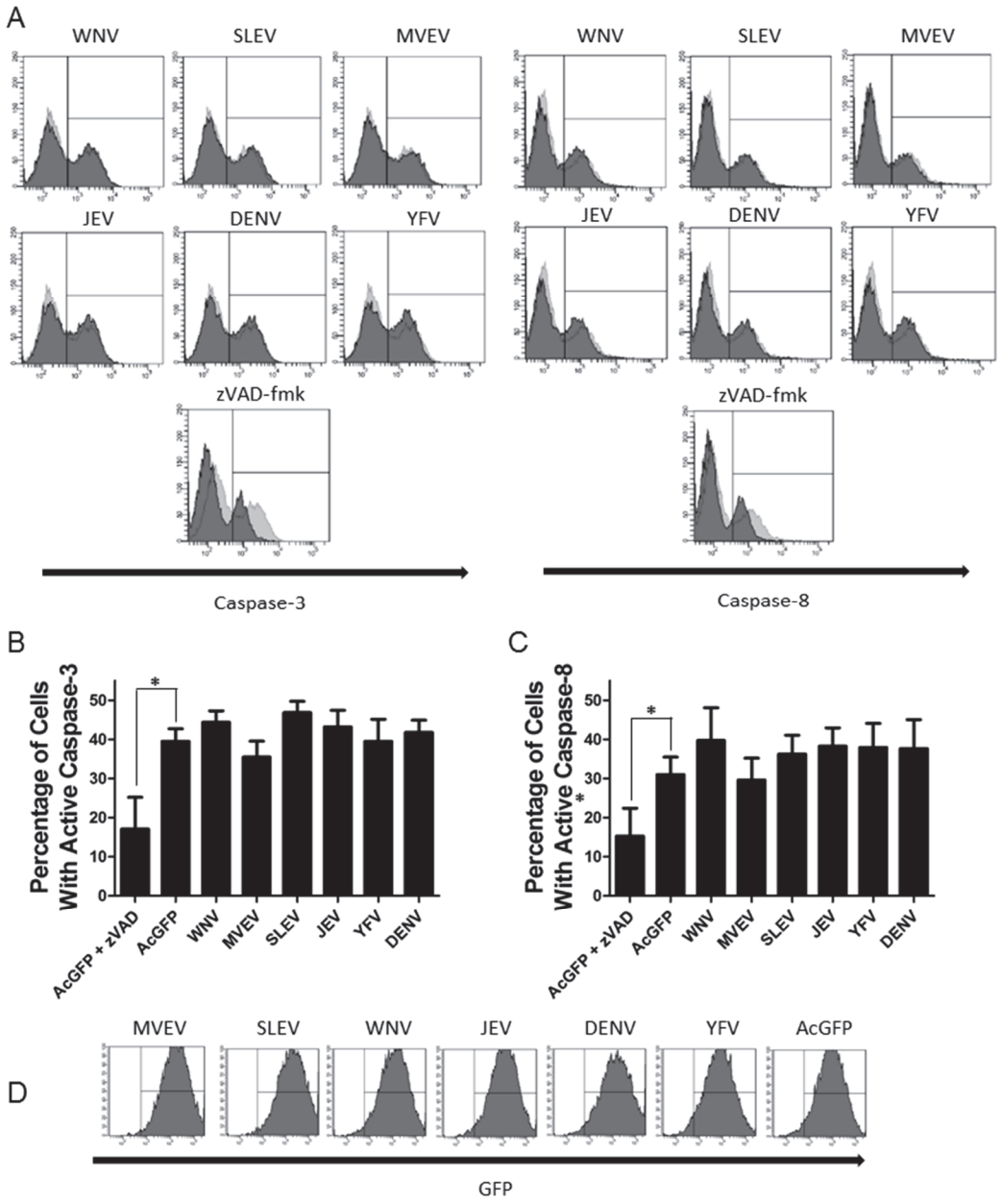

Figure 4.4. Flavivirus capsids do not protect against TNFα challenge. Following transduction with lentiviruses encoding the indicated capsid proteins, cells were incubated for 48 hours before being challenged with TNFα antibody and CHX in serum free medium for 6 hours. Following fixation and flow cytometric analysis, histogram plots were created (A) in which caspase-3 and -8 staining profiles for the indicated capsid proteins (dark histograms) were overlayed with those from the AcGFP only control (lighter gray historgrams). The averages from 3 independent experiments are summarized in B and C, with zVAD-fmk as a control. Plots in D are histograms displaying the level of AcGFP fluorescence in each sample. Cells to the right of the vertical line are considered positive for AcGFP. Results of statistical analyses (t-test) in B and C are indicated (*, $P \leq 0.05$)

4.2.5 Flavivirus capsids do not protect against anti-Fas challenge in 1HAE0 cells.

Previously, I examined the ability of WNV capsid to protect against anti-Fas challenge in A549 and HEL/18 cells (Chapter 3). To expand our understanding of how this process might function in other cell types, I examined their effects in a bronchial epithelial cell line, 1HAE0. Although both A549 (type II pneumocyte) and 1HAE0s (bronchial epithelial cells) originate from lung tissue, their functions differ greatly (Bassinet et al., 2000; Jarrard et al., 1998). Differences in the ability of capsid proteins to affect the onset of apoptosis may reflect a dependence on specific cellular factors in a given cell type or the inability to interact with these factors due to difference in the capsid sequence. Immunoblot analyses were first used to confirm robust expression of the indicated flavivirus capsid proteins, as was performed in A549 cells. Indeed, anti-Fas challenge of flavivirus capsid expressing 1HAE0 cells followed by fixation and FACS analysis demonstrated no protective effect in reference to an AcGFP only control. As a control, cells were treated with zVAD-fmk before challenge with anti-Fas and as expected, these cells exhibited very little activation of caspase-3 (Figure 4.5).

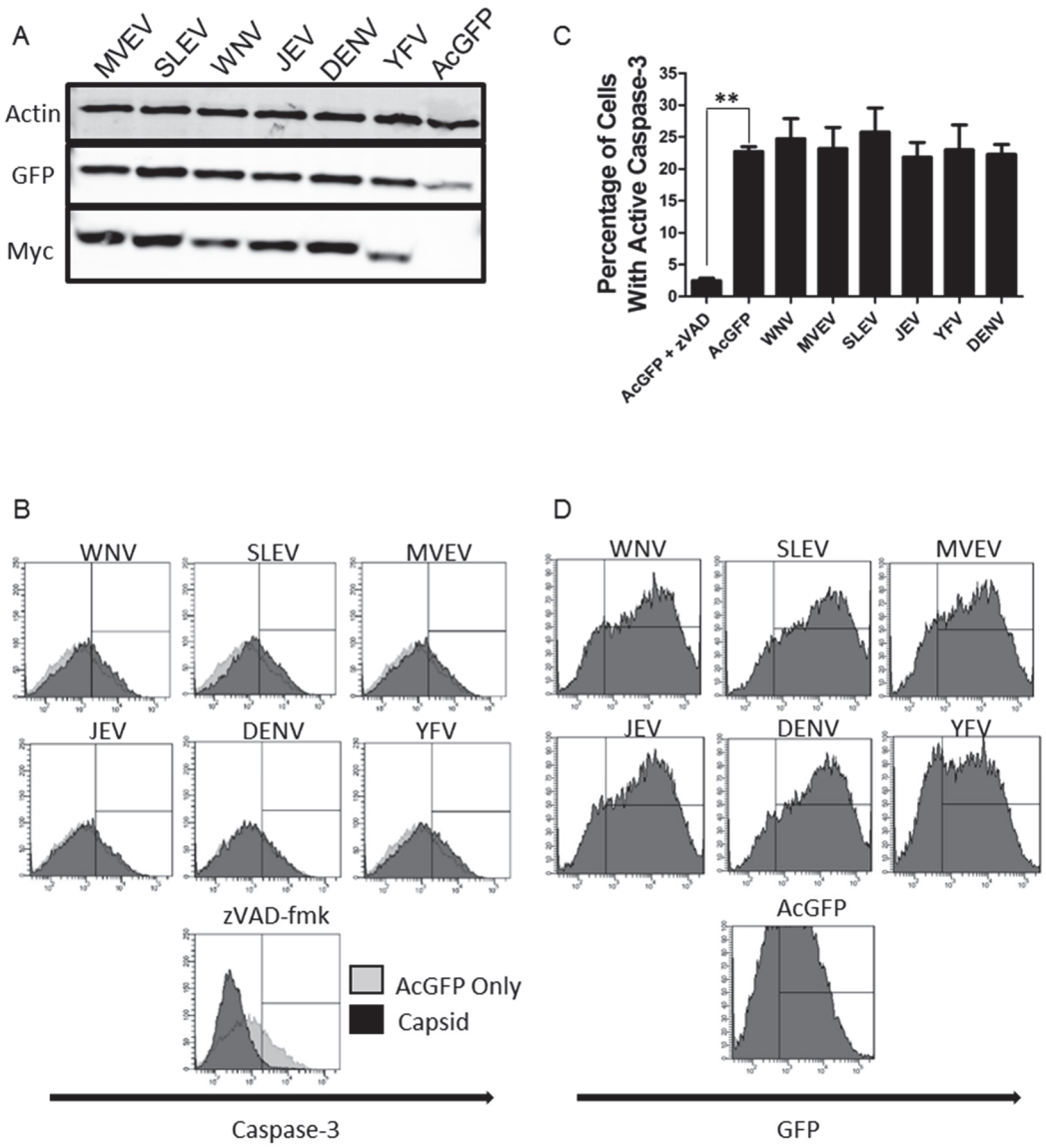

Figure 4.5. Flavivirus capsids do not protect against anti-Fas challenge in 1HAE0 cells. Following transduction with lentiviruses encoding the indicated capsid proteins, cells were incubated for 48 hours before either being lysed and subjected to immunoblotting (A), or challenged with anti-Fas and CHX for 6 hours. Cells were subsequently fixed and stained with activated caspase-3 antibodies. Following flow cytometric analysis, histogram plots were created (B) in which caspase-3 staining profiles for the indicated capsid proteins (dark histograms) are overlaid with those from the AcGFP only control (lighter gray histograms). The results of 3 experiments are summarized in C, with standard error bars shown. Plots in D are histograms displaying the level of AcGFP fluorescence in each sample. Cells to the right of the vertical line are considered positive for AcGFP. Results of statistical analysis (t-test) in C is indicated (***, $P \leq 0.001$).

4.2.6 Flavivirus capsids promote cell viability and maintain phosphorylation of Akt

Activation of Akt has been shown to inhibit the apoptotic program (Andrabi et al., 2007; Brunet et al., 1999; Wang et al., 2008). In Chapter 3, I demonstrated that WNV capsid expression preserves phosphorylation of Akt at serine-473 during growth factor withdrawal. Given the similarity in biological function between the flavivirus capsids examined in this study I determined if other flavivirus capsid proteins can prolong Akt activation during serum withdrawal. Following lentiviral transduction and incubation for 48 hours, cells were shifted to serum-free medium for 24 hours. Lysates were then prepared and analyzed via SDS-PAGE for levels of phospho-Akt S473, corrected for total Akt expression. AcGFP only expressing cells in serum-free medium served as the negative control, while AcGFP only expressing cells maintained in medium containing 10% FBS served as a positive control. In MVEV, SLEV and WNV capsid samples, phospho-Akt levels were significantly higher than the AcGFP only control (Figures 4.6A and B). The capsid proteins of JEV, DENV and YFV failed to produce a significant increase in phosphor-Akt S473 levels. These differences in phosphorylation of Akt may represent distinct mechanistic differences by which flavivirus capsids exert their effects.

To assess whether cell viability and proliferation could be affected by flavivirus capsids, I transduced A549 cells and subjected them to serum withdrawal for 48 hours. The number of cells was determined by analysis of cell suspensions on a Moxi-Z cell counter, which determines viability based on

analysis of cellular diameter. In comparison to the AcGFP only control, all tested capsid proteins caused significant increases in cellular proliferation (Figure 4.6C). To support this concept, viability was assessed via an Alamar blue assay. A549 cells were seeded into a 96-well plate and transduced at an MOT of 10. After 48 hours of incubation in complete medium, a 440 μM Alamar blue stock solution was added to the wells at a concentration of 10% v/v. After 4 hours of incubation, the levels of the reduced form of resazurin salt is measured via fluorimetry. This form is produced via the activity of NADH, which indicates active oxidative respiration and is an indicator of viability and metabolic activity. (Vega-Avila E, 2011). All capsid expressing samples demonstrated a statistically significant increase in metabolic activity compared to the AcGFP only control samples. This result is in concordance with cellular proliferation measurements.

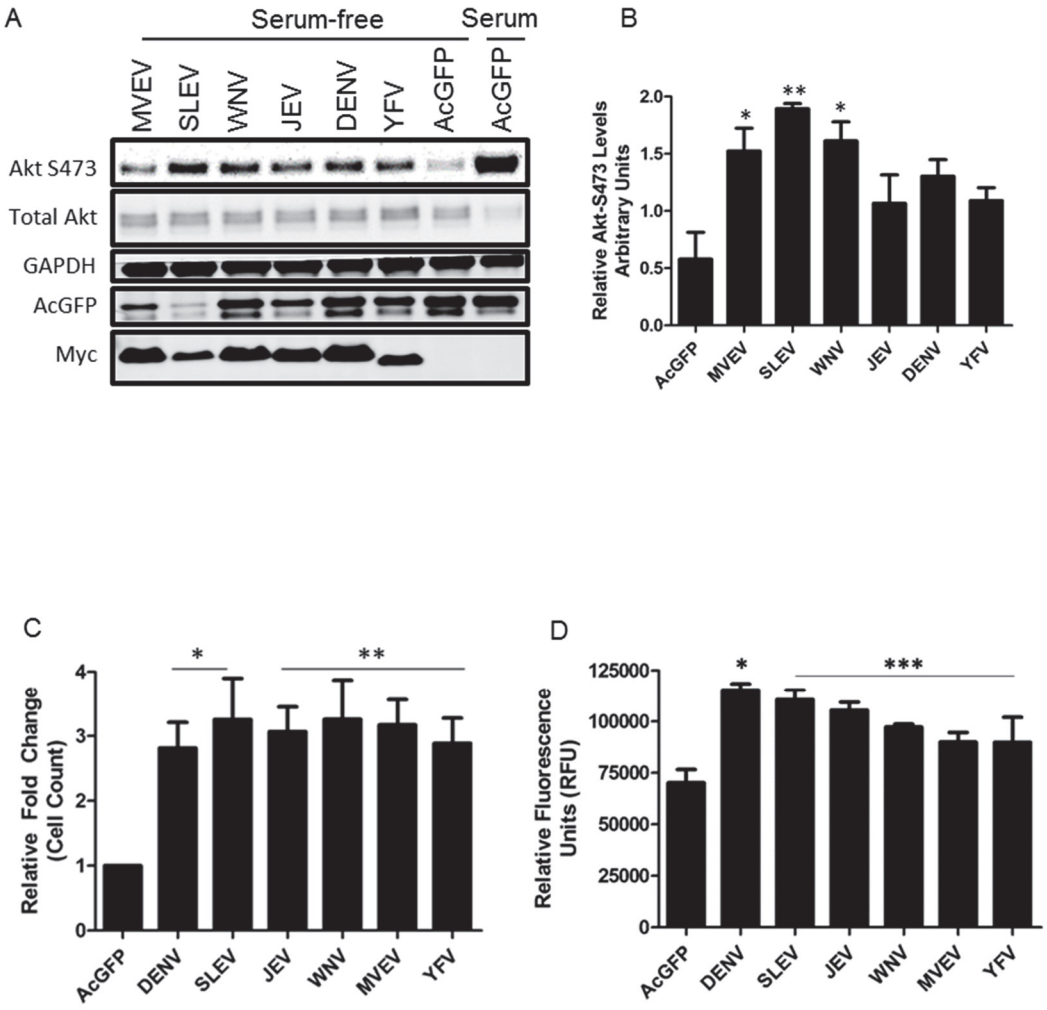

Figure 4.6. Flavivirus capsids promote Akt activation and cellular proliferation. Transduced A549 cells were serum starved for 24 hours, 48 hours post transduction and lysates were prepared and analyzed via immunoblotting for phospho- Akt-S473, Myc, GFP, GAPDH and total Akt as a control in A. The lane marked "Serum" was derived from transduced cells that were maintained in normal growth medium rather than serum-free medium. Band intensities were measured and corrected for total Akt signal and plotted as relative phospho Akt-S473 levels, with AcGFP only serving as a control. The results of 3 separate experiments are plotted in B. In C, cells were shifted to serum free medium 24-hours after transduction and incubated for 48 hours. Cells were then counted on a Moxi-Z cell counter and viable cell counts were analyzed and plotted as a fold-change with respect to the AcGFP only control sample. To assess viability, cells were transduced and incubated for 48 hours before addition of an Alamar blue stock solution to 10% v/v. Fluorescence of the reduced form of Alamar blue (which is indicative of oxidative respiration) was determined and plotted as relative fluorescence units (RFU) (D). With the exception of D, standard error bars are indicated. In D, the range of an average of two experiments performed in

triplicate is displayed. Results of statistical tests (t-test) are shown (*, $P \leq 0.05$) (**, $P \leq 0.01$) (***, $P \leq 0.001$).

4.2.7 Protein Sequence alignment of flavivirus capsids

In order to aid in understanding any potential differences between the abilities of capsid proteins to resist apoptotic stimuli, I performed a protein sequence alignment. Comparison of WNV capsid to MVEV, SLEV, JEV, DENV and YFV capsid reveals that capsid proteins which protect against anti-Fas challenge have sequence features in common (Figure 7). An "MSKK" sequence at positions 1-4 occurs in WNV, MVEV, and SLEV capsid proteins. The closest match among those capsids which do not protect is in JEV capsid, which contains an "MTKK" motif at positions 1-4. The capsids of WNV, MVEV and SLEV also share in common an "FRFTA" sequence at positions 54-58. These similarities may play an important role in providing the protective capacity of WNV, MVEV, and SLEV capsids.

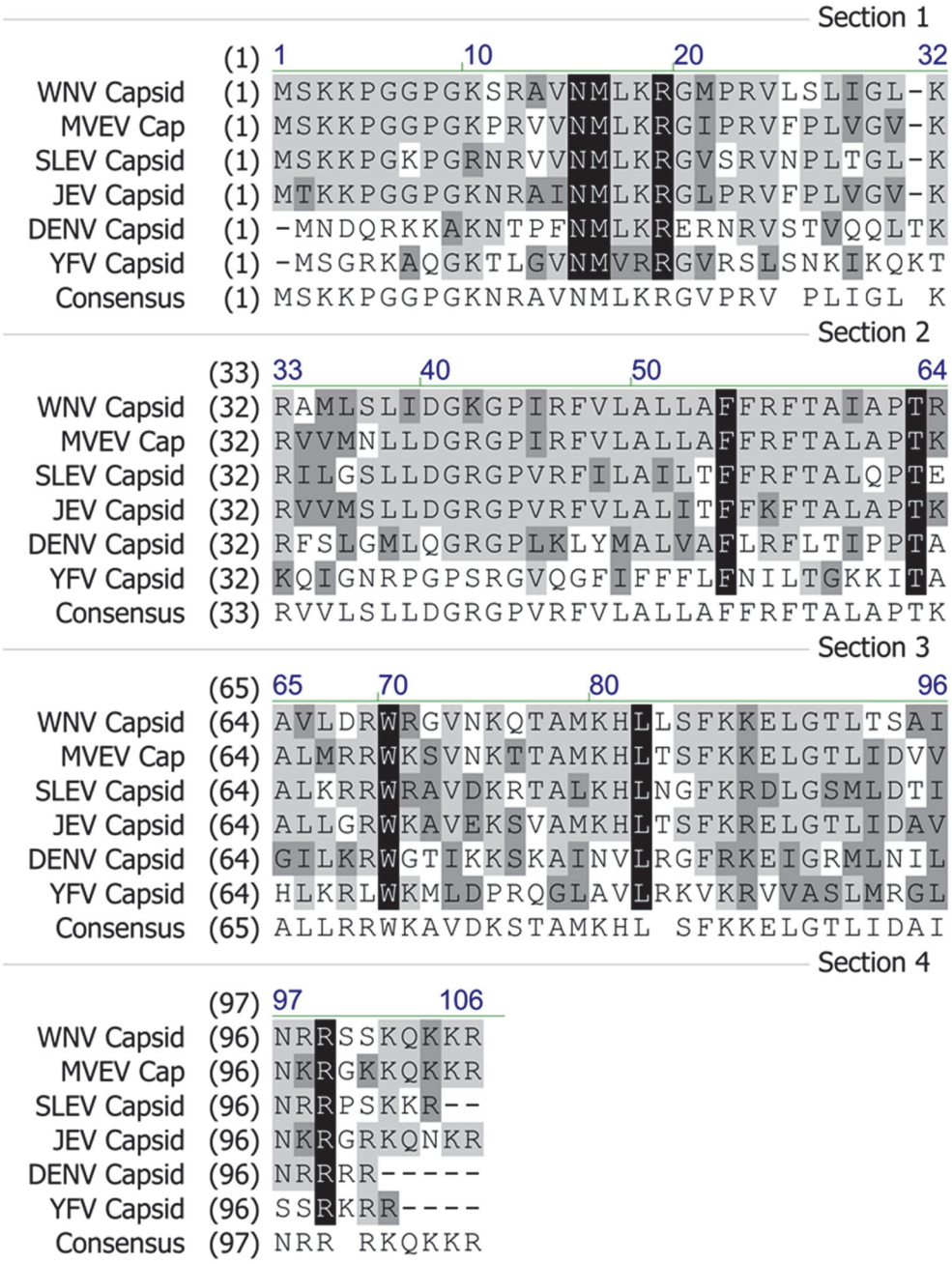

Figure 4.7. Protein sequence alignment of the flavivirus capsids employed in this study. Sequences were obtained from direct strand translation of cDNAs used in the creation of expression constructs for this study. Alignment was carried out using AlignX, with WNV capsid as the first profile. Residues colored light grey indicate a block of identical matches, while those in dark grey are similar. Those residues marked in black are identical in all compared sequences. A consensus based on the sequence of WNV capsid is shown in the last row of the alignment.

4.3 Summary

In this chapter, I examined the anti-apoptotic and cell proliferation enhancing properties of capsid proteins from 6 different flaviviruses. Anti-Fas challenge experiments revealed that in addition to WNV capsid, both MVEV and SLEV capsid proteins offer protection from this agonist in certain cell types. The other flavivirus capsid proteins did not, suggesting that they lack specific sequence motifs required for interaction with critical host factors. It is also possible that those capsid proteins, which did not protect against anti-Fas challenge in A549 cells, do so in other cell types.

In contrast to anti-Fas treatment, A549 cells expressing flavivirus capsid proteins were not resistant to TNFα treatment. These data suggest a protective mechanism that abrogates apoptosis triggered by at least Fas, and perhaps other agonists. These results can direct future studies which seek to understand the specific cellular factors which are required for blockade of apoptosis. The response of capsid expressing cells to other apoptotic agonists can also be examined.

In earlier studies (described in Chapter 3), I showed that expression of WNV capsid protects against anti-Fas challenge in both A549 (Figure 3.4) and HEL/18 (Figure 3.5) cells. However, neither WNV capsid nor any of the other flavivirus capsid proteins protected 1HAE0 cells from anti-Fas treatment. It is possible that this particular cell line lacks a specific factor which is required for capsid-mediated protection. If so, future studies may make use of such

differences in order to determine the identity of the factor or factors required for protection.

In support of the pro-survival role of flavivirus capsid proteins, I found that compared to control cells, phospho-Akt levels were increased in cells expressing MVEV, SLEV and WNV capsid following serum-starvation. These 3 capsid proteins are also the most protective against anti-Fas challenge (Figure 4.2). This correlation strongly suggests that these capsid proteins exert their protective effects through Akt activity. Examination of both cell proliferation and metabolic activities demonstrate that although JEV, DENV and YFV capsid may not protect against anti-Fas challenge, they act to promote both cell proliferation and enhance metabolic activity. This hints at as of yet unknown mechanisms that promote cellular survival and proliferation during growth factor withdrawal and/or stress.

Finally, analysis of the protein sequences of these capsid proteins would suggest that those which protect against anti-Fas challenge share some sequence elements in common. These commonalities provide an avenue for further studies which will determine the role of specific sequence elements in providing anti-apoptotic properties.

Together, these results provide further insight into the biology of flavivirus capsids and their corresponding viruses. Future studies should focus not only on *in vitro* studies in cultured cells but *in vivo* as well, employing recombinant flavivirus strains with engineered mutations in the capsid genes. The ability to

block or reduce the interactions between capsids and the host cell survival machinery may create new possibilities for the synthesis of novel therapeutics and vaccines.

Chapter 5

Discussion

5.1 Overview

The objective of this thesis was to characterize the role of WNV capsid in the modulation of host cell survival during infection. In order to successfully establish a productive infection, viruses must overcome a plethora of host cell defenses, including the activation of cell death pathways. This creates two main paths for evasion: to inhibit the induction of apoptosis to allow time for viral replication, or to enhance it to complement rapid replication kinetics. Given what is known with respect to WNV replication, I hypothesized that WNV capsid is an anti-apoptotic protein that serves to prolong cell survival in order to promote viral replication and spread. Consistent with this prediction, other research groups have published evidence that WNV and other flaviviruses activate cell survival pathways early in the infection process (Lee et al., 2005; Liu et al., 2012; Scherbik and Brinton, 2010; Yang et al., 2012). Blocking the ability of WNV to promote survival signaling leads to rapid onset of apoptosis, and reduced viral titres in cell culture models. In addition, the anti-apoptotic properties of WNV capsid extend to other members of the genus *Flavivirus*, as at least two other capsid proteins protect cells from apoptosis, depending on the agonist employed.

5.2 Roles for the activation of PI3K/Akt signaling in the viral life cycle

5.2.1 Viral binding and entry

The interplay of virus and host is a dynamic process. Starting from the earliest events in infection, all the way through to production of new infectious particles, the host cell employs numerous mechanisms in an attempt to shut down or limit viral replication and spread. At the same time, viruses must evolve strategies which can block or limit these host defenses in order to replicate and produce new virions. One of these critical host defenses is the initiation of PCD by the infected cell. By sacrificing an infected cell, the host is able to limit the ability of a virus to set up a productive infection. For those viruses that are relatively slow at replicating and producing infectious particles, it becomes imperative that they have a means of blocking or delaying this cell death response. This often involves activation of cell survival pathways, commonly those that involve signaling through PI3K/Akt (Hsu et al., 2010; Ji and Liu, 2008; Qin et al., 2011; Wagner and Smiley, 2011).

A study that employed the use of entry defective HSV particles lacking membrane glycoproteins gB, gH or gD examined the ability of virion binding to activate this critical signaling pathway. Activation of Akt by binding of HSV virions in the absence of entry was reported to last for approximately 5 hours, after which it rapidly declined (MacLeod and Minson, 2010). Cheshenko *et al.* subsequently showed that early activation of Akt stimulated by binding of HSV virions stimulates

calcium release and viral entry. Depletion of Akt via the use of siRNAs blocked calcium release, and inhibited plaque formation (Cheshenko et al., 2013). In this way, the activation of a kinase that is well characterized for its ability to promote cell survival also assists viral entry.

Data from studies on HCV demonstrate that cell survival signaling can be triggered by RNA virus binding as well. Specifically, interaction of HCV particles with the cell surface results in transient activation of the PI3K/Akt pathway (Liu et al., 2012). Phosphorylation of Akt at S473 peaks by 30 minutes, and declines until it is undetectable before 24 hours. This effect is likely due to the engagement of the HCV receptors CD81 and claudin-1. Specifically, addition of activating antibodies to these receptors, but not unrelated cell surface molecules had the same effect as HCV binding (Liu et al., 2012). Silencing of Akt via siRNAs led to significant inhibition of HCV infection, as did the use of the inhibitor Akt-V pre-infection. However, use of the inhibitor post-infection did not affect HCV infection, suggesting that this effect is most important for entry of HCV particles. These data, in combination with what is known about the ability of WNV and other flaviviruses to activate PI3K/Akt early in the infection process (section 1.3.1.3) demonstrate an interesting trend in how a number of viruses interact with their hosts.

5.2.2 Promotion of cell survival during replication

Following entry and uncoating of viral particles, the replication of viral genomes and the production of viral proteins triggers a number of antiviral host defenses. These include the initiation of PCD, a process that can be countered by the activation of cell survival pathways. This represents a longer term consequence of PI3K/Akt activation, beyond that which is required for entry of some viruses.

Activation of Akt by viral proteins has been shown to promote the survival of infected cells and phosphorylation of downstream targets such as the kinase complex mTORC1 (Wagner and Smiley, 2011). The HSV proteins VP11 and VP12 can stimulate PI3K/Akt signaling through interaction with PI3K directly or indirectly PI3K complexes. Interestingly, these proteins are part of the viral tegument, which is contained within the nucleocapsid. Similar to WNV capsid, they are exposed to the host cell cytoplasm early in the infection process and are subsequently produced following the initiation of gene transcription and translation. In the aforementioned study, activating phosphorylation of Akt was examined at later times post-infection than those that demonstrated a role for it in viral entry. These later effects were shown to be dependent on VP11 and VP12, and not just binding of virions to the cell surface. Lastly, activation of these kinases has been shown to inhibit apoptosis in oral epithelial cells during HSV infection (Hsu et al., 2010).

The genomes of WNV and other flaviviruses are relatively small compared to DNA viruses. Thus, in order to fulfill the many functions needed for virus replication, assembly and interaction with host cell signaling pathways, products of these genomes must be multifunctional. Capsid is exposed to the host cell cytoplasmic *millieu* probably more than other viral proteins because it is part of the virion itself and is the first viral protein produced following infection. These characteristics make flavivirus capsid proteins well adapted for interfering with early host responses to viral infection such as the initiation of cell death.

5.2.3 Establishment of persistence

A significant body of evidence suggests that PI3K/Akt signaling is a critical process in promoting cell survival, including during viral infection. A logical extension of this concept is that modulation of this host cell machinery could facilitate the establishment of viral persistence. In fact, several viruses which create persistent infections have been shown to affect aspects of PI3K/Akt signaling.

Perhaps the most prominent example of this is provided by HCV, which frequently establishes persistence in hosts following an acute phase of infection. The non-structural protein NS5A interacts with key cellular signaling components such as the adaptor protein Grb2, and the p85 subunit of PI3K (He et al., 2002). The outcome of these interactions is increased tyrosine phosphorylation of Akt, and subsequently higher levels of phospho-BAD. In its dephosphorylated form,

BAD is able to promote apoptosis by blocking the activity of anti-apoptotic Bcl-2 family members (Gupta et al., 2001; Yang et al., 1995). However, when phosphorylated it is inactivated. This leads to its sequestration by 14-3-3 proteins and increases survival of infected cells, lowering the barrier to establishment of persistent infection. Curiously, the effects of NS5A are not merely anti-apoptotic. In addition to activating PI3K/Akt signaling associated with cell survival, NS5A inhibits mitogenic signaling. This is mediated by Grb2 binding, which leads to inhibition of Extracellular Signal Regulated Kinases 1 and 2 (ERK1/2) signaling in the presence of Extracellular Growth Factor (EGF) (He et al., 2002). Thus, mitosis is inhibited in concert with an enhancement of anti-apoptotic signaling. The combination of these two effects likely represents an important set of conditions required for the establishment of persistent infection.

5.3 Role for the interaction of flavivirus capsid proteins with cellular phosphatases

5.3.1 Protein phosphatase 2A

Protein phosphatase 2A describes a large number of dimeric and trimeric Serine/Threonine phosphatases that make up almost 1% of total cellular protein. Indeed, this group of phosphatases accounts for most of the serine/threonine phosphatase activity in mammalian cells (Millward et al., 1999). It is estimated

that 33% of cellular proteins are Serine/Threonine phosphorylated. Given this fact, it is no surprise that PP2A holoenzymes regulate a large number of cellular processes through dephosphorylation including, but not limited to, cell cycle progression, metabolism, and cell death. Generally, PP2A holoenzymes are composed of a core dimeric enzyme referred to as $PP2A_D$, and a structural subunit known as $PP2A_A$. This core enzyme can exist by itself, or in complex with a number of regulatory subunits known as B subunits or $PP2A_B$. These B subunits are members of four distinct classes known as B, B', B'' and B'''. Adding to the diversity of these regulatory subunits, each of them can exist as distinct isoforms. This allows for over 75 distinct PP2A holoenzyme combinations (Sents et al., 2013). In combination with a variety of posttranslational modifications, this diversity in composition allows for a remarkable degree of control over activity and substrate specificity. A detailed examination of the breadth and depth of PP2A biology is not warranted here, however, its role in the modulation of PI3K/Akt activity merits discussion.

PP2A can inhibit the activity of Akt through direct interaction and subsequent dephosphorylation of the residues T308 and S473 (Li et al., 2003). Viral proteins have been shown to affect this process by inhibiting PP2A and thus promoting Akt activation such as polyoma virus small T, and HCV NS5A (Duong et al., 2004; Georgopoulou et al., 2006). These effects can be context dependent as well. As an example, polyoma small T can either promote or inhibit apoptosis, depending on the presence of growth factors (Andrabi et al., 2007). The fact that

viruses would target PP2A activity is not surprising, given its great importance in determining cell fate. The NS5A protein of HCV can act as a PP2A B-subunit mimic that interacts with the core dimeric enzyme to upregulate PP2A enzymatic activity (Georgopoulou et al., 2006; Giannini and Brechot, 2003). This leads to increased viral NS3 helicase activity, and inhibition of IFN-α mediated antiviral signaling, and subsequently, enhanced replication of HCV (Duong et al., 2004). However, these studies did not examine survival signaling to determine if NS5A also altered substrate specificity as well.

5.3.2 Inhibitor 2 of PP2A

The activity of PP2A is also regulated by interaction with inhibitor proteins, specifically, I_1^{PP2A} and I_2^{PP2A}. These serve to reduce PP2A activity, yet all of the contexts in which this activity is important are not clear. I_2^{PP2A} has been shown to bind WNV capsid, an interaction which affects PP2A activity (Hunt et al., 2007). Total PP2A activity was examined using an *in vitro* phosphatase assay in which dephosphorylation of a radioactive substrate was measured. Interestingly, an increase in PP2A activity was observed when WNV capsid was expressed via transfection. This study was the first report that WNV capsid could affect PP2A activity. However, it is not known how WNV capsid may alter the activity of specific PP2A holoenzymes to mediate effects such as inhibition of Fas-mediated apoptosis. The sequestration or blockade of some PP2A holoenzymes and not

others may allow for enhanced activity of PI3K/Akt, increasing survival during anti-Fas challenge.

A diverse set of PP2A complexes is known to regulate a large number of cellular processes including those that determine cell fate. The idea that viral proteins have evolved to manipulate PP2A complexes to create a more permissive environment for infection and replication is well supported by the literature (Law et al., 2013; Mori et al., 2013; Shanker et al., 2013). The list of viruses which interface with PI3K/Akt as well as PP2A is constantly growing. This list includes WNV, and potentially other flaviviruses.

5.4 A role for flavivirus capsids in inhibiting host cell apoptosis

5.4.1 Death receptor-mediated apoptosis

Initiation of apoptosis through death receptors on the cell surface is one of the major PCD pathways (section 1.2.1.2). This process is thought to be important for the clearance of virus infected cells, along with PCD triggered by intrinsic mechanisms. Of particular relevance to this thesis is the binding of ligands to the Fas receptor and TNF receptor. The activation of these receptors is known to occur in a variety of cell types, which express FasL or secrete TNF. Additionally, these effects can be mediated in a paracrine and/or autocrine manner. My experimental data indicate that flavivirus capsids can affect multiple points in the apoptotic program (Figure 5.1)

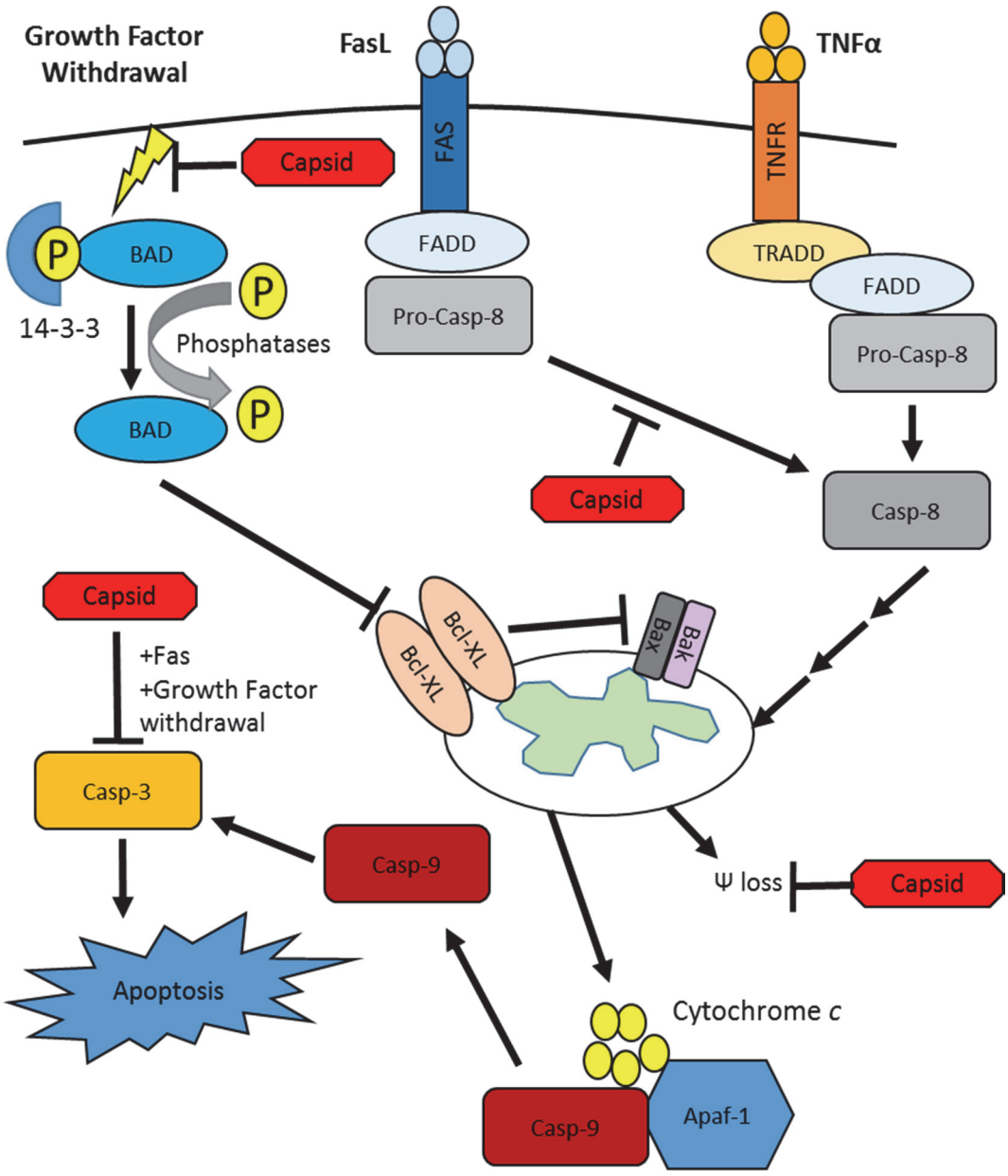

Figure 5.1. Overview of the apoptotic program inhibited by WNV capsid. Apoptosis triggered by 3 different mechanisms is depicted. The shapes labelled "capsid" point out steps in the apoptotic program that are inhibited by capsid (confirmed by experimental data). Note that capsid does not inhibit apoptosis initiated by TNFα. Withdrawal of growth factors leads to the accumulation of stress signals and affects the action of several BH3-only proteins such as Bad, a key player in promoting apoptosis via serum starvation. Following dephosphorylation, Bad binds to and inhibits the activity of the pro-survival protein Bcl-XL, allowing for the activity of the pro-apoptotic BH3-only proteins Bax and Bak to dominate. Note the greek symbol Ψ, which represents mitochondrial membrane potential.

5.4.1.1 Fas-mediated apoptosis

During viral infection, Fas-mediated apoptosis is triggered by several cell types of the host immune system. This occurs in an attempt to eliminate infected cells, ideally before they are able to produce a large number of progeny virions.

The ability of various flavivirus capsids to inhibit the progression of Fas-mediated apoptosis is likely dependent on their ability to interact with specific host cell factors. As stated previously, viruses with comparatively small genomes must by necessity encode proteins that are multifunctional. This allows for the interaction of viral proteins with numerous cellular factors. Although flavivirus capsid proteins share similar features, differences in primary sequence likely allow for binding with different cohorts of proteins. Given data that indicate a link between WNV capsid and a PP2A binding protein, it is possible that inhibition of a specific PP2A complexe(s) is responsible for capsid's anti-apoptotic properties (Hunt et al., 2007). Determining if MVEV and SLEV capsid binding proteins include PP2A subunits or regulatory proteins will provide more detailed information on how these proteins inhibit Fas-mediated apoptosis.This concept fits well with what is known with respect to PI3K/Akt activity and its interaction with PP2A. Capsid proteins that are unable to decrease the onset of apoptosis in response to Fas may lack the ability to interact with a key protein necessary for blocking dephosphorylation of specific Akt substrates by PP2A involved in Fas signaling.

As an example of this, the cellular protein c-FLIP is known to be regulated by PI3K/Akt (Quintavalle et al., 2010; Wang et al., 2008). This caspase-like protein

lacks any protease activity but is capable of forming heteromers with pro-caspase-8 to inhibit proteolytic processing. This activity is enhanced by Akt in two ways: The direct phosphorylation and stabilization of c-FLIP, and the increase in mRNA levels stimulated by Akt-directed phosphorylation of transcription factors (Figure 5.2). Through maintaining activation of PI3K/Akt by blocking specific PP2A complexes, capsid could potentially increase both transcription and protein stability of c-FLIP, which would then antagonize Fas-mediated caspase-8 activation.

Variation in the expression or availability of critical host cell-encoded capsid-binding proteins that are required for enhancement of cell survival can also vary by cell type. Data from experiments carried out in Section 4.2.5 indicates that although WNV capsid can protect against anti-Fas challenge in A549 and HEL/18 cells, this is not the case in 1HAE0 cells. This may reflect the absence of a specific capsid binding protein which is required for protection. Capsid proteins that lack the ability to block or sequester specific PP2A complexes that dephosphorylate Akt and its substrates would be unable to inhibit apoptosis. This idea is further supported by data from section 4.2.6 which show that only those capsid proteins which protect against anti-Fas treatment are capable of enhancing Akt phosphorylation. Future studies may well make use of this difference to identify the identity of this factor.

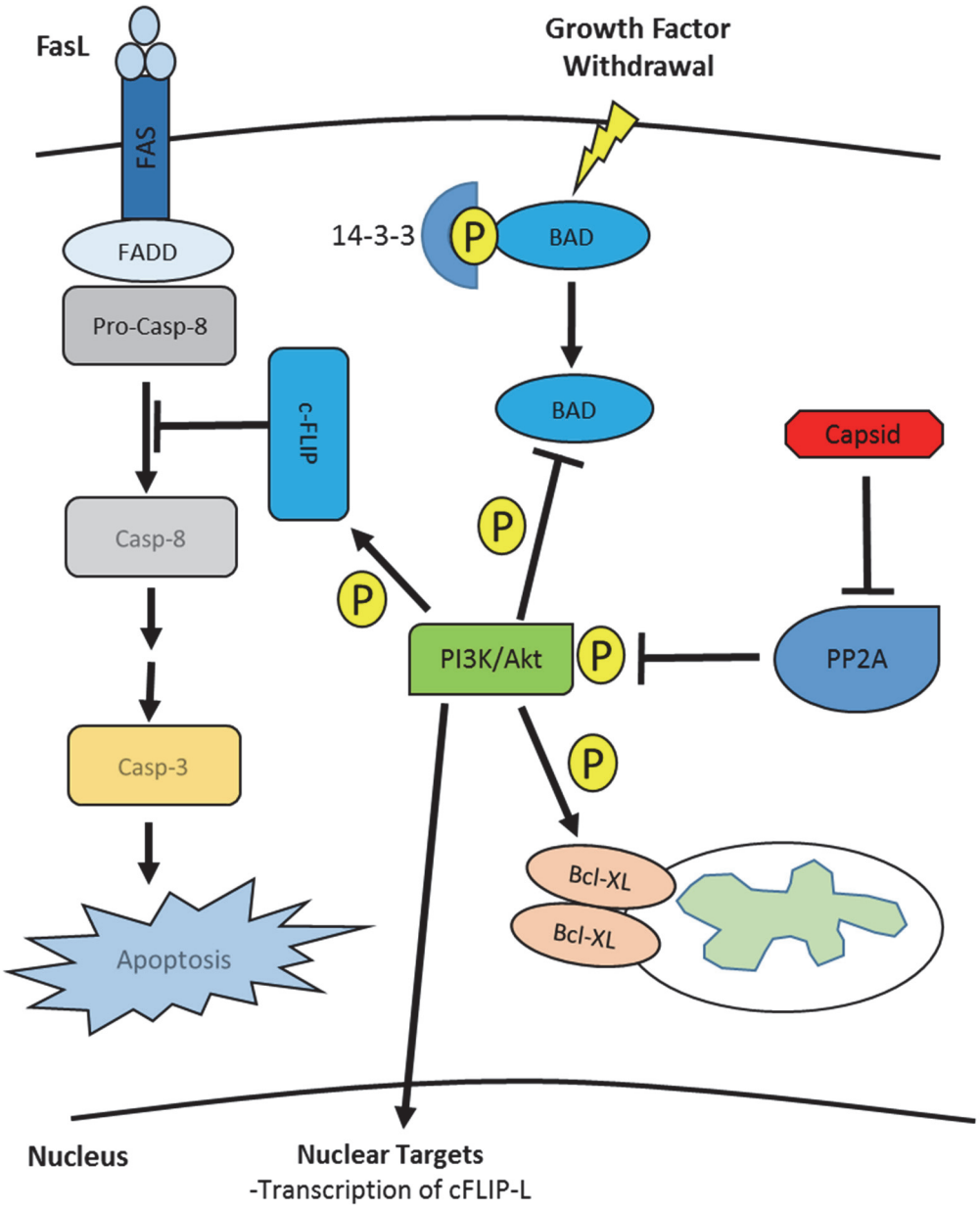

Figure 5.2. Model of how enhanced PI3K/Akt activity can prevent apoptosis initiated by Fas or growth factor withdrawal. By interfering with the activities of specific PP2A complexes, capsid inhibits dephosphorylation, and thus inactivation of Akt. This allows Akt to act at multiple steps in the apoptotic program, enhancing the phosphorylation and inactivation of Bad, increasing c-FLIP-L levels, and inactivating pro-apoptotic transcription factors. Additionally, the anti-apoptotic activity of Bcl-XL is enhanced by Akt phosphorylation, promoting retention of mitochondrial membrane potential, and inhibition of cytochrome *c* release.

5.4.1.2 TNFα

The anti-viral effects of TNFα during viral infection vary with respect to the virus and cell type (Wortzman et al., 2013). Depending on context, TNFα can trigger cell death or activate cell survival pathways (reviewed in (Napetschnig and Wu, 2013; Ramseyer and Garvin, 2013; Waters et al., 2013)). TNFα also induces inflammatory reactions that are important for clearing pathogens. Indeed, TNFα plays a pivotal role in orchestrating the actions of both cellular and humoral immunity, to resolve infections.

The role of TNFα in WNV infection is likely that of protection and inflammatory response intiation (Shrestha et al., 2008). Treatment of neurons *ex-vivo* with TNFα, followed by WNV infection reduces caspase-3 activation and promotes survival (Zhang et al., 2010). In this regard, it is not surprising that flavivirus capsids do not protect against TNFα during apoptotic challenge. This is likely due to the differing mechanisms by which TNFα can initiate the apoptotic program in comparison to Fas, which is detailed below.

Through interaction with the TRADD protein, TNFR recruits FADD and subsequently pro-caspase-8 (Figure 5.3). An adapter protein known as TNFα receptor associated factor 2 interacts with TRADD (Nishitoh et al., 1998). This protein can recruit and activate the kinase apoptosis stimulating kinase 1, which is normally kept in an inactive complex with its inhibitor thioredoxin (Tobiume et al., 2002). However, during the application of cellular stress, thioredoxin is dissociated, and apoptosis stimulating kinase 1 can be activated. This leads to

signal transduction that ultimately activates the pro-apoptotic kinase JNK, which can then phosphorylate several targets to bring about cell death (Bogoyevitch and Kobe, 2006). Of note is the E3 ubiquitin ligase Itch, which upon JNK phosphorylation is able to ubiquitinate several anti-apoptotic substrates including c-FLIP (Chang et al., 2006; Schlatter et al., 2011). This relieves repression of caspase-8 activation and potentiates apoptosis; thereby providing a possible mechanism by which TNFα-induced apoptosis is not affected by expression of WNV capsid (Figure 5.3).

5.4.2 Flavivirus capsid protein sequence analysis

The comparison of the protein sequences of capsids employed in this study reveals indicates that those capsid proteins which protect against anti-Fas challenge share sequence features in common (Figure 4.6). The N-termini of WNV, MVEV and SLEV capsids contain an "MSKK" motif which is not present in other examined capsid proteins (Figure 4.7). The closest match is an "MTKK" from JEV capsid, which does not protect against Fas. This suggests that the serine residue at position 2 may be important. Another motif "FRFTA" is common to WNV, MVEV and SLEV capsids. This 5-amino acid residue stretch is mostly hydrophobic and may be in part responsible for mediating interactions with binding partners. Mutational analysis of these and other residues will reveal important information about how these capsid proteins inhibit Fas-mediated apoptosis.

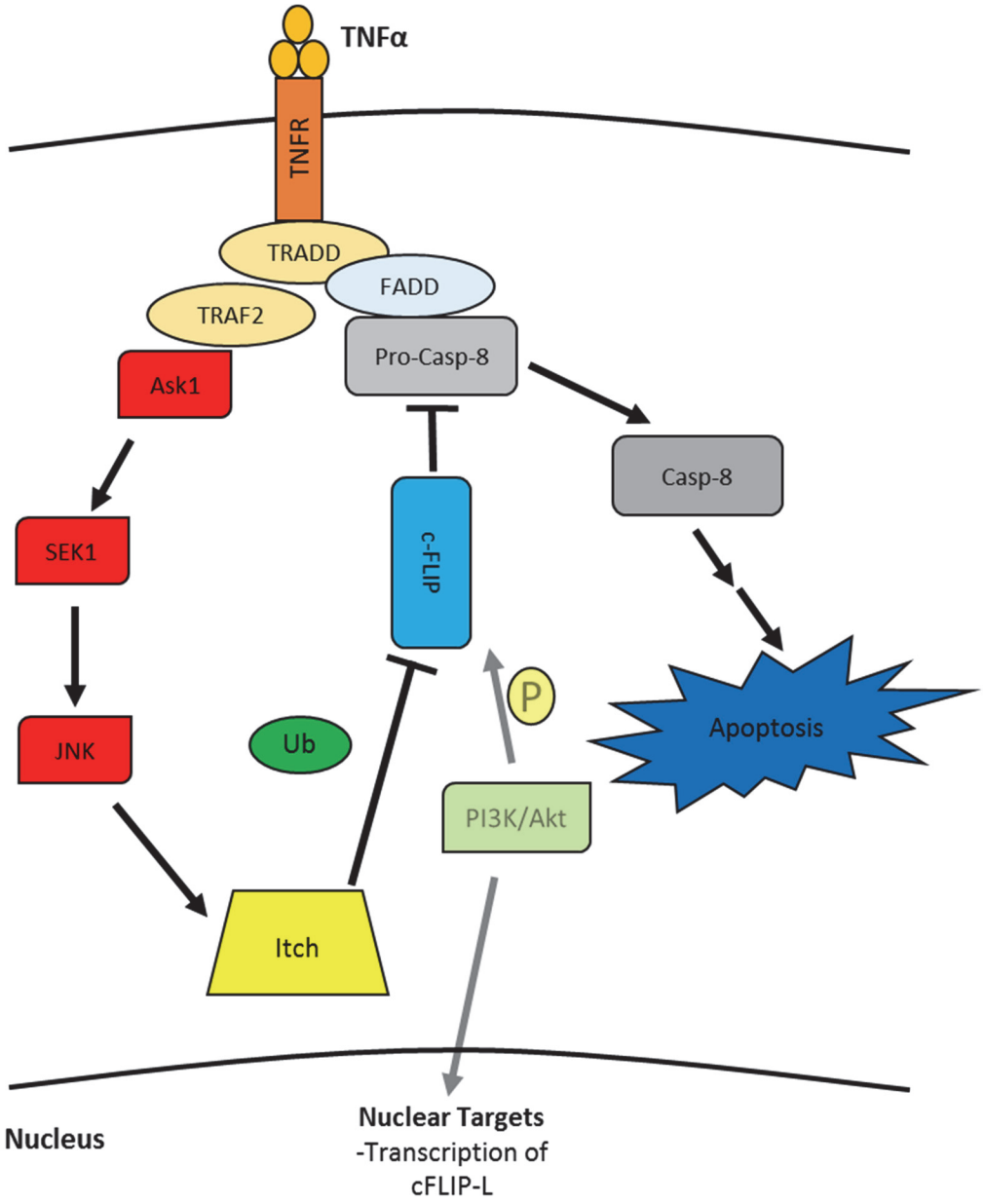

Figure 5.3. Model depicting why TNFα-induced apoptosis is resistant to capsid expression. In contrast to Fas-mediated apoptosis, binding of TNFα can promote either survival or apoptosis. Interaction of TRAF2 with the kinase Ask1 under conditions of stress, promotes JNK activation and the subsequent enhancement of Itch activity. This E3 ubiquitin ligase then promotes degradation of c-FLIP, a caspase-like molecule (lacks protease activity) that inhibits caspase-8 activation. It is likely that these events predominate over the actions of Akt, which serves to both stabilize c-FLIP-L through phosphorylation, and increase its levels through enhanced transcription.

5.5 Cellular proliferation and metabolism

The effects of growth factor withdrawal in cell culture can include cell cycle arrest and eventually, apoptosis (Maurer et al., 2006). The kinetics of these processes can vary with the cell line examined. The observation that those capsid proteins that block Fas-mediated apoptosis also significantly enhance Akt phosphorylation at serine-473 creates a distinct possibility that they may also enhance proliferation as well. The activity of Akt has been extensively studied in the context of its mitogenic capabilities, and is of great interest as a target for oncotherapy (reviewed in (Cecconi et al., 2012; Fyffe and Falasca, 2013; Wu et al., 2013)). The results of the serum starvation experiments in section 4.2.6 would indicate that both those capsids which enhance Akt phosphorylation and those that do not can promote cell division and metabolism (Figure 4.6). This observation suggests that this function is independent of Akt activation and hints at an alternate mechanism that these capsid proteins have in common. Alternatively, resistance to anti-fas mediated apoptosis may be a "knock on" effect of enhanced cellular metabolism and proliferation, which includes enhanced glucose utilization and oxidative respiration. The activation of Akt has been strongly associated with enhancement of glucose utilization, in addition to enhanced translation and cell growth. This includes modulation of insulin induced signaling, which forms a central part of glucose metabolism (Cordero-Espinoza and Hagen, 2013; Sylow et al., 2013; Tsuchiya et al., 2013).

Although many molecular events take place during growth factor withdrawal, a key player is the BH3 only protein BAD (Section 1.2.3.4). During growth factor withdrawal, BAD is dephosphorylated, and is then able to participate in the intrinsic pathway of apoptosis. Increased cellular proliferation combined with enhanced mitochondrial respiration suggests that BAD phosphorylation is preserved. Future studies will examine this possibility.

5.6 Future directions and perspective

The interaction of a viral pathogen with its host organism occurs as a complex series of events in which the primary goal of the virus is simply to replicate and produce infectious particles. At the same time, complex metazoan hosts such as humans employ a large number of intrinsic, innate and adaptive immune responses in an attempt eliminate the foreign invader. If this response is inadequate or too robust, the host can fail to clear the pathogen, or inflict severe damage upon itself. It is evasion of this appropriate and balanced immune response that viral pathogens have evolved to avoid through a number of strategies. Thus, viral disease can be thought of as the consequence of an inappropriate immune response against a pathogen which has evolved to avoid it.

The inhibition of PCD by WNV and other capsids is very likely one of these immune avoidance mechanisms that serves to stave off the host response long enough to permit sufficient replication and spread. The data presented in this thesis detail the ability of WNV and other flavivirus capsids to inhibit the

progression of cell death by Fas ligation, a mechanism that is common in both innate and adaptive immune responses. Although studies have examined the role of FasL in CNS infection and subsequent mortality, the contribution of WNV capsid to successful replication in peripheral tissues remains unknown. Thus, *in vivo* studies which investigate the role of the PI3K/Akt dependent apoptosis inhibition will add greater depth to our understanding of WNV induced disease. Blockade of the protective effects of capsid would likely inhibit early virus replication, and allow for a more effective immune response.

In order to create possibilities for therapies that target the ability of capsid to function as an inhibitor of apoptosis, further studies on the macromolecular basis of this phenomenon are needed. Given the fact that WNV capsid is known to interact with the PP2A binding protein I_2^{PP2A}, and because capsid prolongs Akt phosphorylation when growth factors are reduced, PP2A is likely at the center of this mechanism. The regulation of PP2A activity is complex, as many different holoenzyme combinations can be regulated via a variety of protein-protein interactions and post translational modifications.

The mitogenic and metabolic effects of these capsid proteins do not yet have a molecular basis. A comprehensive study of the host cell factors which interact with these capsid proteins will reveal commonalities that are responsible for this phenomenon. Eventually, a greater number of therapeutic targets will be revealed, improving the state of vaccination and treatment for all flaviviruses.

References

Centers for Disease Control - West Nile Virus and Other Arboviral Diseases — United States, 2012.*2013,*

Aguirre, A., Shoji, K.F., Saez, J.C., Henriquez, M., and Quest, A.F. (2013). FasL-triggered death of Jurkat cells requires caspase 8-induced, ATP-dependent cross-talk between Fas and the purinergic receptor P2X(7). J. Cell. Physiol. *228,* 485-493.

Ahmed, N.N., Franke, T.F., Bellacosa, A., Datta, K., Gonzalez-Portal, M.E., Taguchi, T., Testa, J.R., and Tsichlis, P.N. (1993). The proteins encoded by c-akt and v-akt differ in post-translational modification, subcellular localization and oncogenic potential. Oncogene *8,* 1957-1963.

Alessi, D.R., Deak, M., Casamayor, A., Caudwell, F.B., Morrice, N., Norman, D.G., Gaffney, P., Reese, C.B., MacDougall, C.N., Harbison, D., Ashworth, A., and Bownes, M. (1997). 3-Phosphoinositide-dependent protein kinase-1 (PDK1): structural and functional homology with the Drosophila DSTPK61 kinase. Curr. Biol. *7,* 776-789.

Alessi, D.R., James, S.R., Downes, C.P., Holmes, A.B., Gaffney, P.R., Reese, C.B., and Cohen, P. (1997). Characterization of a 3-phosphoinositide-dependent protein kinase which phosphorylates and activates protein kinase Balpha. Curr. Biol. *7,* 261-269.

Alessi, D.R., Kozlowski, M.T., Weng, Q.P., Morrice, N., and Avruch, J. (1998). 3-Phosphoinositide-dependent protein kinase 1 (PDK1) phosphorylates and activates the p70 S6 kinase in vivo and in vitro. Curr. Biol. *8,* 69-81.

Alvarez, D.E., Filomatori, C.V., and Gamarnik, A.V. (2008). Functional analysis of dengue virus cyclization sequences located at the 5' and 3'UTRs. Virology *375,* 223-235.

Amberg, S.M., and Rice, C.M. (1999). Mutagenesis of the NS2B-NS3-mediated cleavage site in the flavivirus capsid protein demonstrates a requirement for coordinated processing. J. Virol. *73,* 8083-8094.

Andrabi, S., Gjoerup, O.V., Kean, J.A., Roberts, T.M., and Schaffhausen, B. (2007). Protein phosphatase 2A regulates life and death decisions via Akt in a context-dependent manner. Proc. Natl. Acad. Sci. U. S. A. *104,* 19011-19016.

Anez, G., Grinev, A., Chancey, C., Ball, C., Akolkar, N., Land, K.J., Winkelman, V., Stramer, S.L., Kramer, L.D., and Rios, M. (2013). Evolutionary dynamics of West

Nile virus in the United States, 1999-2011: phylogeny, selection pressure and evolutionary time-scale analysis. PLoS Negl Trop. Dis. *7,* e2245.

Balachandran, S., Roberts, P.C., Kipperman, T., Bhalla, K.N., Compans, R.W., Archer, D.R., and Barber, G.N. (2000). Alpha/beta interferons potentiate virus-induced apoptosis through activation of the FADD/Caspase-8 death signaling pathway. J. Virol. *74,* 1513-1523.

Barba, G., Harper, F., Harada, T., Kohara, M., Goulinet, S., Matsuura, Y., Eder, G., Schaff, Z., Chapman, M.J., Miyamura, T., and Brechot, C. (1997). Hepatitis C virus core protein shows a cytoplasmic localization and associates to cellular lipid storage droplets. Proc. Natl. Acad. Sci. U. S. A. *94,* 1200-1205.

Bassinet, L., Gueirard, P., Maitre, B., Housset, B., Gounon, P., and Guiso, N. (2000). Role of adhesins and toxins in invasion of human tracheal epithelial cells by Bordetella pertussis. Infect. Immun. *68,* 1934-1941.

Beasley, D.W., Whiteman, M.C., Zhang, S., Huang, C.Y., Schneider, B.S., Smith, D.R., Gromowski, G.D., Higgs, S., Kinney, R.M., and Barrett, A.D. (2005). Envelope protein glycosylation status influences mouse neuroinvasion phenotype of genetic lineage 1 West Nile virus strains. J. Virol. *79,* 8339-8347.

Beer-Romero, P., Glass, S., and Rolfe, M. (1997). Antisense targeting of E6AP elevates p53 in HPV-infected cells but not in normal cells. Oncogene *14,* 595-602.

Bellacosa, A., Franke, T.F., Gonzalez-Portal, M.E., Datta, K., Taguchi, T., Gardner, J., Cheng, J.Q., Testa, J.R., and Tsichlis, P.N. (1993). Structure, expression and chromosomal mapping of c-akt: relationship to v-akt and its implications. Oncogene *8,* 745-754.

Berg, P.J., Smallfield, S., and Svien, L. (2010). An investigation of depression and fatigue post West Nile virus infection. S. D. Med. *63,* 127-9, 131-3.

Beroukhim, R., Mermel, C.H., Porter, D., Wei, G., Raychaudhuri, S., Donovan, J., Barretina, J., Boehm, J.S., Dobson, J., Urashima, M.*, et al.* (2010). The landscape of somatic copy-number alteration across human cancers. Nature *463,* 899-905.

Bhuvanakantham, R., Chong, M.K., and Ng, M.L. (2009). Specific interaction of capsid protein and importin-alpha/beta influences West Nile virus production. Biochem. Biophys. Res. Commun. *389,* 63-69.

Bhuvanakantham, R., Chong, M.K., and Ng, M.L. (2009). Specific interaction of capsid protein and importin-alpha/beta influences West Nile virus production. Biochem. Biophys. Res. Commun. *389,* 63-69.

Bhuvanakantham, R., and Ng, M.L. (2013). West Nile virus and dengue virus capsid protein negates the antiviral activity of human Sec3 protein through the proteasome pathway. Cell. Microbiol.

Blakely, P.K., Kleinschmidt-DeMasters, B.K., Tyler, K.L., and Irani, D.N. (2009). Disrupted glutamate transporter expression in the spinal cord with acute flaccid paralysis caused by West Nile virus infection. J. Neuropathol. Exp. Neurol. *68,* 1061-1072.

Bluml, S., Scheinecker, C., Smolen, J.S., and Redlich, K. (2012). Targeting TNF receptors in rheumatoid arthritis. Int. Immunol. *24,* 275-281.

Bogoyevitch, M.A., and Kobe, B. (2006). Uses for JNK: the many and varied substrates of the c-Jun N-terminal kinases. Microbiol. Mol. Biol. Rev. *70,* 1061-1095.

Bradbury, J. (2005). Toll gate for West Nile virus brain entry. Lancet Infect. Dis. *5,* 9.

Bradfute, S.B., Swanson, P.E., Smith, M.A., Watanabe, E., McDunn, J.E., Hotchkiss, R.S., and Bavari, S. (2010). Mechanisms and consequences of ebolavirus-induced lymphocyte apoptosis. J. Immunol. *184,* 327-335.

Brenner, D., Krammer, P.H., and Arnold, R. (2008). Concepts of activated T cell death. Crit. Rev. Oncol. Hematol. *66,* 52-64.

Brunet, A., Bonni, A., Zigmond, M.J., Lin, M.Z., Juo, P., Hu, L.S., Anderson, M.J., Arden, K.C., Blenis, J., and Greenberg, M.E. (1999). Akt promotes cell survival by phosphorylating and inhibiting a Forkhead transcription factor. Cell *96,* 857-868.

Cabal-Hierro, L., and Lazo, P.S. (2012). Signal transduction by tumor necrosis factor receptors. Cell. Signal. *24,* 1297-1305.

Cabal-Hierro, L., and Lazo, P.S. (2012). Signal transduction by tumor necrosis factor receptors. Cell. Signal. *24,* 1297-1305.

Cantarini, L., Lucherini, O.M., Muscari, I., Frediani, B., Galeazzi, M., Brizi, M.G., Simonini, G., and Cimaz, R. (2012). Tumour necrosis factor receptor-associated periodic syndrome (TRAPS): state of the art and future perspectives. Autoimmun. Rev. *12,* 38-43.

Carbone, M., Rizzo, P., Grimley, P.M., Procopio, A., Mew, D.J., Shridhar, V., de Bartolomeis, A., Esposito, V., Giuliano, M.T., Steinberg, S.M.*, et al.* (1997). Simian

virus-40 large-T antigen binds p53 in human mesotheliomas. Nat. Med. *3,* 908-912.

Carmona-Gutierrez, D., Eisenberg, T., Buttner, S., Meisinger, C., Kroemer, G., and Madeo, F. (2010). Apoptosis in yeast: triggers, pathways, subroutines. Cell Death Differ. *17,* 763-773.

Carnero, A. (2010). The PKB/AKT pathway in cancer. Curr. Pharm. Des. *16,* 34-44.

Carson, P.J., Konewko, P., Wold, K.S., Mariani, P., Goli, S., Bergloff, P., and Crosby, R.D. (2006). Long-term clinical and neuropsychological outcomes of West Nile virus infection. Clin. Infect. Dis. *43,* 723-730.

Cecconi, S., Mauro, A., Cellini, V., and Patacchiola, F. (2012). The role of Akt signalling in the mammalian ovary. Int. J. Dev. Biol. *56,* 809-817.

Centers For Disease Control. West Nile Virus and Other Arboviral Diseases — United States, 2012.*2013,*

Chang, L., Kamata, H., Solinas, G., Luo, J.L., Maeda, S., Venuprasad, K., Liu, Y.C., and Karin, M. (2006). The E3 ubiquitin ligase itch couples JNK activation to TNFalpha-induced cell death by inducing c-FLIP(L) turnover. Cell *124,* 601-613.

Checkley, M.A., Luttge, B.G., and Freed, E.O. (2011). HIV-1 envelope glycoprotein biosynthesis, trafficking, and incorporation. J. Mol. Biol. *410,* 582-608.

Chen, R., Kim, O., Yang, J., Sato, K., Eisenmann, K.M., McCarthy, J., Chen, H., and Qiu, Y. (2001). Regulation of Akt/PKB activation by tyrosine phosphorylation. J. Biol. Chem. *276,* 31858-31862.

Cheng, E.H., Nicholas, J., Bellows, D.S., Hayward, G.S., Guo, H.G., Reitz, M.S., and Hardwick, J.M. (1997). A Bcl-2 homolog encoded by Kaposi sarcoma-associated virus, human herpesvirus 8, inhibits apoptosis but does not heterodimerize with Bax or Bak. Proc. Natl. Acad. Sci. U. S. A. *94,* 690-694.

Cheshenko, N., Trepanier, J.B., Stefanidou, M., Buckley, N., Gonzalez, P., Jacobs, W., and Herold, B.C. (2013). HSV activates Akt to trigger calcium release and promote viral entry: novel candidate target for treatment and suppression. FASEB J. *27,* 2584-2599.

Chipuk, J.E., Kuwana, T., Bouchier-Hayes, L., Droin, N.M., Newmeyer, D.D., Schuler, M., and Green, D.R. (2004). Direct activation of Bax by p53 mediates mitochondrial membrane permeabilization and apoptosis. Science *303,* 1010-1014.

Chung, W.M., Buseman, C.M., Joyner, S.N., Hughes, S.M., Fomby, T.B., Luby, J.P., and Haley, R.W. (2013). The 2012 West Nile encephalitis epidemic in Dallas, Texas. JAMA *310,* 297-307.

Ciuffreda, L., Di Sanza, C., Incani, U.C., and Milella, M. (2010). The mTOR pathway: a new target in cancer therapy. Curr. Cancer. Drug Targets *10,* 484-495.

Clinton, G.M., Little, S.P., Hagen, F.S., and Huang, A.S. (1978). The matrix (M) protein of vesicular stomatitis virus regulates transcription. Cell *15,* 1455-1462.

Cohen, P., Alessi, D.R., and Cross, D.A. (1997). PDK1, one of the missing links in insulin signal transduction? FEBS Lett. *410,* 3-10.

Cordero-Espinoza, L., and Hagen, T. (2013). Increased concentrations of Fructose-2,6-bisphosphate contribute to the Warburg effect in PTEN-deficient cells. J. Biol. Chem.

Daffis, S., Samuel, M.A., Suthar, M.S., Gale, M.,Jr, and Diamond, M.S. (2008). Toll-like receptor 3 has a protective role against West Nile virus infection. J. Virol. *82,* 10349-10358.

Daffis, S., Szretter, K.J., Schriewer, J., Li, J., Youn, S., Errett, J., Lin, T.Y., Schneller, S., Zust, R., Dong, H.*, et al.* (2010). 2'-O methylation of the viral mRNA cap evades host restriction by IFIT family members. Nature *468,* 452-456.

Darman, J., Backovic, S., Dike, S., Maragakis, N.J., Krishnan, C., Rothstein, J.D., Irani, D.N., and Kerr, D.A. (2004). Viral-induced spinal motor neuron death is non-cell-autonomous and involves glutamate excitotoxicity. J. Neurosci. *24,* 7566-7575.

Das, S., Chakraborty, S., and Basu, A. (2010). Critical role of lipid rafts in virus entry and activation of phosphoinositide 3' kinase/Akt signaling during early stages of Japanese encephalitis virus infection in neural stem/progenitor cells. J. Neurochem. *115,* 537-549.

Desbien, A.L., Kappler, J.W., and Marrack, P. (2009). The Epstein-Barr virus Bcl-2 homolog, BHRF1, blocks apoptosis by binding to a limited amount of Bim. Proc. Natl. Acad. Sci. U. S. A. *106,* 5663-5668.

Diamond, M.S., and Klein, R.S. (2004). West Nile virus: crossing the blood-brain barrier. Nat. Med. *10,* 1294-1295.

Dieterle, A.M., Bohler, P., Keppeler, H., Alers, S., Berleth, N., Driessen, S., Hieke, N., Pietkiewicz, S., Loffler, A.S., Peter, C.*, et al.* (2013). PDK1 controls upstream PI3K expression and PIP generation. Oncogene

Doble, B.W., and Woodgett, J.R. (2003). GSK-3: tricks of the trade for a multi-tasking kinase. J. Cell. Sci. *116,* 1175-1186.

Dokland, T., Walsh, M., Mackenzie, J.M., Khromykh, A.A., Ee, K.H., and Wang, S. (2004). West Nile virus core protein; tetramer structure and ribbon formation. Structure *12,* 1157-1163.

Dong, H., Ren, S., Li, H., and Shi, P.Y. (2008). Separate molecules of West Nile virus methyltransferase can independently catalyze the N7 and 2'-O methylations of viral RNA cap. Virology *377,* 1-6.

Duong, F.H., Filipowicz, M., Tripodi, M., La Monica, N., and Heim, M.H. (2004). Hepatitis C virus inhibits interferon signaling through up-regulation of protein phosphatase 2A. Gastroenterology *126,* 263-277.

Enserink, M. (2002). Infectious disease. West Nile's surprisingly swift continental sweep. Science *297,* 1988-1989.

Ergunay, K., Gunay, F., Oter, K., Kasap, O.E., Orsten, S., Akkutay, A.Z., Erdem, H., Ozkul, A., and Alten, B. (2013). Arboviral Surveillance of Field-Collected Mosquitoes Reveals Circulation of West Nile Virus Lineage 1 Strains in Eastern Thrace, Turkey. Vector Borne Zoonotic Dis.

Fernandez-Garcia, M.D., Mazzon, M., Jacobs, M., and Amara, A. (2009). Pathogenesis of flavivirus infections: using and abusing the host cell. Cell. Host Microbe *5,* 318-328.

Fiandalo, M.V., and Kyprianou, N. (2012). Caspase control: protagonists of cancer cell apoptosis. Exp. Oncol. *34,* 165-175.

Friesen, K.M., and Johnson, G.D. (2013). Mosquito and West Nile virus surveillance in northeast Montana, U.S.A., 2005 and 2006. Med. Vet. Entomol.

Fuchs, Y., and Steller, H. (2011). Programmed cell death in animal development and disease. Cell *147,* 742-758.

Fyffe, C., and Falasca, M. (2013). 3-Phosphoinositide-dependent protein kinase-1 as an emerging target in the management of breast cancer. Cancer. Manag. Res. *5,* 271-280.

Gaddy, D.F., and Lyles, D.S. (2007). Oncolytic vesicular stomatitis virus induces apoptosis via signaling through PKR, Fas, and Daxx. J. Virol. *81,* 2792-2804.

Galluzzi, L., Kepp, O., and Kroemer, G. (2012). Mitochondria: master regulators of danger signalling. Nat. Rev. Mol. Cell Biol. *13,* 780-788.

Galluzzi, L., Kepp, O., Trojel-Hansen, C., and Kroemer, G. (2012). Mitochondrial control of cellular life, stress, and death. Circ. Res. *111,* 1198-1207.

Georgopoulou, U., Tsitoura, P., Kalamvoki, M., and Mavromara, P. (2006). The protein phosphatase 2A represents a novel cellular target for hepatitis C virus NS5A protein. Biochimie *88,* 651-662.

Giannini, C., and Brechot, C. (2003). Hepatitis C virus biology. Cell Death Differ. *10 Suppl 1,* S27-38.

Gingras, A.C., Raught, B., and Sonenberg, N. (2001). Control of translation by the target of rapamycin proteins. Prog. Mol. Subcell. Biol. *27,* 143-174.

Gingras, A.C., Raught, B., and Sonenberg, N. (2001). Regulation of translation initiation by FRAP/mTOR. Genes Dev. *15,* 807-826.

Gollins, S.W., and Porterfield, J.S. (1986). pH-dependent fusion between the flavivirus West Nile and liposomal model membranes. J. Gen. Virol. *67 (Pt 1),* 157-166.

Gollins, S.W., and Porterfield, J.S. (1986). The uncoating and infectivity of the flavivirus West Nile on interaction with cells: effects of pH and ammonium chloride. J. Gen. Virol. *67 (Pt 9),* 1941-1950.

Gorchakov, R., Frolova, E., Williams, B.R., Rice, C.M., and Frolov, I. (2004). PKR-dependent and -independent mechanisms are involved in translational shutoff during Sindbis virus infection. J. Virol. *78,* 8455-8467.

Granot, T., Venticinque, L., Tseng, J.C., and Meruelo, D. (2011). Activation of cytotoxic and regulatory functions of NK cells by Sindbis viral vectors. PLoS One *6,* e20598.

Gupta, S., Radha, V., Furukawa, Y., and Swarup, G. (2001). Direct transcriptional activation of human caspase-1 by tumor suppressor p53. J. Biol. Chem. *276,* 10585-10588.

Hanna, S.L., Pierson, T.C., Sanchez, M.D., Ahmed, A.A., Murtadha, M.M., and Doms, R.W. (2005). N-linked glycosylation of west nile virus envelope proteins influences particle assembly and infectivity. J. Virol. *79,* 13262-13274.

He, Y., Nakao, H., Tan, S.L., Polyak, S.J., Neddermann, P., Vijaysri, S., Jacobs, B.L., and Katze, M.G. (2002). Subversion of cell signaling pathways by hepatitis C virus nonstructural 5A protein via interaction with Grb2 and P85 phosphatidylinositol 3-kinase. J. Virol. *76,* 9207-9217.

Henderson, S., Huen, D., Rowe, M., Dawson, C., Johnson, G., and Rickinson, A. (1993). Epstein-Barr virus-coded BHRF1 protein, a viral homologue of Bcl-2, protects human B cells from programmed cell death. Proc. Natl. Acad. Sci. U. S. A. *90,* 8479-8483.

Hers, I., Vincent, E.E., and Tavare, J.M. (2011). Akt signalling in health and disease. Cell. Signal. *23,* 1515-1527.

Hsu, M.J., Wu, C.Y., Chiang, H.H., Lai, Y.L., and Hung, S.L. (2010). PI3K/Akt signaling mediated apoptosis blockage and viral gene expression in oral epithelial cells during herpes simplex virus infection. Virus Res. *153,* 36-43.

Huang, D.C., Cory, S., and Strasser, A. (1997). Bcl-2, Bcl-XL and adenovirus protein E1B19kD are functionally equivalent in their ability to inhibit cell death. Oncogene *14,* 405-414.

Huang, L., Kinnucan, E., Wang, G., Beaudenon, S., Howley, P.M., Huibregtse, J.M., and Pavletich, N.P. (1999). Structure of an E6AP-UbcH7 complex: insights into ubiquitination by the E2-E3 enzyme cascade. Science *286,* 1321-1326.

Huang, P.Y., Guo, J.H., and Hwang, L.H. (2012). Oncolytic Sindbis virus targets tumors defective in the interferon response and induces significant bystander antitumor immunity in vivo. Mol. Ther. *20,* 298-305.

Hunt, T.A., Urbanowski, M.D., Kakani, K., Law, L.M., Brinton, M.A., and Hobman, T.C. (2007). Interactions between the West Nile virus capsid protein and the host cell-encoded phosphatase inhibitor, I(2)(PP2A). Cell. Microbiol. *9,* 2756-2766.

Hunt, T.A., Urbanowski, M.D., Kakani, K., Law, L.M., Brinton, M.A., and Hobman, T.C. (2007). Interactions between the West Nile virus capsid protein and the host cell-encoded phosphatase inhibitor, I2PP2A. Cell. Microbiol. *9,* 2756-2766.

Ilkow, C.S., Goping, I.S., and Hobman, T.C. (2011). The Rubella virus capsid is an anti-apoptotic protein that attenuates the pore-forming ability of Bax. PLoS Pathog. *7,* e1001291.

Isoyama, T., Kuge, S., and Nomoto, A. (2002). The core protein of hepatitis C virus is imported into the nucleus by transport receptor Kap123p but inhibits Kap121p-dependent nuclear import of yeast AP1-like transcription factor in yeast cells. J. Biol. Chem. *277,* 39634-39641.

Jarrard, J.A., Linnoila, R.I., Lee, H., Steinberg, S.M., Witschi, H., and Szabo, E. (1998). MUC1 is a novel marker for the type II pneumocyte lineage during lung carcinogenesis. Cancer Res. *58,* 5582-5589.

Ji, W.T., and Liu, H.J. (2008). PI3K-Akt signaling and viral infection. Recent. Pat. Biotechnol. *2,* 218-226.

Kazlauskas, A., and Cooper, J.A. (1990). Phosphorylation of the PDGF receptor beta subunit creates a tight binding site for phosphatidylinositol 3 kinase. EMBO J. *9,* 3279-3286.

Khromykh, A.A., Meka, H., Guyatt, K.J., and Westaway, E.G. (2001). Essential role of cyclization sequences in flavivirus RNA replication. J. Virol. *75,* 6719-6728.

Kilpatrick, A.M., and Pape, W.J. (2013). Predicting Human West Nile Virus Infections With Mosquito Surveillance Data. Am. J. Epidemiol.

Kofler, R.M., Heinz, F.X., and Mandl, C.W. (2002). Capsid protein C of tick-borne encephalitis virus tolerates large internal deletions and is a favorable target for attenuation of virulence. J. Virol. *76,* 3534-3543.

Kofler, R.M., Leitner, A., O'Riordain, G., Heinz, F.X., and Mandl, C.W. (2003). Spontaneous mutations restore the viability of tick-borne encephalitis virus mutants with large deletions in protein C. J. Virol. *77,* 443-451.

Kong, K.F., Delroux, K., Wang, X., Qian, F., Arjona, A., Malawista, S.E., Fikrig, E., and Montgomery, R.R. (2008). Dysregulation of TLR3 impairs the innate immune response to West Nile virus in the elderly. J. Virol. *82,* 7613-7623.

Koyama, A.H. (1995). Induction of apoptotic DNA fragmentation by the infection of vesicular stomatitis virus. Virus Res. *37,* 285-290.

Koyama, N., Kobayashi, K., Yamazaki, H., and Tomoda, H. (2008). Inhibition of lipid droplet accumulation in mouse macrophages by stemphone derivatives. J. Antibiot. (Tokyo) *61,* 509-514.

Kvansakul, M., Wei, A.H., Fletcher, J.I., Willis, S.N., Chen, L., Roberts, A.W., Huang, D.C., and Colman, P.M. (2010). Structural basis for apoptosis inhibition by Epstein-Barr virus BHRF1. PLoS Pathog. *6,* e1001236.

Lampman, R.L., Krasavin, N.M., Ward, M.P., Beveroth, T.A., Lankau, E.W., Alto, B.W., Muturi, E., and Novak, R.J. (2013). West Nile virus infection rates and avian serology in east-central Illinois. J. Am. Mosq. Control Assoc. *29,* 108-122.

Lavrik, I.N., and Krammer, P.H. (2012). Regulation of CD95/Fas signaling at the DISC. Cell Death Differ. *19,* 36-41.

Law, A.H., Tam, A.H., Lee, D.C., and Lau, A.S. (2013). A Role for Protein Phosphatase 2A in Regulating p38 Mitogen Activated Protein Kinase Activation and Tumor Necrosis Factor-Alpha Expression during Influenza Virus Infection. Int. J. Mol. Sci. *14,* 7327-7340.

Lee, C.J., Liao, C.L., and Lin, Y.L. (2005). Flavivirus activates phosphatidylinositol 3-kinase signaling to block caspase-dependent apoptotic cell death at the early stage of virus infection. J. Virol. *79,* 8388-8399.

Lee, J.M., and Bernstein, A. (1993). P53 Mutations Increase Resistance to Ionizing Radiation. Proc. Natl. Acad. Sci. U. S. A. *90,* 5742-5746.

Li, H., Zhu, H., Xu, C.J., and Yuan, J. (1998). Cleavage of BID by caspase 8 mediates the mitochondrial damage in the Fas pathway of apoptosis. Cell *94,* 491-501.

Li, L., Ren, C.H., Tahir, S.A., Ren, C., and Thompson, T.C. (2003). Caveolin-1 maintains activated Akt in prostate cancer cells through scaffolding domain binding site interactions with and inhibition of serine/threonine protein phosphatases PP1 and PP2A. Mol. Cell. Biol. *23,* 9389-9404.

Lin, P., Bush, J.A., Cheung, K.J.,Jr, and Li, G. (2002). Tissue-specific regulation of Fas/APO-1/CD95 expression by p53. Int. J. Oncol. *21,* 261-264.

Lindenbach, B.D., and Rice, C.M. (2003). Molecular biology of flaviviruses. Adv. Virus Res. *59,* 23-61.

Liu, Z., Tian, Y., Machida, K., Lai, M.M., Luo, G., Foung, S.K., and Ou, J.H. (2012). Transient activation of the PI3K-AKT pathway by hepatitis C virus to enhance viral entry. J. Biol. Chem. *287,* 41922-41930.

Liu, Z., Tian, Y., Machida, K., Lai, M.M., Luo, G., Foung, S.K., and Ou, J.H. (2012). Transient activation of the PI3K-AKT pathway by hepatitis C virus to enhance viral entry. J. Biol. Chem. *287,* 41922-41930.

Liu, Z., Tian, Y., Machida, K., Lai, M.M., Luo, G., Foung, S.K., and Ou, J.H. (2012). Transient activation of the PI3K-AKT pathway by hepatitis C virus to enhance viral entry. J. Biol. Chem. *287,* 41922-41930.

Lo, M.K., Tilgner, M., Bernard, K.A., and Shi, P.Y. (2003). Functional analysis of mosquito-borne flavivirus conserved sequence elements within 3' untranslated region of West Nile virus by use of a reporting replicon that differentiates between viral translation and RNA replication. J. Virol. *77,* 10004-10014.

Lobigs, M., Lee, E., Ng, M.L., Pavy, M., and Lobigs, P. (2010). A flavivirus signal peptide balances the catalytic activity of two proteases and thereby facilitates virus morphogenesis. Virology *401,* 80-89.

Lorenz, I.C., Allison, S.L., Heinz, F.X., and Helenius, A. (2002). Folding and dimerization of tick-borne encephalitis virus envelope proteins prM and E in the endoplasmic reticulum. J. Virol. *76,* 5480-5491.

Machain-Williams, C., Reagan, K., Wang, T., Zeidner, N.S., and Blair, C.D. (2013). Immunization with Culex tarsalis mosquito salivary gland extract modulates West Nile virus infection and disease in mice. Viral Immunol. *26,* 84-92.

Mackenzie, J.S., Gubler, D.J., and Petersen, L.R. (2004). Emerging flaviviruses: the spread and resurgence of Japanese encephalitis, West Nile and dengue viruses. Nat. Med. *10,* S98-109.

Mackenzie, J.S., and Williams, D.T. (2009). The zoonotic flaviviruses of southern, south-eastern and eastern Asia, and Australasia: the potential for emergent viruses. Zoonoses Public. Health. *56,* 338-356.

MacLeod, I.J., and Minson, T. (2010). Binding of herpes simplex virus type-1 virions leads to the induction of intracellular signalling in the absence of virus entry. PLoS One *5,* e9560.

Malik, A.R., Urbanska, M., Macias, M., Skalecka, A., and Jaworski, J. (2013). Beyond control of protein translation: what we have learned about the non-canonical regulation and function of mammalian target of rapamycin (mTOR). Biochim. Biophys. Acta *1834,* 1434-1448.

Markman, B., Tao, J.J., and Scaltriti, M. (2013). PI3K pathway inhibitors: better not left alone. Curr. Pharm. Des. *19,* 895-906.

Martins, I.C., Gomes-Neto, F., Faustino, A.F., Carvalho, F.A., Carneiro, F.A., Bozza, P.T., Mohana-Borges, R., Castanho, M.A., Almeida, F.C., Santos, N.C., and Da Poian, A.T. (2012). The disordered N-terminal region of dengue virus capsid protein contains a lipid-droplet-binding motif. Biochem. J. *444,* 405-415.

Matissek, K.J., Mossalam, M., Okal, A., and Lim, C.S. (2013). The DNA Binding Domain of p53 Is Sufficient To Trigger a Potent Apoptotic Response at the Mitochondria. Mol. Pharm.

Maurer, U., Charvet, C., Wagman, A.S., Dejardin, E., and Green, D.R. (2006). Glycogen synthase kinase-3 regulates mitochondrial outer membrane permeabilization and apoptosis by destabilization of MCL-1. Mol. Cell *21,* 749-760.

Meier, R., and Hemmings, B.A. (1999). Regulation of protein kinase B. J. Recept. Signal Transduct. Res. *19,* 121-128.

Methner, A., and Zipp, F. (2013). Multiple sclerosis in 2012: Novel therapeutic options and drug targets in MS. Nat. Rev. Neurol. *9,* 72-73.

Millward, T.A., Zolnierowicz, S., and Hemmings, B.A. (1999). Regulation of protein kinase cascades by protein phosphatase 2A. Trends Biochem. Sci. *24,* 186-191.

Mori, N., Ishikawa, C., Uchihara, J.N., and Yasumoto, T. (2013). Protein phosphatase 2A as a potential target for treatment of adult T cell leukemia. Curr. Cancer. Drug Targets *13,* 829-842.

Mori, Y., Okabayashi, T., Yamashita, T., Zhao, Z., Wakita, T., Yasui, K., Hasebe, F., Tadano, M., Konishi, E., Moriishi, K., and Matsuura, Y. (2005). Nuclear localization of Japanese encephalitis virus core protein enhances viral replication. J. Virol. *79,* 3448-3458.

Mori, Y., Yamashita, T., Tanaka, Y., Tsuda, Y., Abe, T., Moriishi, K., and Matsuura, Y. (2007). Processing of capsid protein by cathepsin L plays a crucial role in replication of Japanese encephalitis virus in neural and macrophage cells. J. Virol. *81,* 8477-8487.

Moriishi, K., Koura, M., and Matsuura, Y. (2002). Induction of Bad-mediated apoptosis by Sindbis virus infection: involvement of pro-survival members of the Bcl-2 family. Virology *292,* 258-271.

Mukherjee, S., Lin, T.Y., Dowd, K.A., Manhart, C.J., and Pierson, T.C. (2011). The infectivity of prM-containing partially mature West Nile virus does not require the activity of cellular furin-like proteases. J. Virol. *85,* 12067-12072.

Namatame, I., Tomoda, H., Ishibashi, S., and Omura, S. (2004). Antiatherogenic activity of fungal beauveriolides, inhibitors of lipid droplet accumulation in macrophages. Proc. Natl. Acad. Sci. U. S. A. *101,* 737-742.

Napetschnig, J., and Wu, H. (2013). Molecular basis of NF-kappaB signaling. Annu. Rev. Biophys. *42,* 443-468.

Nayak, R., Farris, K.D., and Pintel, D.J. (2008). E4Orf6-E1B-55k-dependent degradation of de novo-generated adeno-associated virus type 5 Rep52 and capsid proteins employs a cullin 5-containing E3 ligase complex. J. Virol. *82,* 3803-3808.

Nishitoh, H., Saitoh, M., Mochida, Y., Takeda, K., Nakano, H., Rothe, M., Miyazono, K., and Ichijo, H. (1998). ASK1 is essential for JNK/SAPK activation by TRAF2. Mol. Cell *2,* 389-395.

Nolan, M.S., Hause, A.M., and Murray, K.O. (2012). Findings of Long-Term Depression up to 8 Years Post Infection From West Nile Virus. J. Clin. Psychol. *68,* 801-808.

Oltersdorf, T., Elmore, S.W., Shoemaker, A.R., Armstrong, R.C., Augeri, D.J., Belli, B.A., Bruncko, M., Deckwerth, T.L., Dinges, J., Hajduk, P.J.*, et al.* (2005). An inhibitor of Bcl-2 family proteins induces regression of solid tumours. Nature *435,* 677-681.

Parquet, M.C., Kumatori, A., Hasebe, F., Morita, K., and Igarashi, A. (2001). West Nile virus-induced bax-dependent apoptosis. FEBS Lett. *500,* 17-24.

Paterson, R. (2005). How West Nile virus crosses the blood-brain barrier. Lancet Neurol. *4,* 18.

Pearce, A.F., and Lyles, D.S. (2009). Vesicular stomatitis virus induces apoptosis primarily through Bak rather than Bax by inactivating Mcl-1 and Bcl-XL. J. Virol. *83,* 9102-9112.

Pennella, M.A., Liu, Y., Woo, J.L., Kim, C.A., and Berk, A.J. (2010). Adenovirus E1B 55-kilodalton protein is a p53-SUMO1 E3 ligase that represses p53 and stimulates its nuclear export through interactions with promyelocytic leukemia nuclear bodies. J. Virol. *84,* 12210-12225.

Plemper, R.K. (2011). Cell entry of enveloped viruses. Curr. Opin. Virol. *1,* 92-100.

Qin, D., Feng, N., Fan, W., Ma, X., Yan, Q., Lv, Z., Zeng, Y., Zhu, J., and Lu, C. (2011). Activation of PI3K/AKT and ERK MAPK signal pathways is required for the induction of lytic cycle replication of Kaposi's sarcoma-associated herpesvirus by herpes simplex virus type 1. BMC Microbiol. *11,* 240-2180-11-240.

Querido, E., Blanchette, P., Yan, Q., Kamura, T., Morrison, M., Boivin, D., Kaelin, W.G., Conaway, R.C., Conaway, J.W., and Branton, P.E. (2001). Degradation of p53 by adenovirus E4orf6 and E1B55K proteins occurs via a novel mechanism involving a Cullin-containing complex. Genes Dev. *15,* 3104-3117.

Quetglas, J.I., Ruiz-Guillen, M., Aranda, A., Casales, E., Bezunartea, J., and Smerdou, C. (2010). Alphavirus vectors for cancer therapy. Virus Res. *153,* 179-196.

Quintavalle, C., Incoronato, M., Puca, L., Acunzo, M., Zanca, C., Romano, G., Garofalo, M., Iaboni, M., Croce, C.M., and Condorelli, G. (2010). c-FLIPL enhances anti-apoptotic Akt functions by modulation of Gsk3beta activity. Cell Death Differ. *17,* 1908-1916.

Ramseyer, V.D., and Garvin, J.L. (2013). Tumor necrosis factor-alpha: regulation of renal function and blood pressure. Am. J. Physiol. Renal Physiol. *304,* F1231-42.

Raught, B., and Gingras, A.C. (1999). eIF4E activity is regulated at multiple levels. Int. J. Biochem. Cell Biol. *31,* 43-57.

Ray, R.B., Basu, A., Steele, R., Beyene, A., McHowat, J., Meyer, K., Ghosh, A.K., and Ray, R. (2004). Ebola virus glycoprotein-mediated anoikis of primary human cardiac microvascular endothelial cells. Virology *321,* 181-188.

Salvesen, G.S. (2002). Caspases: opening the boxes and interpreting the arrows. Cell Death Differ. *9,* 3-5.

Sampath, A., and Padmanabhan, R. (2009). Molecular targets for flavivirus drug discovery. Antiviral Res. *81,* 6-15.

Samsa, M.M., Mondotte, J.A., Iglesias, N.G., Assuncao-Miranda, I., Barbosa-Lima, G., Da Poian, A.T., Bozza, P.T., and Gamarnik, A.V. (2009). Dengue virus capsid protein usurps lipid droplets for viral particle formation. PLoS Pathog. *5,* e1000632.

Sangiambut, S., Keelapang, P., Aaskov, J., Puttikhunt, C., Kasinrerk, W., Malasit, P., and Sittisombut, N. (2008). Multiple regions in dengue virus capsid protein contribute to nuclear localization during virus infection. J. Gen. Virol. *89,* 1254-1264.

Schache, P., Gurlevik, E., Struver, N., Woller, N., Malek, N., Zender, L., Manns, M., Wirth, T., Kuhnel, F., and Kubicka, S. (2009). VSV virotherapy improves

chemotherapy by triggering apoptosis due to proteasomal degradation of Mcl-1. Gene Ther. *16,* 849-861.

Scherbik, S.V., and Brinton, M.A. (2010). Virus-induced Ca2+ influx extends survival of west nile virus-infected cells. J. Virol. *84,* 8721-8731.

Schlatter, R., Schmich, K., Lutz, A., Trefzger, J., Sawodny, O., Ederer, M., and Merfort, I. (2011). Modeling the TNFalpha-induced apoptosis pathway in hepatocytes. PLoS One *6,* e18646.

Sents, W., Ivanova, E., Lambrecht, C., Haesen, D., and Janssens, V. (2013). The biogenesis of active protein phosphatase 2A holoenzymes: a tightly regulated process creating phosphatase specificity. FEBS J. *280,* 644-661.

Shanker, V., Trincucci, G., Heim, H.M., and Duong, H.T. (2013). Protein phosphatase 2A impairs IFNalpha-induced antiviral activity against the hepatitis C virus through the inhibition of STAT1 tyrosine phosphorylation. J. Viral Hepat. *20,* 612-621.

Shaw, P., Bovey, R., Tardy, S., Sahli, R., Sordat, B., and Costa, J. (1992). Induction of apoptosis by wild-type p53 in a human colon tumor-derived cell line. Proc. Natl. Acad. Sci. U. S. A. *89,* 4495-4499.

Shrestha, B., Zhang, B., Purtha, W.E., Klein, R.S., and Diamond, M.S. (2008). Tumor necrosis factor alpha protects against lethal West Nile virus infection by promoting trafficking of mononuclear leukocytes into the central nervous system. J. Virol. *82,* 8956-8964.

Slomovitz, B.M., and Coleman, R.L. (2012). The PI3K/AKT/mTOR pathway as a therapeutic target in endometrial cancer. Clin. Cancer Res. *18,* 5856-5864.

Smit, J.M., Moesker, B., Rodenhuis-Zybert, I., and Wilschut, J. (2011). Flavivirus cell entry and membrane fusion. Viruses *3,* 160-171.

Solomon, T., and Vaughn, D.W. (2002). Pathogenesis and clinical features of Japanese encephalitis and West Nile virus infections. Curr. Top. Microbiol. Immunol. *267,* 171-194.

Song, M.S., Salmena, L., and Pandolfi, P.P. (2012). The functions and regulation of the PTEN tumour suppressor. Nat. Rev. Mol. Cell Biol. *13,* 283-296.

Speck, S.H., and Virgin, H.W. (1999). Host and viral genetics of chronic infection: a mouse model of gamma-herpesvirus pathogenesis. Curr. Opin. Microbiol. *2,* 403-409.

Speeckaert, M.M., Speeckaert, R., Laute, M., Vanholder, R., and Delanghe, J.R. (2012). Tumor necrosis factor receptors: biology and therapeutic potential in kidney diseases. Am. J. Nephrol. *36,* 261-270.

Spencer, S.L., and Sorger, P.K. (2011). Measuring and modeling apoptosis in single cells. Cell *144,* 926-939.

Srivastava, S.P., Kumar, K.U., and Kaufman, R.J. (1998). Phosphorylation of eukaryotic translation initiation factor 2 mediates apoptosis in response to activation of the double-stranded RNA-dependent protein kinase. J. Biol. Chem. *273,* 2416-2423.

Stadler, K., Allison, S.L., Schalich, J., and Heinz, F.X. (1997). Proteolytic activation of tick-borne encephalitis virus by furin. J. Virol. *71,* 8475-8481.

Stocks, C.E., and Lobigs, M. (1995). Posttranslational signal peptidase cleavage at the flavivirus C-prM junction in vitro. J. Virol. *69,* 8123-8126.

Suthar, M.S., Diamond, M.S., and Gale, M.,Jr. (2013). West Nile virus infection and immunity. Nat. Rev. Microbiol. *11,* 115-128.

Sylow, L., Kleinert, M., Pehmoller, C., Prats, C., Chiu, T.T., Klip, A., Richter, E.A., and Jensen, T.E. (2013). Akt and Rac1 signalling are jointly required for insulin-stimulated glucose uptake in skeletal muscle and downregulated in insulin resistance. Cell. Signal.

Szretter, K.J., Daniels, B.P., Cho, H., Gainey, M.D., Yokoyama, W.M., Gale, M.,Jr, Virgin, H.W., Klein, R.S., Sen, G.C., and Diamond, M.S. (2012). 2'-O methylation of the viral mRNA cap by West Nile virus evades ifit1-dependent and -independent mechanisms of host restriction in vivo. PLoS Pathog. *8,* e1002698.

Talis, A.L., Huibregtse, J.M., and Howley, P.M. (1998). The role of E6AP in the regulation of p53 protein levels in human papillomavirus (HPV)-positive and HPV-negative cells. J. Biol. Chem. *273,* 6439-6445.

Thomas, M., and Banks, L. (1998). Inhibition of Bak-induced apoptosis by HPV-18 E6. Oncogene *17,* 2943-2954.

Thurner, C., Witwer, C., Hofacker, I.L., and Stadler, P.F. (2004). Conserved RNA secondary structures in Flaviviridae genomes. J. Gen. Virol. *85,* 1113-1124.

Tobiume, K., Saitoh, M., and Ichijo, H. (2002). Activation of apoptosis signal-regulating kinase 1 by the stress-induced activating phosphorylation of pre-formed oligomer. J. Cell. Physiol. *191,* 95-104.

Trent, D.W., Kinney, R.M., Johnson, B.J., Vorndam, A.V., Grant, J.A., Deubel, V., Rice, C.M., and Hahn, C. (1987). Partial nucleotide sequence of St. Louis encephalitis virus RNA: structural proteins, NS1, ns2a, and ns2b. Virology *156,* 293-304.

Tsuchiya, A., Kanno, T., and Nishizaki, T. (2013). PI3 kinase directly phosphorylates Akt1/2 at Ser473/474 in the insulin signal transduction pathway. J. Endocrinol.

Tsuda, Y., Mori, Y., Abe, T., Yamashita, T., Okamoto, T., Ichimura, T., Moriishi, K., and Matsuura, Y. (2006). Nucleolar protein B23 interacts with Japanese encephalitis virus core protein and participates in viral replication. Microbiol. Immunol. *50,* 225-234.

Urbanowski, M.D., and Hobman, T.C. (2013). The West Nile virus capsid protein blocks apoptosis through a phosphatidylinositol 3-kinase-dependent mechanism. J. Virol. *87,* 872-881.

Urbanowski, M.D., Ilkow, C.S., and Hobman, T.C. (2008). Modulation of signaling pathways by RNA virus capsid proteins. Cell. Signal. *20,* 1227-1236.

Vega-Avila E, P.M. (2011). An overview of colorimetric assay methods used to assess survival or proliferation of mammalian cells**.** Proc West Pharmacol Soc. *54,* 4-10.

Venticinque, L., and Meruelo, D. (2010). Sindbis viral vector induced apoptosis requires translational inhibition and signaling through Mcl-1 and Bak. Mol. Cancer. *9,* 37-4598-9-37.

Vercammen, E., Staal, J., and Beyaert, R. (2008). Sensing of viral infection and activation of innate immunity by toll-like receptor 3. Clin. Microbiol. Rev. *21,* 13-25.

Wagner, M.J., and Smiley, J.R. (2011). Herpes simplex virus requires VP11/12 to activate Src family kinase-phosphoinositide 3-kinase-Akt signaling. J. Virol. *85,* 2803-2812.

Wang, K., Yin, X.M., Chao, D.T., Milliman, C.L., and Korsmeyer, S.J. (1996). BID: a novel BH3 domain-only death agonist. Genes Dev. *10,* 2859-2869.

Wang, T., Town, T., Alexopoulou, L., Anderson, J.F., Fikrig, E., and Flavell, R.A. (2004). Toll-like receptor 3 mediates West Nile virus entry into the brain causing lethal encephalitis. Nat. Med. *10,* 1366-1373.

Wang, X., Chen, W., Zeng, W., Bai, L., Tesfaigzi, Y., Belinsky, S.A., and Lin, Y. (2008). Akt-mediated eminent expression of c-FLIP and Mcl-1 confers acquired resistance to TRAIL-induced cytotoxicity to lung cancer cells. Mol. Cancer. Ther. *7,* 1156-1163.

Waters, J.P., Pober, J.S., and Bradley, J.R. (2013). Tumour necrosis factor in infectious disease. J. Pathol. *230,* 132-147.

Waters, J.P., Pober, J.S., and Bradley, J.R. (2013). Tumour necrosis factor in infectious disease. J. Pathol. *230,* 132-147.

Wei, L., Zhu, S., Wang, J., and Liu, J. (2012). Activation of the phosphatidylinositol 3-kinase/Akt signaling pathway during porcine circovirus type 2 infection facilitates cell survival and viral replication. J. Virol. *86,* 13589-13597.

Wicker, J.A., Whiteman, M.C., Beasley, D.W., Davis, C.T., Zhang, S., Schneider, B.S., Higgs, S., Kinney, R.M., and Barrett, A.D. (2006). A single amino acid substitution in the central portion of the West Nile virus NS4B protein confers a highly attenuated phenotype in mice. Virology *349,* 245-253.

Wolf, K., Beimforde, N., Falzarano, D., Feldmann, H., and Schnittler, H.J. (2011). The Ebola virus soluble glycoprotein (sGP) does not affect lymphocyte apoptosis and adhesion to activated endothelium. J. Infect. Dis. *204 Suppl 3,* S947-52.

Woodgett, J.R. (2001). Judging a protein by more than its name: GSK-3. Sci. STKE *2001,* re12.

Wortzman, M.E., Lin, G.H., and Watts, T.H. (2013). Intrinsic TNF/TNFR2 Interactions Fine-Tune the CD8 T Cell Response to Respiratory Influenza Virus Infection in Mice. PLoS One *8,* e68911.

Wu, J., Chen, C., and Zhao, K.N. (2013). Phosphatidylinositol 3-kinase signaling as a therapeutic target for cervical cancer. Curr. Cancer. Drug Targets *13,* 143-156.

Xu, Z., Anderson, R., and Hobman, T.C. (2011). The capsid-binding nucleolar helicase DDX56 is important for infectivity of West Nile virus. J. Virol. *85,* 5571-5580.

Xu, Z., and Hobman, T.C. (2012). The helicase activity of DDX56 is required for its role in assembly of infectious West Nile virus particles. Virology *433,* 226-235.

Yamazaki, H., Kobayashi, K., Matsuda, D., Nonaka, K., Masuma, R., Omura, S., and Tomoda, H. (2009). Pentacecilides, new inhibitors of lipid droplet formation in mouse macrophages, produced by Penicillium cecidicola FKI-3765-1: I.

Taxonomy, fermentation, isolation and biological properties. J. Antibiot. (Tokyo) *62,* 195-200.

Yang, C.M., Lin, C.C., Lee, I.T., Lin, Y.H., Yang, C.M., Chen, W.J., Jou, M.J., and Hsiao, L.D. (2012). Japanese encephalitis virus induces matrix metalloproteinase-9 expression via a ROS/c-Src/PDGFR/PI3K/Akt/MAPKs-dependent AP-1 pathway in rat brain astrocytes. J. Neuroinflammation *9,* 12-2094-9-12.

Yang, E., Zha, J., Jockel, J., Boise, L.H., Thompson, C.B., and Korsmeyer, S.J. (1995). Bad, a heterodimeric partner for Bcl-XL and Bcl-2, displaces Bax and promotes cell death. Cell *80,* 285-291.

Yang, M.R., Lee, S.R., Oh, W., Lee, E.W., Yeh, J.Y., Nah, J.J., Joo, Y.S., Shin, J., Lee, H.W., Pyo, S., and Song, J. (2008). West Nile virus capsid protein induces p53-mediated apoptosis via the sequestration of HDM2 to the nucleolus. Cell. Microbiol. *10,* 165-176.

Yonish-Rouach, E., Resnitzky, D., Lotem, J., Sachs, L., Kimchi, A., and Oren, M. (1991). Wild-type p53 induces apoptosis of myeloid leukaemic cells that is inhibited by interleukin-6. Nature *352,* 345-347.

Youle, R.J., and Strasser, A. (2008). The BCL-2 protein family: opposing activities that mediate cell death. Nat. Rev. Mol. Cell Biol. *9,* 47-59.

Zhang, B., Dong, H., Zhou, Y., and Shi, P.Y. (2008). Genetic interactions among the West Nile virus methyltransferase, the RNA-dependent RNA polymerase, and the 5' stem-loop of genomic RNA. J. Virol. *82,* 7047-7058.

Zhang, B., Patel, J., Croyle, M., Diamond, M.S., and Klein, R.S. (2010). TNF-alpha-dependent regulation of CXCR3 expression modulates neuronal survival during West Nile virus encephalitis. J. Neuroimmunol. *224,* 28-38.

Zhang, J., Xu, X., and Liu, Y. (2004). Activation-induced cell death in T cells and autoimmunity. Cell. Mol. Immunol. *1,* 186-192.

Zhang, Y., Corver, J., Chipman, P.R., Zhang, W., Pletnev, S.V., Sedlak, D., Baker, T.S., Strauss, J.H., Kuhn, R.J., and Rossmann, M.G. (2003). Structures of immature flavivirus particles. EMBO J. *22,* 2604-2613.

Zhang, Y., Kaufmann, B., Chipman, P.R., Kuhn, R.J., and Rossmann, M.G. (2007). Structure of immature West Nile virus. J. Virol. *81,* 6141-6145.

Zhou, Y., Ray, D., Zhao, Y., Dong, H., Ren, S., Li, Z., Guo, Y., Bernard, K.A., Shi, P.Y., and Li, H. (2007). Structure and function of flavivirus NS5 methyltransferase. J. Virol. *81,* 3891-3903.

Appendix A

Appendix A

Transcriptiomics of flavivirus capsid-expressing cells

The production of capsid proteins in vast excess of what is required for the formation and secretion of virions creates an opportunity for these proteins to play non-structural roles. A key and striking feature of flavivirus capsid proteins is their localization to the nuclei of host cells. With these facts in mind, I sought to determine if expression of flavivirus capsid proteins affects affect a prominent nuclear process, host gene transcription. Regulation of host gene transcription is one manner in which capsid could alter the host environment to evade the immune response, and/or promote the availability of factors required for replication.

Microarray analyses was used to compare the relative activities of host genes in response to expression of WNV, MVEV, SLEV, JEV, DENV or YFV capsids, or an AcGFP only control. Total cellular RNA was extracted, labeled, and hybridized to Affymetrix PrimeView human genome arrays. Fluorescence data were collected and subsequently analyzed to determine the fold increase or decrease of specific mRNA levels in relation to a control. Analysis of transcriptional data indicated that in all cases, there was very little change in gene expression brought about by capsid expression. Nonetheless, the lack of significant effects on host gene expression may provide insight into the means by which WNV and other flavivirus capsids inhibit apoptosis. For example, these studies suggest their role in blocking apoptosis does not require alteration of transcription and/or mRNA stability.

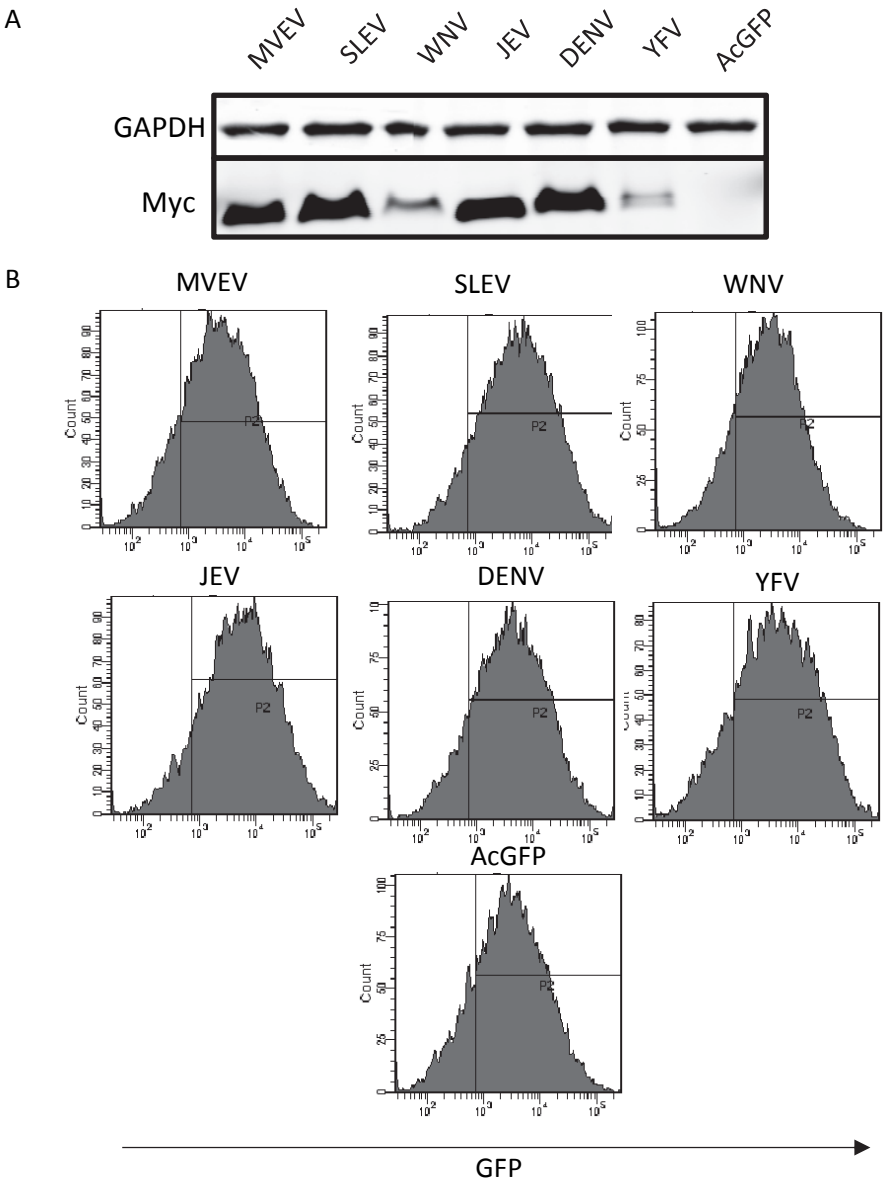

Figure 1. Expression of myc-tagged flavivirus capsids in A549 cells. In parallel with samples used for RNA preparation, cells were lysed for analyses via immunoblotting, and fixed for FACS analyses. Immunoblotting was used to determine the levels of capsid protein expression (myc), with GAPDH as a loading control (A). Fixed cells were subjected to FACS analysis in which levels of AcGFP fluorescence were measured to determine transduction efficiency. Those events to the right of the vertical line are considered positive for AcGFP (B).

Increase
Decrease

Fold Change	Gene Title
2.207269	methionine adenosyltransferase II, alpha
2.1345756	
2.0683093	hexosaminidase A (alpha polypeptide)
2.0112154	ankyrin repeat domain 20 family, member A5
2.0058951	eukaryotic translation initiation factor 4A2 /// small nucleolar RNA, H/ACA box 63
2.0003874	LUC7-like 3 (S. cerevisiae)
-2.008511	TAO kinase 3
-2.0576928	cyclin-dependent kinase 12
-2.081243	guanine nucleotide binding protein (G protein), beta polypeptide 4
-2.1133611	RAP1A, member of RAS oncogene family

YFV Capsid

Fold Change	Gene Title
2.7898867	ADP-ribosyltransferase 3
2.6840024	
2.353025	eukaryotic translation initiation factor 4A2 /// small nucleolar RNA, H/ACA box 4
2.2919207	calpastatin
2.287129	heterogeneous nuclear ribonucleoprotein M
2.2714918	chaperonin containing TCP1, subunit 5 (epsilon)
2.1903577	annexin A1
2.1800194	dynein, cytoplasmic 1, intermediate chain 2 /// heterogeneous nuclear ribonucleoprotein M
2.1734378	heterogeneous nuclear ribonucleoprotein M
2.1451209	
2.0712311	insulin-like 4 (placenta)
-2.0111403	heat shock 22kDa protein 8
-2.0124815	immunity-related GTPase family, Q
-2.0130608	RAB3B, member RAS oncogene family
-2.0151906	zinc finger protein 264
-2.03633	glutaminase
-2.1845362	neurofilament, light polypeptide
-2.1911528	annexin A5
-2.19692	jun proto-oncogene
-2.2028902	RAP1A, member of RAS oncogene family
-2.3727021	actin, alpha 2, smooth muscle, aorta

WNV Capsid

Figure 2. Lists of genes that changed 2-fold or greater (relative to control (AcGFP) in response to capsid expression. After transduction of A549 cells with the indicated capsid expressing lentivirus at an MOT of 10, total cellular RNA was harvested, labelled, and hybridizied to Affymetrix PrimeView human genome arrays. Collection of raw data was followed with processing by analysis software that calculated fold change values for each gene specific probe in comparison to a control. Those genes which demonstrated a ≥2-fold change in expression level were placed in tables for each capsid protein in which green represents an increase, and red represents a decrease.

Fold Change	Gene Title
2.0026393	chromosome 8 open reading frame 59
-2.0884378	glutaminase
-2.1141715	zinc finger protein 264

DENV Capsid

Fold Change	Gene Title
2.5120199	integrin beta 3 binding protein (beta3-endonexin)
2.428367	ADP-ribosyltransferase 3
2.399336	integrin beta 3 binding protein (beta3-endonexin)
2.3615649	integrin beta 3 binding protein (beta3-endonexin)
2.3218148	chromosome 8 open reading frame 59
2.2507122	chromosome 8 open reading frame 59
2.0915987	C-type lectin domain family 2, member B
2.0687706	chromosome 13 open reading frame 27
2.0485122	troponin T type 3 (skeletal, fast)
2.0395525	insulin-like 4 (placenta)
2.0114553	ribosomal protein S15a
-2.0128055	glutaminase
-2.021641	insulin-like growth factor binding protein 1
-2.052217	myosin, heavy chain 9, non-muscle
-2.0593665	coatomer protein complex, subunit alpha
-2.1649728	inositol 1,4,5-triphosphate receptor interacting protein-like 2
-2.1983953	multiple EGF-like-domains 8
-2.2280538	GLI pathogenesis-related 1
-2.2778873	zinc finger protein 264

JEV Capsid

Figure 2 *(con't)*.

Fold Change	Gene Title
3.453274	heterogeneous nuclear ribonucleoprotein M
3.3809085	heterogeneous nuclear ribonucleoprotein M
3.3646042	chaperonin containing TCP1, subunit 6 (zeta) pseudogene 1
3.1467052	dynein, cytoplasmic 1, intermediate chain 2
3.120906	
3.023375	calpastatin
2.8661432	transformer 2 alpha homolog (Drosophila)
2.791713	
2.7682981	CTAGE family, member 15, pseudogene
2.764913	neuregulin 1
2.726124	polymerase (DNA directed), theta
2.669989	integrin beta 3 binding protein (beta3-endonexin)
2.6652746	eukaryotic translation initiation factor 4A2 /// small nucleolar RNA, H/ACA box 4
2.6473513	ankyrin repeat domain 20 family, member A5
2.5821993	WD repeat domain 61
2.5622807	chromosome 12 open reading frame 48
2.5377982	integrin beta 3 binding protein (beta3-endonexin)
2.489072	ribosomal protein L10
2.4878006	chromosome 8 open reading frame 59
2.4741344	annexin A1
2.46964	COBW domain containing 1
2.4647498	PTPRF interacting protein, binding protein 1 (liprin beta 1)
2.4568393	integrin beta 3 binding protein (beta3-endonexin)
2.4003417	insulin-like 4 (placenta)
2.3876934	ADP-ribosyltransferase 3
2.3596463	small nucleolar RNA, H/ACA box 32
2.3482337	small nucleolar RNA, H/ACA box 25
2.3373573	
2.3155987	coiled-coil domain containing 144A
2.3083355	chromosome Y open reading frame 15B
2.2928958	exocyst complex component 4
2.2921803	endogenous Borna-like N element-2
2.28421	metastasis associated lung adenocarcinoma transcript 1 (non-protein coding)
2.2792332	RUN and FYVE domain containing 2
2.2724123	small nucleolar RNA, H/ACA box 18
2.2666378	chaperonin containing TCP1, subunit 5 (epsilon)
2.264268	TBC1 domain family, member 8 (with GRAM domain)
2.258827	ribosomal protein S27a
2.2533844	chromosome 8 open reading frame 59

Increase

Decrease

Continued on next page

SLEV Capsid

Figure 2 *(con't)*.

Fold Change	Gene Title
2.251001	cytochrome P450, family 4, subfamily F, polypeptide 3
2.2499356	ribosomal protein S27a
2.236204	PRP38 pre-mRNA processing factor 38 (yeast) domain containing B
2.224897	histocompatibility (minor) 13
2.223179	
2.21709	glutamate-cysteine ligase, catalytic subunit
2.2134533	amyloid beta (A4) precursor protein-binding, family B, member 2
2.2100372	numb homolog (Drosophila)
2.2053883	mitogen-activated protein kinase 14
2.2033467	chromosome 7 open reading frame 54
2.190517	cytoplasmic linker associated protein 2
2.1866982	polycystic kidney disease 1 (autosomal dominant) pseudogene 1
2.1593893	Ribosomal protein S3A
2.1507413	serine/threonine kinase 4
2.1488173	ADP-ribosylation factor-like 17A
2.1449225	coiled-coil domain containing 150
2.1441767	pleckstrin homology domain containing, family H (with MyTH4 domain) member 2
2.1433966	C-type lectin domain family 2, member B
2.1417134	MIR17 host gene (non-protein coding)
2.141004	ribosomal protein L10
2.1203976	tumor protein p53
2.1195982	ovostatin homolog 2-like /// ovostatin homolog 2-like /// ovostatin 2
2.0968726	paired immunoglobin-like type 2 receptor beta
2.0960937	Rho guanine nucleotide exchange factor (GEF) 10
2.0883894	NOP2/Sun domain family, member 5 pseudogene 2
2.087475	methionine adenosyltransferase II, alpha
2.0853057	COBW domain containing 2 /// COBW domain containing 5 /// COBW domain containing 7
2.0830867	EH domain binding protein 1
2.07797	cell division cycle associated 2
2.0747569	eukaryotic translation initiation factor 4A2 /// small nucleolar RNA, H/ACA box 63
2.072767	RAB12, member RAS oncogene family
2.069103	phosphodiesterase 7A
2.0670025	histone cluster 1, H4k
2.0644362	meningioma expressed antigen 5 (hyaluronidase)
2.0596557	DEAH (Asp-Glu-Ala-Asp/His) box polypeptide 57
2.0596557	DEAH (Asp-Glu-Ala-Asp/His) box polypeptide 57
2.0593555	GALI1870
2.0521193	gamma-aminobutyric acid (GABA) A receptor, epsilon
2.0407836	myeloma overexpressed 2
2.0407028	natural killer-tumor recognition sequence
2.0370114	chromosome 13 open reading frame 27

Continued on next page

SLEV Capsid

Figure 2 *(con't)*.

Fold Change	Gene Title
2.036509	mediator complex subunit 31
2.0363517	CTAGE family, member 5
2.0327365	histone cluster 1, H2bn
2.030652	chromosome Y open reading frame 15B
2.028055	crystallin, gamma S
2.0259347	ribosomal protein L37a
2.0246701	ribosomal protein S15a
2.0238845	X-ray repair complementing defective repair in Chinese hamster cells 2
2.0236278	hexosaminidase A (alpha polypeptide)
2.0185816	heterogeneous nuclear ribonucleoprotein A2/B1
2.015046	similar to Uncharacterized protein KIAA0220
2.0143094	cyclin L2
2.0123272	BCL2-like 11 (apoptosis facilitator)
2.0114002	splicing factor, arginine/serine-rich 18
2.0111163	cytoplasmic linker associated protein 2
2.0059729	C1D nuclear receptor corepressor
2.0025506	hypothetical LOC100506548 /// ribosomal protein L37
2.0024467	DEAD/H (Asp-Glu-Ala-Asp/His) box polypeptide 11
2.0023243	LUC7-like 3 (S. cerevisiae)
-2.0398073	coatomer protein complex, subunit alpha
-2.0400884	kinesin-associated protein 3
-2.0531695	NADH dehydrogenase (ubiquinone) Fe-S protein 1, 75kDa (NADH-coenzyme Q reductase)
-2.056747	cell cycle progression 1
-2.0709784	actin, alpha 2, smooth muscle, aorta
-2.1357281	3-ketodihydrosphingosine reductase
-2.1693356	neurofilament, light polypeptide
-2.176037	cell cycle progression 1
-2.2416408	annexin A5
-2.2541568	jun proto-oncogene
-2.2543998	glutaminase
-2.264334	vascular endothelial zinc finger 1
-2.2852807	keratin 19
-2.2950072	proteasome (prosome, macropain) subunit, beta type, 8 (large multifunctional peptidase 7)

Increase

Decrease

SLEV Capsid

Figure 2 *(con't)*.

Fold Change	Gene Title
2.1782908	integrin beta 3 binding protein (beta3-endonexin)
2.1258564	integrin beta 3 binding protein (beta3-endonexin)
2.1186666	chromosome 8 open reading frame 59
2.087511	integrin beta 3 binding protein (beta3-endonexin)
2.0280323	insulin-like 4 (placenta)
2.0026393	chromosome 8 open reading frame 59
-2.0075738	microtubule-associated protein 1B
-2.0133643	sparc/osteonectin, cwcv and kazal-like domains proteoglycan (testican) 1
-2.0197861	phosphoglucomutase 2-like 1
-2.036934	spectrin, beta, non-erythrocytic 1
-2.0780642	multiple EGF-like-domains 8
-2.078573	serpin peptidase inhibitor, clade E (nexin, plasminogen activator inhibitor type 1), member 1
-2.1036727	glutaminase
-2.1262963	insulin-like growth factor 2 (somatomedin A) /// INS-IGF2 readthrough transcript
-2.682525	RAP1A, member of RAS oncogene family

MVEV Capsid

Figure 2 *(con't)*.